Synthesis and Evaluation of SOD-ZMOF-Chitosan Adsorbent for Post-Combustion Carbon dioxide Capture

Singo Muofhe Comfort

A dissertation submitted to the Faculty of Engineering and the Built Environment, University of the Witwatersrand, Johannesburg, in fulfilment of the requirements for the degree of Master of Science in Engineering

Supervisor: Prof. M.O. Daramola

September, 2017

DECLARATION

I declare that this dissertation is my own unaided work. It is being submitted to the Master of Science to the University of the Witwatersrand, Johannesburg. It has not been submitted before any degree or examination to any other University.

……

(Signature of Candidate)

……day of…….year…….

day *month* *year*

ABSTRACT

South Africa emits large amounts of carbon dioxide (CO_2) due to its reliance on coal. The emission of CO_2 needs to be reduced for clean sustainable energy generation. Research efforts have therefore been devoted to reducing CO_2 emissions by developing cost-effective methods for capturing and storing it. Amine-based absorption using monoethanolamine solvent is the most mature technique for CO_2 capture despite its huge energy consumption, corrosiveness and difficulty in solvent regeneration. However, CO_2 removal by solid adsorbents is a promising alternative because it consumes less energy, and can be operated at moderate temperature and pressure. Metal organic frameworks have received attention as a CO_2 adsorbent because they have large surface areas, open metal sites, high porosity and they require less energy for regeneration.

This research was aimed at optimizing and scaling-up SOD-ZMOF through structural modification for enhanced CO_2 adsorption by impregnating it with chitosan. Scaled-up SOD-ZMOF samples were prepared as described elsewhere and impregnated with Chitosan. Physiochemical properties obtained using X-ray diffraction (XRD), Fourier transform infrared spectroscopy (FTIR), and Nitrogen physisorption showed that SOD-ZMOF and SOD-ZMOF-chitosan were successfully synthesized. Qualitatively, the surface area of the SOD-ZMOF synthesized using the scaled up protocol is lower than the one prepared using the non-scaled-up protocol

XRD pattern of SOD-ZMOF showed that it was crystalline and was in agreement with literature. The XRD peaks of the SOD-ZMOF decreased after chitosan impregnation showing that chitosan was impregnated on SOD-ZMOF. The FTIR spectrum of SOD-ZMOF showed functional groups present in organic linker used to synthesize SOD-ZMOF, and that of the SOD-ZMOF-chitosan revealed the same functional groups but with disappearance of carboxylic acid functional group. N_2 physisorption showed a decrease in BET surface area and pore volume after chitosan impregnation on SOD-ZMOF as well.

Performance evaluation of the material was carried out with a demonstration adsorption set-up using a 15%/85% CO_2/N_2 mixture and as a thermal gravimetric analysis (TGA) using 100% CO_2. For both the packed-bed column and the TGA experiments, evaluation was conducted on SOD-ZMOF and SOD-ZMOF with chitosan for comparison. About 50 mg of the adsorbent was used at 25 ^oC, 1 bar and 25 ml/min for the packed-bed column. For the adsorption with the TGA, 11 mg of adsorbent was used at 25 ℃, 1 bar and 60 ml/min.

SOD-ZMOF showed improved adsorption capacity after chitosan impregnation. CO_2 adsorption capacity of SOD-ZMOF increased by 16% and 39% using packed-bed column and TGA, respectively, after chitosan impregnation. The increase in adsorption capacity was attributed to the impregnated chitosan that has amine groups that display a high affinity for CO_2.

A traditional approach was used to investigate the effect of adsorption temperature and inlet gas flowrate on the CO_2 adsorption capacity of SOD-ZMOF-chitosan. This was done using both the parked bed column and the TGA. Temperature range of 25-80 ℃ and inlet gas flowrate range of 25-90 ml/min were investigated. Adsorption capacity increased with a decrease in temperature and inlet gas flowrate. For the packed-bed column, maximum of 781 mg CO_2/ g adsorbent was obtained at 25℃, 1 bar, 25 ml/min and for the TGA a maximum CO_2 adsorption capacity of 23 mg/ g adsorbent at 25 ℃, 1 bar, and 60 ml/min was obtained.

ACKNOWLEDGEMENTS

I would like to acknowledge my supervisors, Prof. Michael Daramola and Dr Olugbenga Oluwasina for their efforts. Thank you so much for your help, support, and patience and pieces of advice. Thank you too for assisting me and giving me the courage to continue when it seemed impossible. I appreciate you so much. Thank very much to ABB for providing the gas analyser that was used in this project.

I really acknowledge the national research fund South Africa (NRF) and South African centre of carbon capture and storage (SACCCS) for the financial support. Thank you so much to the stuff at the school of chemical and metallurgical engineering at Wits University for your assistance.

I would also like to thank my mom and dad. Mom you are a true definition of what a mother is. Thank you so much for your support, for the strength, prayers and words of encouragement. Your unconditional love is irresistible. To my siblings, Rendani, Gundo and Khahule, I say thank you so much guys for your support, love and prayers. You guys are the best and I love you so much.

PUBLICATIONS

1. **Singo**, **M. C,** Molepo, X. C., Oluwasina, Olugbenga O., Daramola, M.O. Chitosan-impregnated SOD-Metal Organic Frameworks (SOD-ZMOF) for CO_2 capture: Synthesis and performance evaluation, *Energy Procedia,114 (2017), 2429-2440.* ***(Accepted).***

2. Yoro, K.O., **Singo, M.C,** Mulopo, J.L., Daramola, M.O., Modelling and Experimental Study of the CO_2 Adsorption Behaviour of Polyaspartamide as an Adsorbent during Post-Combustion CO_2 Capture, *Energy Procedia, 114 (2017), 1643–1664.* ***(Accepted).***

CONFERENCE PROCEEDINGS AND PRESENTATIONS

1. **Muofhe. C .Singo**, Xitivhane. C. Molepo, Olugbenga O. Oluwasina, Michael.O.Daramola. Chitosan-impregnated SOD-Metal Organic Frameworks (SOD-ZMOF) for CO_2 capture: Synthesis and performance evaluation. **Poster presentation**. 13th International Conference on Greenhouse Gas Control Technologies, GHGT-13, 14-18 November 2016. Lausanne, Switzerland.
2. Kelvin O. Yoro, **Muofhe Singo**, Jean L. Mulopo, Michael. O. Daramola. Modeling and Experimental Study of the CO_2 Adsorption Behavior of Polyaspartamide as an Adsorbent during Post-Combustion CO_2 Capture. **Poster presentation**. 13th International Conference on Greenhouse Gas Control Technologies, GHGT-13, 14-18 November 2016, Lausanne, Switzerland.
3. **Muofhe. C .Singo**, Xitivhane. C. Molepo Olugbenga O. Oluwasina, Michael.O.Daramola. Comparative Study of the CO_2 Adsorption Capacity of SOD-zeolite Metal Organic Frameworks (SOD-ZMOF) and Chitosan-impregnated SOD-ZMOF for Post-combustion CO_2 Capture**. Oral presentation**. *International Conference on Environment, Materials and Green Technology,* 24-25th November 2016 - VUT Southern Gauteng Science & Technology Park– Educity Campus, South Africa.

4. ***Muofhe. C .Singo,*** Olugbenga. Oluwasina, Michael.O.Daramola. Synthesis of chitosan-impregnated SOD-zeolite metal organic frameworks (SOD-ZMOF) for carbon dioxide (CO_2) capture: a preliminary investigation. **Oral presentation**. 33rd

International Pittsburgh Coal Conference, Cape Town, South Africa, 8 - 12 August 2016

5. Yoro, K.O., **Singo, M.C**, Daramola, M.O., Mulopo, J.L., Mathematical Modelling of Adsorption Behaviour of SOD-ZMOF/Chitosan Adsorbent during Post-Combustion CO_2 Capture, ISBN #: 1-890977-33-0 - **Oral Presentation**, *33rd International Pittsburgh Coal Conference*, 8th – 12th August 2016, Cape Town, South Africa

6. ***Muofhe. C .Singo***, Michael O. Daramola. Synthesis, Performance Evaluation and Optimization of the metal organic framework supported ionic liquid Adsorbent for post-combustion CO_2 Capture. **Oral presentation**. 6th National Student Colloquium, University of the Witwatersrand, Johannesburg, 05 June 2015

7. ***Muofhe. C .Singo***, Michael O. Daramola. Synthesis, Performance Evaluation and Optimization of the SOD-ZMOF / PAA Adsorbent for CO_2 Capture. **Oral Presentation**. Carbon Capture Workshop, University of the Western Cape, Cape Town, South Africa. 2 – 4 March 2015.

Contents

DECLARATION i

ABSTRACT ii

ACKNOWLEDGEMENTS iv

PUBLICATIONS v

CONFERENCE PROCEEDINGS AND PRESENTATIONS v

LIST OF FIGURES x

LIST OF TABLES xiii

NOMENCLATURE xv

CHAPTER 1: INTRODUCTION 1

1.1. Motivation and Background 1

1.2. Problem statement and Aim 4

1.3. Research questions 5

1.4. Objectives of the study 5

1.5. Scope of study 5

1.6. Expected outcomes 5

References 6

CHAPTER 2: LITERATURE REVIEW 8

2.1. Introduction 8

2.2. CO_2 emissions 8

2.3. Reduction of CO_2 emissions 12

2.4. Carbon Capture and Storage 13

2.4.1. CO_2 transport and storage 13

2.4.2. Carbon Capture 15

2.5. Summary 50

References 51

CHAPTER 3: EXPERIMENTAL PROCEDURE 59

3.1. Materials and Adsorption equipment 60

3.1.1. Materials 60

3.1.2. Description of Adsorption equipment 60
3.2. Synthesis of SOD-ZMOF-chitosan composite 60
3.2.1. Synthesis of SOD-ZMOF 60
3.2.2. Production of chitosan 60
3.2.3. Development of SOD-ZMOF-chitosan composite adsorbent 61
3.3. Characterisation techniques 61
3.4. Performance evaluation 62
3.4.1. TGA performance evaluation 62
3.4.2. Packed-bed column evaluation 62
References 64
CHAPTER 4: SYNTHESIS AND CHARATERISATION OF SOD-ZMOF-CHITOSAN COMPOSITE ADSORBENT 65
4.1. Introduction 65
4.2. Experimental 65
4.2.1. Synthesis 65
4.2.2. Characterisation techniques for SOD-ZMOF and SOD-ZMOF-chitosan 65
4.3. Results and Discussion 66
4.3.1. Physicochemical characterization 66
4.3.2. Surface area and pore volume 69
4.4. Summary 71
References 71
CHAPTER 5: PERFORMANCE EVALUATION OF SOD-ZMOF-CHITOSAN COMPOSITE ADSORBENT FOR CO_2 CAPTURE 73
5.1. Introduction 73
5.2. Experimental 73
5.3. Results and discussion 73
5.3.1. TGA performance evaluation 73
5.3.2. CO_2 adsorption capacity in packed-bed column 75
5.4. Results compared with literature 78
5.5. Summary 80

References 80
CHAPTER 6: INFLUENCE OF OPERATING CONDITIONS ON CO_2 ADSORPTION CAPACITY OF SOD-ZMOF COMPOSITE 82
6.1. Introduction 82
6.2. Experimental 82
6.3. Results and discussion 83
6.3.1. CO_2 adsorption capacity behaviour with time in TGA and packed-bed column 83
6.3.2. CO_2 adsorption behaviour with temperature in TGA and packed-bed column 85
6.3.3. Effect of gas Flowrate on the CO_2 adsorption capacity of SOD-ZMOF-chitosan 86
6.4. Summary 88
References 89
CHAPTER 7: CONCLUSIONS AND RECOMMENDATIONS 90
7.1. Conclusions 90
6.5. Recommendations 92
APPENDICES 94
Appendix A 94
Appendix B: Adsorption runs and calculations results 95
B1. TGA 95
B1.2: Adsorption capacity as a function of time calculations 101
Appendix C: Adsorption Equipment 111
C1. Packed-bed column 111
Appendix D: Published papers 113

LIST OF FIGURES

Figure 1.1: Total primary energy consumption in South Africa, 2013……...1

Figure 2.1: Summary of literature review……..8

Figure 2.2: Global major sources of anthropogenic sources of greenhouse gases ……..…..…9

Figure 2.3: Anthropogenic sources of CO_2 emissions……...……..……10

Figure 2.4: Diagram illustrating concept of carbon capture and storage…….13

Figure 2.5: Overview of pre-combustion capture ……..…….……16

Figure 2:6. Overview of Oxy-combustion capture …….……17

Figure 2.7: Overview of Post-combustion capture …….……18

Figure 2.8: absorption/ regeneration process……..…..……19

Figure 2.9: Separation by cryogenic distillation…….……23

Figure 2.10: Separation of CO_2 using membrane……..….…..……25

Figure 2.11: Classification of adsorption isotherms …….…..…….29

Figure 2.12: Adsorption Mechanism of carbon dioxide…….…..……30

Figure 2.13: Overview of TSA process…….……...……31

Figure 2.14: Overview of PSA process…….……...…32

Figure 2.15: Overview of fixed/packed-bed adsorption system……..……33

Figure 2.16: Overview of metal organic framework …….……39

Figure 2.17: Formation of different ZMOFs due to the use of different SDA's ...……43

Figure 2.18: Structure of chitin……..…….…….47

Figure 2.19: Structure of chitosan …….…….…….48

Figure 3.1: Summary of research methodology…….……..……59

Figure 3.2: process flow diagram for the adsorption set-up…….……63

Figure 4.1: Characterisation methods used to analyse SOD-ZMOF, chitosan and SOD-ZMOF…….……..……66

Figure 4.2: XRD pattern of SOD-ZMOF before and after impregnation…….……67

Figure 4.3: FTIR spectra of SOD-ZMOFs and chitosan impregnation……...……..……68

Figure 4.4: FTIR spectra of SOD-ZMOFs dried at different temperatures …….……70

Figure 5.1: Profile of TGA adsorption profile…….……74

Figure 5.2: CO2 adsorption capacity of MOFs and chitosan using TGA ……...75

Figure 5.3: Concentration profile of adsorption equipment depicted in Figure 3.2 ……76

Figure 5.4: CO_2 adsorption capacity of the MOFs and Chitosan using packed-bed column...77

Figure 5.5: Overview of how gas flows in A) Packed-bed column. B) TGA ……78

Figure 6.1: Adsorption capacity as a function of time using the TGA ……...…84

Figure 6.2: Adsorption capacity as a function of time using the packed-bed 86…….……85

Figure 6.3: Effect of temperature on CO_2 adsorption capacity of SOD-ZMOF-chitosan using the TGA…….……...……86

Figure 6.4: Effect of temperature on CO_2 adsorption capacity of SOD-ZMOF-chitosan using packed-bed column…….……..…86

Figure 6.5: Effect of gas Flowrate on CO2 adsorption capacity of SOD-ZMOF-chitosan using the TGA…….……..87

Figure 6.6: Effect of gas Flowrate on CO2 adsorption capacity of SOD-ZMOF-chitosan using Packed-bed column…….……88

Figure B1: TGA for SOD-ZMOF at a flowrate of 30 ml/min, 1 bar and 25℃……95

Figure B.2: TGA for chitosan at a flowrate of 30 ml/min, 1 bar and 25℃……..…96

Figure B.3: TGA for SOD-ZMOF-chitosan at a flowrate of 30 ml/min, 1 bar and 25℃……96

Figure B.4: TGA for SOD-ZMOF-chitosan at a flowrate of 45 ml/min, 1 bar and 25℃……97

Figure B.5: TGA for SOD-ZMOF-chitosan at a flowrate of 55 ml/min, 1 bar and 25℃……97

Figure B.6: TGA for SOD-ZMOF-chitosan at a flowrate of 70 ml/min, 1 bar and 25℃……98

Figure B.7: TGA for SOD-ZMOF-chitosan at a flowrate of 90 ml/min, 1 bar and 25℃……98

Figure B.8: TGA for SOD-ZMOF-chitosan at a flowrate of 60 ml/min, 1 bar and 40℃……99

Figure B.9: TGA for SOD-ZMOF-chitosan at a flowrate of 60 ml/min, 1 bar and 55℃……99

Figure B.10: TGA for SOD-ZMOF-chitosan at a flowrate of 60 ml/min, 1 bar and 70℃…100

Figure B.11: TGA for SOD-ZMOF-chitosan at a flowrate of 60 ml/min, 1 bar and 85℃…100

Figure C2: packed-bed column adsorption set-up……112

LIST OF TABLES

Table 2.1: Pros and Cons of CO_2 transport options……..……..14

Table 2.2: Membrane transport mechanisms …….…….……26

Table 2.3: comparison of physisorption and chemisorption …….…….……..…28

Table 2.4: MOFs examined for CO_2 storage capacity …….…….……..…42

Table 2.5: Textual properties of ZMOFs …….…….…….……44

Table 3.1: Operating conditions investigated…….…..…….……62

Table 4.1: Interpretation of characteristics of IR absorption……...……68

Table 4.2: BET surface area, pore volume and pore size of SOD-ZMOF and SOD-ZMOF-chitosan samples……..…..……69

Table 5.1: Comparison of adsorbents and adsorption methods……79

Table 6.1: Investigated operating conditions for packed bed and TGA……..83

Table B1: TGA Adsorption capacity calculations for at 25℃, 1 bar and 30 ml/min …..…..101

Table B2: TGA Adsorption capacity calculations for at 25℃, 1 bar and 45 ml/min……102

Table B3: TGA Adsorption capacity calculations for at 25℃, 1 bar and 60 ml/min……103

Table B4: TGA Adsorption capacity calculations for at 25℃, 1 bar and 75 ml/min……104

Table B5: TGA Adsorption capacity calculations for at 25℃, 1 bar and 90 ml/min……105

Table B6: TGA Adsorption capacity calculations for at 40℃, 1 bar and 60ml/min …….106

Table B7: TGA Adsorption capacity calculations for at 55℃, 1 bar and 60 ml/min ……107

Table B8: TGA Adsorption capacity calculations for at 70℃, 1 bar and 60 ml/min …….....108

Table B9: Packed-bed Adsorption capacity calculations for at 25℃, 1 bar and 25 ml/min ……..……..……109

Table B10: Packed-bed Adsorption capacity calculations for at 40℃, 1 bar and 25 ml/min……..……..……..……109

Table B11: Packed-bed Adsorption capacity calculations for at 55℃, 1 bar and 25 ml/min. ……110

Table B12: Packed-bed Adsorption capacity calculations for at 25℃, 1 bar and 50 ml/min ……..……..……..…..…110

Figure C2: packed-bed column adsorption set-up……..…..……..……..……112

NOMENCLATURE

ASU: Air Separation Unit

AMP: 2-amino-2-methyl-1-propanol

CO_2: Carbon dioxide

BET: Brunauer, Emmett, and Teller

CCS: Carbon Capture and Storage

DMF: Dimethylformamide

EDA: Ethylenediamine

EOR: Enhanced oil recovery

FTIR: Fourier transform infrared

GHG: Greenhouse gases

IEA: International Energy Agency

IL: Ionic liquid

MDEA: Methyldiethanolamine

MEA: Monoethanolamine

MOFs: Metal organic frameworks

N_2: Nitrogen

O_2: Oxygen

PZ: Piperazine

PSA: Pressure swing adsorption

SACCCS: South African Centre for Carbon Capture and Storage

TGA: Thermal gravimetric Analysis

TSA: Temperature swing adsorption

SOD-ZMOF: Sodalite zeolite-like metal organic framework

SOD-ZMOF-Chitosan: Chitosan impregnated Sodalite-like metal organic framework

XRD: X-ray diffraction

CHAPTER 1: INTRODUCTION

1.1. Motivation and Background

South Africa is largely dependent on coal for energy generation (Nyajowa, 2014). In 2013, it was reported that 72% South African primary energy was generated from coal and the remaining percentage was from oil, nuclear, natural and renewables (see Figure 1.1) (EIA, 2015).

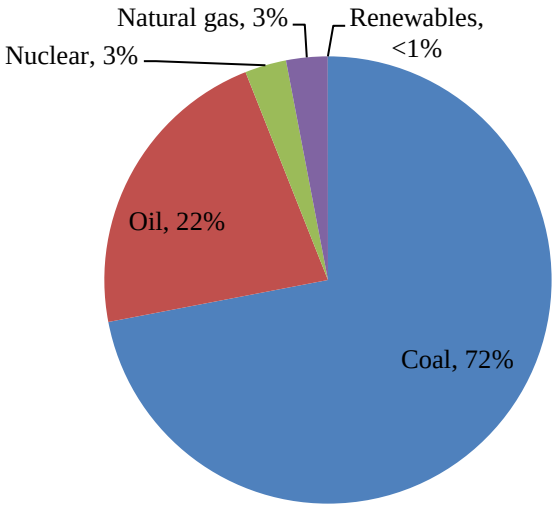

Figure 1.1: Total primary energy consumption in South Africa, 2013 (adapted from EIA (2015))

To date about 90% of South Africa's electricity needs is provided from coal (Nyajoya 2014). It is likely that coal will remain the main source of energy in the next decade because it is available, cheap and also due to lake of suitable alternatives to coal as energy source (Eskom, 2015). Coal is combusted for electricity generation. This exhausts high levels of carbon dioxide (CO_2) into the atmosphere. CO_2 is a major greenhouse gas which substantially causes the greenhouse effect which is known to be the major cause of global warming. Global warming then results to climate change and related environmental disasters. Much effort has been devoted in finding ways of reducing the amount of CO_2 being released to the atmosphere. Carbon capture and storage (CCS) technology is the most common and most identified way. This is because CCS makes it possible to continue using coal for energy generation while reducing the amount of CO_2 being released to the atmosphere (Lackner, 2009). CCS comprises three main steps. First CO_2 is captured from point sources such as coal power plants, cement plants and other industries that burn fossil fuels for energy source.

Second stage is transportation of CO_2 to storage site, and finally storage of CO_2 where CO_2 is stored in a way that will not affect the environment (Li *et al*., 2011).

The South African centre for Carbon Capture and Storage (SACCCS) has been established to investigate the feasibility of CCS in South Africa. SACCCS's strategy is to develop and implement a roadmap for the implementation of CCS in South Africa by 2025 (SACCCS, 2015). In 2004, a preliminary investigation was done to determine if South Africa has potential storage sites for CO_2 (SACCCS, 2015). Results from this investigation showed that South Africa has potential storage sites for CO_2 storage.

In CCS; CO_2 needs to be captured first before it is stored, hence the scope of this research was focused at CO_2 capture. Capture is the most expensive stage in CCS (Li *et al*., 2011). They are three different methodologies for capturing CO_2 from point sources. CO_2 can be captured before and also after combustion of fossil fuels. When CO_2 is captured before combustion the method is called pre-combustion and when captured after combustion the method can be post-combustion or Oxy-combustion (Lee & Park, 2015). The difference is that in post-combustion air is used and in oxy-combustion pure oxygen is used. Thus oxy-combustion is more expensive than post-combustion because an extra stage is required to separate oxygen from air (Lee & Park, 2015). The CO_2 concentration in the gas stream, pressure of gas stream and type of fossil fuel are responsible in selecting the type of capture method (IPCC, 2015). This study focused on post-combustion capture. Different technologies have been developed and investigated for capture methodologies. These technologies include absorption, adsorption, and membrane separation, cryogenic and microbial technologies (Lee & Park, 2015).

Adsorptive CO_2 removal using solid adsorbents has been shown to be very effective. This method presents the benefits of low toxic secondary products and easy to operate (Imeteaz & Sung, 2014). Adsorption process can be carried out at low temperatures, thus it is less energy intensive compared to absorption (Imeteaz & Sung, 2014). There are a number of solid adsorbents that has been developed and investigated for CO_2 capture, but metal organic frameworks (MOFs) have drawn much attention over the past decade (Chen *et al*, 2011). This is explained in that MOFs have large surface area, adjustable pore sizes, open metal sites and less energy for regeneration. Rowsell and Yaghi (2004) defined MOFs as organic-inorganic porous solids that contain metal ions linked to organic ligands. The two assemble together to form extended frameworks through coordination bonds (Rowsell & Yaghi, 2004).

Several types of MOFs have been developed and investigated for capturing CO_2. One of the most recent that is reported in the literature is the zeolite-like metal organic framework (ZMOF). This is a type of MOF with zeolite-like topology. ZMOFs have been investigated for CO_2 capture by Chen *et al* (2011). Their study focused on investigating adsorption of CO_2 by ZMOFs associated with Sodalite and rod topologies (SOD-ZMOF and rod-ZMOF). Chen *et al* (2011) further modified the SOD-ZMOFs by incorporating some alkali metals in the framework through ion exchange. Both the SOD-ZMOF and the modified framework displayed a relatively high CO_2 adsorption capacity as compared to other types of MOFs which proved that SOD-ZMOF is a potential adsorbent for CO_2 capture.

Additionally, the properties of MOFs can be enhanced by incorporating appropriate functional groups to the MOF structure through grafting, impregnation and ion exchange to improve its CO_2 adsorption capacity (Imeteaz & Sung, 2014). The Amine functional group is of particular interest for incorporating in solid adsorbents. This is because the interaction between basic modified amine active sites and acidic CO_2 enables adsorption by covalent bonding (Yu *et al.*, 2012). A major advantage of amine based adsorbents is that they require low heat of regeneration as compared to aqueous amines (Yu *et al.*, 2012). Chen *et al*, grafted ethylenediamine (EDA) on SOD-ZMOF to enhance its adsorption capacity, and the EDA-grafted SOD-ZMOF gave a 30% increase in adsorption capacity as compared to the ordinary SOD-ZMOF (Chen *et al*., 2013), thus the adsorption capacity of SOD-ZMOF can be enhanced for CO_2 capture.

According to Shukla *et al.* (2012), chitosan is a bio-degradable, bio-renewable, bio-compatible and non-toxic polymer derived from chitin (Shukla *et al*, 2013). Chitosan is obtained from naturally occurring sources such as insects, arthropods, shellfish, shrimp, prawns, crabs and fungi (Shukla *et al*, 2013). Due to properties such as biocompatibility, biodegradability, high permeability, non-toxicity high viscosity, high solubility in various media, ability to form films and capability to bind with various metal ions and cost effectiveness, chitosan has gained growing interest over the past few years (Sashiwa & Aiba, 2004). The aforementioned properties have enabled chitosan to be applied for different uses in food industry, cosmetics, and agriculture, waste water treatment and biomedical (Shukla *et al.*, 2013).

Chitosan is a green material and is the second largest most abundant polymer on earth (Ma *et al.*, 2015) The presence of functionalities such as amine ($-NH_2$) and hydroxyl (-OH) in the

chitosan molecules provides basis for interaction with other materials (Xie *et al*.,2013). Therefore, of recent chitosan has been receiving great attention to be used as novel functional composite material (Shukla *et al.,* 2013). Chitosan can be blended with porous materials to form composite chitosan modified materials (Shukla *et al.,* 2013). Numerous works has been reported on composite modified materials (Shukla *et al.,* 2013), but as far as could be ascertained no study on SOD-ZMOF-chitosan composite have appeared in literature.

Chitosan, being a biodegradable organic material with several anime groups depending on its degree of deacetylation, can be a green material that could be used as a substitute to synthetic liquid amine. Also, the final product; SOD-ZMOF-chitosan would have very little environmental effect. Against this background, this research was aimed at designing a composite adsorbent from SOD-ZMOF and chitosan for capturing CO_2.

1.2. Problem statement and Aim

Absorption process, with monoethanolamine (MEA) as absorbent, is the most mature technology that can be applied for post-combustion CO_2 capture (Garðarsdóttir *at al*., 2015). The advantage of using MEA is that it combines strongly and selectively with CO_2 and solubility process of CO_2 into MEA is relatively fast and inexpensive (Khan *et al.,* 2016). However, the main problem that industries face with this method is corrosion as MEA is more corrosive than most secondary and tertiary amines (Pires *et al*, 2011). Another problem is that the process is energy intensive as most of the energy required for CO_2 capture is consumed in heating the CO_2 rich MEA in the stripper column in order to regenerate the solvent (Pires *et al*, 2011). This calls for efficient alternative method for CO_2 capture from point sources.

Amine based adsorbents have drawbacks such as high cost and environmental negative impacts associated with synthetic amines; making it challenging for commercial application of this adsorbents (Yu *et al*, 2012). This calls for an alternative material that has strong affinity for CO_2 but with less production cost and less environmental negative impacts. This work proposed chitosan as an alternative source of amine functional group to be impregnated on SOD-ZMOF.

1.3. Research questions

This study provided answers to the following questions:

i) Can up-scaling synthesis protocol for producing SOD-ZMOF affect physicochemical properties of the synthesized crystals?
ii) Can SOD-ZMOF-chitosan composite adsorbent be synthesized successfully?
iii) What will be the performance of the adsorbent for post-combustion CO_2 capture?
iv) What will be the effect of operating variables on the CO_2 adsorption capacity of the material?

1.4. Objectives of the study

This research aimed at optimizing and up-scaling the synthesis of ZMOFs (SOD-ZMOF in particular) through structural modification or formation of composite material for enhanced CO_2 adsorption. Also, the project explored the synergy between SOD-ZMOF and chitosan in the synthesis of a composite adsorbent for CO_2 capture. Specific objectives of this work were:

(i) To scale-up the synthesis of SOD-ZMOF and compare results with those from literature
(ii) To investigate the CO_2 adsorption capacity of the material in (i) by impregnating it with chitosan and evaluating the performance of the material for CO_2 capture
(iii) To investigate the effect of operating variables such as temperature and flowrate on CO_2 adsorption capacity of the adsorbent in (ii).

1.5. Scope of study

This study was limited to the scale-up of the synthesis, characterization and evaluation of the SOD-ZMOF-chitosan for post-combustion CO_2 capture. The study also investigated the influence of the operating variables on the adsorption capacity of the adsorbent. The study does not focus on CO_2 transportation and storage after storage.

1.6. Expected outcomes

The expected outcomes of this research were:

i) Successfully synthesized SOD-ZMOF-chitosan composite adsorbent for CO_2 capture

ii) Information on the performance of the adsorbent in (i) for CO_2 capture and effect of operating variables on the performance

iii) Communication of the findings journal papers, conference proceedings and in a report

References

1. Chen C, Kim J, Park, D, & Ahn, W. Ethylenediamine grafting on zeolite like metal organic frameworks (ZMOF) for CO_2 capture. *Materials letters*. 2013; 344:347.
2. Chen C, Kim J, Yang D, Ahn, W. Carbon dioxide adsorption over zeolite-like metal organic frameworks (ZMOFs) having a SOD topology: structure and ion exchange effect. *Chemical Engineering Journal*. 2011; 1134:1139.
3. Eskom. (2015). coal power. (ESKOM) Retrieved October 8, 2015, from coal power: http://www.eskom.co.za/AboutElectricity/ElectricityTechnologies/Pages/Coal_Power.aspx
4. Garðarsdóttir S, Normann F, Andersson K, Prölß K, Emilsdóttir S, Johnsson F. Post-combustion CO_2capture applied to a state-of-the-art coal-fired power plant—The influence of dynamic process conditions. *International Journal of Greenhouse Gas Control.* 2015; 51:62
5. Imteaz A, Sung H. Composite of metal organic framework: Preparation and Application in adsorption. *Materials today*. 2014; 136:146.
6. International Energy agency (EIA). CO_2 emissions from Fuel combustions highlights. *IEA Publications*. 2015; 1:139
7. Intergovernmental Panel on Climate Change (IPCC). Carbon dioxide capture and storage. *Cambridge University Press*. 2005; 51:52
8. Khan A, Haldera GN, Saha AK. Comparing CO_2 removal characteristics of aqueous solutions of monoethanolamine, 2-amino-2-methyl-1-propanol, methyldiethanolamine and piperazine through absorption process. *International Journal of Greenhouse Gas Control.* 2014; 1666:1676
9. Lackner K. Carbon Capture: sequestration and storage (2009).
10. Lee S, Park S. A review on solid adsorbents for carbon dioxide capture. *Journal of Industrial and Engineering Chemistry*. 2015; 1:11

11. Li J, Ma Y, McCarthy MC, Sculley J, Yu J, Jeong H, Balbuena PB, Zhou H. Carbon dioxide capture-related gas adsorption and separation in metal-organic frameworks. *Coordination Chemistry Reviews*. 2011; 1791:1823
12. Ma J, Xin C, Tan C. Preparation, physicochemical and pharmaceutical characterization of chitosan from Catharsius molossus residue. *International Journal of Biological Macromolecules*. 2015; 547:556
13. Xie J, Li C, Chi L, Wu D. Chitosan modified zeolite as a versatile adsorbent for the removal of different Pollutants from water. *Fuel*. 2013; 480:485
14. Nyajowa W. (2014). South Africa's coal demands and trends. (SHAM MEDIA corp) Retrieved October 8, 2015, from South Africa's coal demands and trends: http://www.sham-media.net/article.php?45
15. Pires J, Martins F, Aliuim-Ferraz M, Simoes, M. Recent developments on carbon capture and storage: An overview. *Chemical Engineering Research and Design*. 2011; 1446:1460
16. Rowsell J, Yaghi O. Metal-organic frameworks: a new class of porous materials. *Microporous and Mesoporous Materials*. 2004; 3:14.
17. SACCCS. (2015). Roadmap/stratergy. Retrieved December 7, 2015, from SACCCS: http://www.sacccs.org.za/roadmap/
18. Shukla S, Mishra A, Arotiba O, Mamba B. Chitosan-based nanomaterials: A state-of the-art review. *International Journal of Biological Macromolecules*. 2013; 46:58.
19. Sashiwa H, Aiba A. chemically modified chitin and chitosan as biomaterials. *Progress in polymer science*. 2004; 887:908
20. Yu C, Huang C, Tan C. A Review of CO_2 Capture by Absorption and Adsorption. *Taiwan Association for Aerosol Research*. 2012; 745:769-12

CHAPTER 2: LITERATURE REVIEW

2.1. Introduction

This chapter discusses the CO_2 problem in detail and reviews work that has been done on reduction of CO_2 emissions. It also looks at why and how climate change is a challenge the whole world is facing today as well as the effects caused by climate change at present. The Chapter discusses the technologies, methods and materials that have been developed and investigated for reducing the amount of CO_2 being released into the atmosphere. In addition, this chapters looks at the advantages and disadvantages of developed technologies, methods and materials. This chapter concludes with a summary of all the investigated technologies, methods and materials. Figure 2.1 depicts an overview of this chapter.

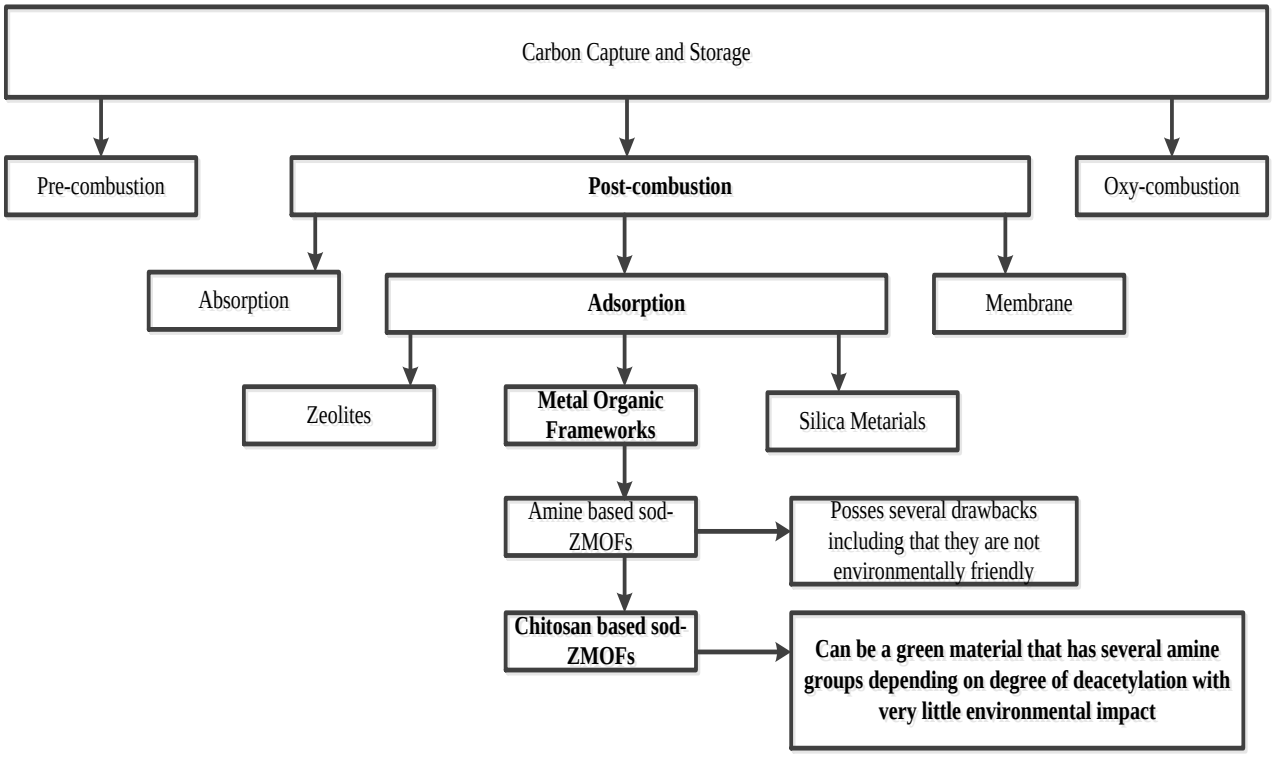

Figure 2.1: Overview of literature review

2.2. CO_2 emissions

Carbon dioxide is a colourless and odourless gas that is produced from human or natural sources. CO_2 is also naturally present in the atmosphere as it is part of the earth's carbon cycle. Additional CO_2 is also produces through human activities such as those highlighted in Figure 2.2. CO_2 produced from human activities is called anthropogenic CO_2. In the past the atmospheric sink was large enough to accommodate for additional CO_2 produced from

anthropogenic activities. However, since the beginning of industrial revolution the CO_2 concentration in the atmosphere has increased from 280 parts per million (ppm) by volume to 397 ppm by volume in 2014 and has continued to increase with an average of about 2 ppm annually in the last decade (IEA, 2015). The increase in atmospheric CO_2 concentration is known to be due to anthropogenic activities. Among many anthropogenic sources that are known to produce greenhouse gases the use of fossil fuel contributes the largest amount of greenhouse gases emissions released in the atmosphere as depicted in Figure 2.3 (Le Quéré *et al*, 2012). In most parts of the world, fossil fuels are the main source of energy production.

Figure 2.2 shows that 68 % of greenhouse gases produced from anthropogenic activities are from the energy production sector. Out of the 68% of greenhouse gases emissions produced from energy generation; 90% of the emissions are CO_2 emissions (IEA, 2015). This is because when fossil fuels are combusted for energy production CO_2 is an inevitable product from the energy production process. About 80-85% of global primary needs are provided from fossil fuels resources (Susarla *et al*., 2015). In 2011, the international energy agency (IEA) predicted that the amount CO_2 emissions from the use of fossil fuels will be 40.2 GT by the year 2030 (Ziobrowski *et al*, 2016).

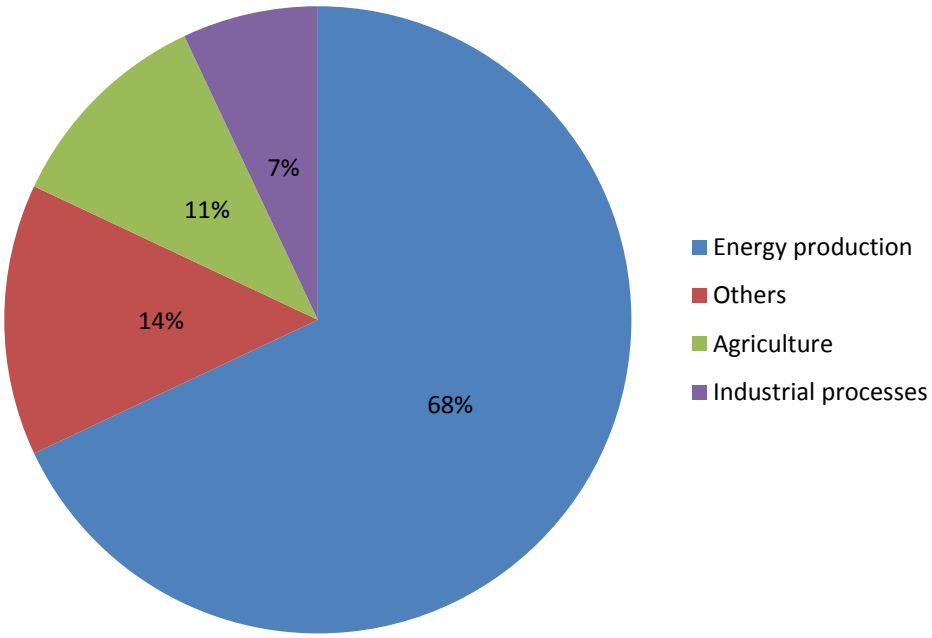

Figure 2.2: Global major sources of anthropogenic sources of greenhouse gases (Adapted from EIA, 2015)

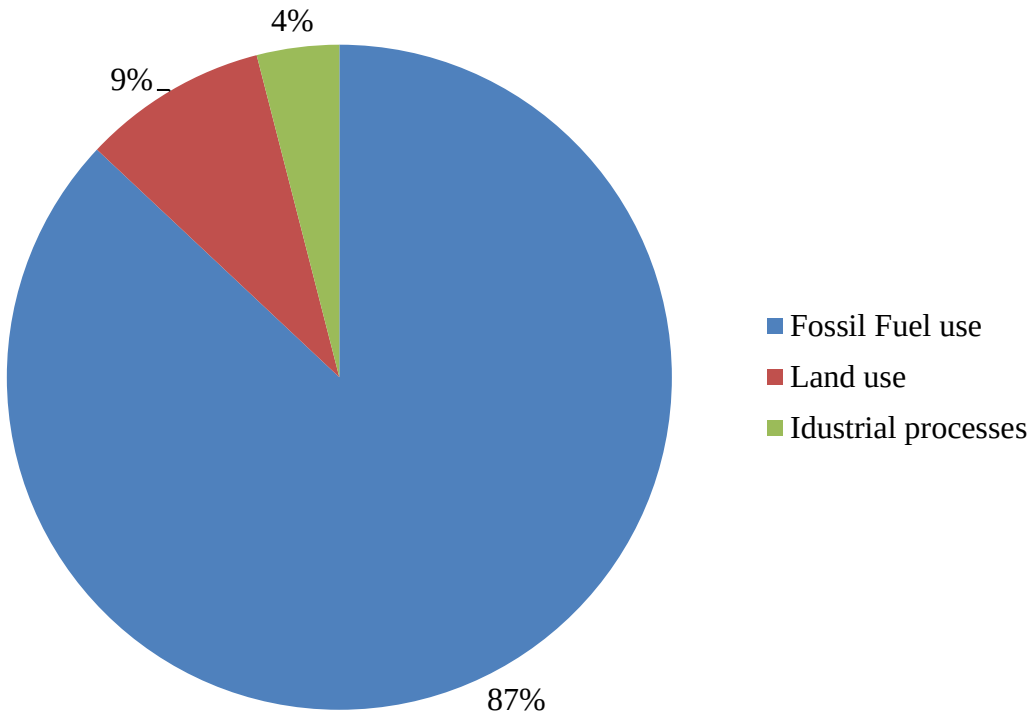

Figure 2.3: Anthropogenic sources of CO_2 emissions (Adapted from Le Quéré *et al*, 2012)

The problem is CO_2 is a major greenhouse gas accounting for 80% of the impact and has drastic consequences on the environment (Freije *et al*, 2016). Increase in atmospheric concentration of greenhouse gases such as CO_2 results in a phenomenon called greenhouse effect that results in global warming. The greenhouse effect is when the temperature of the earth increase due to the trapping of heat in the atmosphere by greenhouse gases (Anderson *et al*, 2016). The earth's temperature increases more than it would if the only source of warming was from direct sunlight (Anderson *et al*, 2016). This is because greenhouse gases absorb some of the heat that would otherwise have escaped from the atmosphere to outer space. This heat is then redirected back to the earth, thus making it warmer (Venkataramanan & Smitha, 2011). This increase in average temperature of the earth is called global warming (Venkataramanan & Smitha, 2011). The major effect of global warming is climate change (Venkataramanan & Smitha, 2011). According to Venkataramanan & Smitha (2011) as the earth is getting warmer disasters like hurricanes, floods and droughts are occurring more frequently. Other possible effects of increasing temperatures include:

- Oceans

The oceans serve as sink for CO_2, however increased atmospheric concentrations of CO_2 in the ocean has led to ocean acidification which changes the pH of the ocean environment (Venkataramanan & Smitha, 2011). Increased temperatures result in the ocean unable to absorb excess CO_2. More effects of global warming on the ocean includes rising sea levels due to thermal expansions and melting of glaciers (Venkataramanan & Smitha, 2011). Sea level rise is one of the certain effects of global warming, because of the 10 to 20 cm rise over the cause of the 20^{th} century which was 10 times more than average rate over the previous three thousand years (Venkataramanan & Smitha, 2011). Venkataramanan & Smitha (2011) reported that the effect of sea rise will be severe in some places due to geologic factors.

- Weather

High temperatures speed up evaporation of water from oceans and thus increase the amount of water vapor in the air which leads to heavy rains (Wang & Chameides, 2005). Heavy rainfall is known to increase the risk of flooding. With increase in temperatures, droughts are expected to occur frequently (Wang & Chameides, 2005). Increase in temperature results in high rate of evaporation and if precipitation doesn't replace the lost moisture from the soil then the soil will grow drier and this can affect the agricultural industry (Wang & Chameides, 2005).

- Health

Increase in temperatures results in outbreaks of vector borne diseases by lengthening the season during which vectors are active and expanding the geographic range of tropical mosquito-borne diseases, such as malaria, dengue fever and yellow fever (Wang & Chameides, 2005). It is reported that malaria kills one to two million people annually (Wang & Chameides, 2005).

This are just a few possible effects caused by increased temperatures and it is evident that effort has to be made in order to find ways of preventing the worst from happening due to increasing atmospheric concentration of CO_2. It is of great significance to find possible ways of reducing the amount of CO_2 concentration in the atmosphere.

2.3. Reduction of CO_2 emissions

It is important to identify factors that contribute to high CO_2 emissions, in order to minimize them. The modified Kaya identity (Equation 2.1) provides direct relationship between anthropogenic CO_2 emissions represented by C and human population (P), economic development indicated by the gross domestic product, (GDP), energy production (E), carbon-based fuels used for energy production (C) and CO_2 sinks, S_{CO2} (Bachu, 2008; Pires *et al*, 2011).

$$\boldsymbol{C = P\frac{GDP}{P}\frac{E}{GDP}\frac{C}{E} - S_{CO_2}} \quad \textbf{(2.1)}$$

According to Equation 2.1, increase in anthropogenic CO_2 emissions is directly proportional to the human population increase per capita GDP, the energy intensity of the economy (E/GDP) and carbon intensity of the energy system (C/E) (Bachu, 2008; Pires *et al*, 2011). Based on equation 2.1, there are 5 ways in which anthropogenic CO_2 emissions can be reduced (Bachu, 2008; Pires *et al*, 2011). The first two ways involves the reduction of population and economic outputs which are not a realistic solution due to policy implementation (Bachu, 2008). The third and fourth ways involves increasing energy efficiency and switching completely or partially to renewable energy such as wind, solar, nuclear, biomass to replace coal (Bachu, 2008; Pires *et al*, 2011). However, the high cost of renewable energy compared to the abundance of fossil fuels availability is delaying the introduction of green renewable energy (Bachu, 2008; Pires *et al.*, 2011). Furthermore, the use of biomass could lead to conflict with other land and water uses as well as food production and forestation (Bachu, 2008) .The fifth term, S_{CO_2} representing CO_2 sinks involves the continuous use of coal for energy generation and the use of CCS technology to stabilize CO_2 emissions (Bachu, 2008; Pires *et al.*, 2011).

Pires *et al* (2011) reported that coal will remain the main source of energy in this century. Maintaining the CO_2 emissions from fossil fuels is the most indicated technology to stabilize atmospheric CO_2 emissions (Pires *et al*, 2011). This could be achieved using a technology called carbon capture and storage (CCS). CCS involves CO_2 capture from fixed generation sources, transporting it to storage site and storing it in geological sites (Pires *et al*, 2011). Point sources include power plants, cement manufacturing plants, refineries, iron and steel industries as well as petrochemical industries. CCS is considered the only technology that can reduce CO_2 emissions from the power generation industry (Cebrucean *et al*, 2014). The IEA

(2014) reported that CCS can reduce total energy production related emissions by 14% by the year 2050 (IEA, 2014).

2.4. Carbon Capture and Storage

CCS is the most identified and commonly used technology for stabilizing CO_2 emissions in the atmosphere. The main advantages of CCS are that it is deployable in a number of industries and it allows the continued use of fossil fuels for energy production with low CO_2 emissions (Stanley, 2014). It involves CO_2 capture at point sources of generation such as cement factories, steel production and coal power plants; compressing it to a supercritical fluid to be transported and then storing it in geographical sites (Zhang & Huisingh., 2017). Figure 2.3 illustrates an overview of the CCS process. CCS comprises of three main steps as observed in figure 2.4: CO_2 capture, transportation and storage.

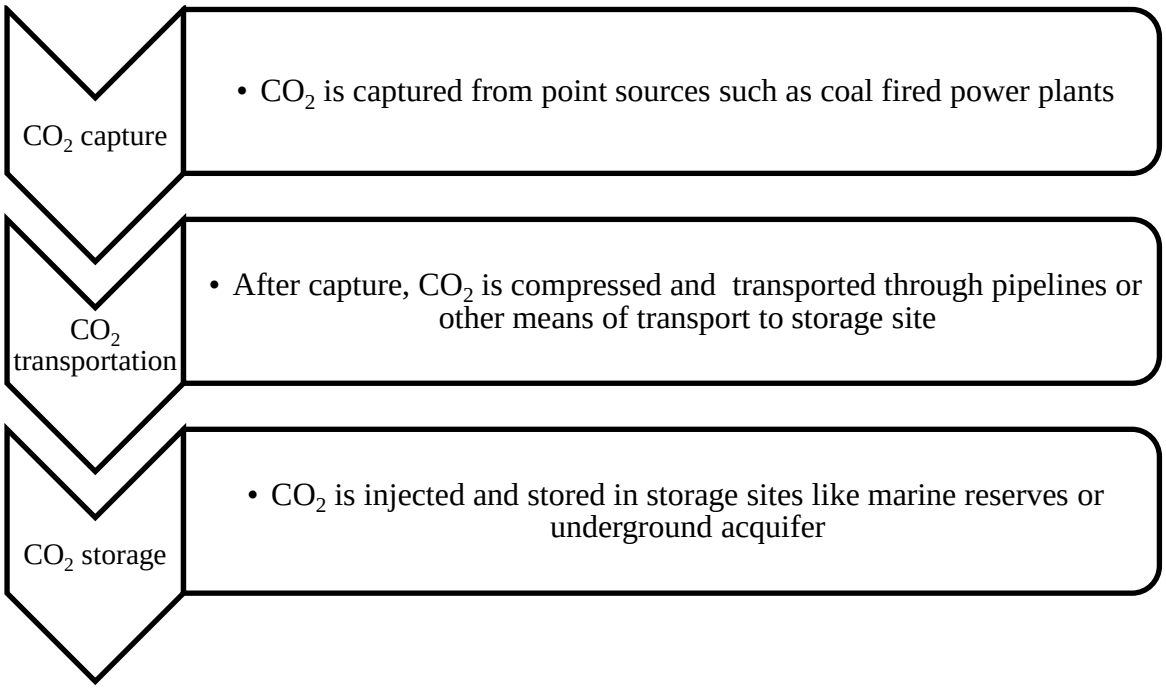

Figure 2.4: Diagram illustrating concept of carbon capture and storage

2.4.1. CO_2 transport and storage

After capturing CO_2; it is compressed to liquid and supercritical fluid before it is transported and stored. CO_2 is transported by either pipelines, trucks or ship to a place where it will be stored (Zhang & Huisingh., 2017). Table 2.1 gives the advantages and disadvantages of the aforementioned CO_2 transportation options.

Table 2.1: Pros and Cons of CO_2 transport options (Adapted from Zhang & Huisingh., 2017))

Transport option	Advantages	Disadvantages
Trucks	Good for transportation of small amount of CO_2	• High CO_2 leakage risk • High Transport costs • Only small amount of CO_2 can be transported per load
Pipelines	• Has been used in industry for more than 40 years • Large amount of CO_2 can be transported per load • Low Transport costs • Low CO_2 leakage risk	• Pipeline integrity • Flow assurance • Safety and operational considerations
Ships	• Low transport costs • Large amount of CO_2 can be transported per load • Low CO_2 leakage risk	• Extra costs may be incurred as CO_2 needs to be compressed first

When CO_2 is transported by trucks it is to be stored in land, when transported by pipelines it can be stored in either land or sea and when transported by ship it is stored in sea (Zhang & Huisingh., 2017). CCS keeps CO_2 out of the atmosphere by capturing it from power plants and injecting it in deep reservoirs that contain fluids for thousands of years (Zhang & Huisingh., 2017).

CO_2 storage involves injecting captured CO_2 from point sources into geological sites (Zhang & Huisingh., 2017). Thus captured CO_2 does not go back to the atmosphere therefore reducing the amount of CO_2 that is being released into the atmosphere. The captured CO_2 could be purely for the purpose of storage or for utilization. A mature example of utilization of CO_2 is the enhanced oil recovery (EOR) from depleted oil reservoirs (Zhang & Huisingh.,

2017). EOR is a process whereby CO_2 is used to recover oil. EOR has been practiced in Canada at the Weyburn oilfield since 1954 and also in USA at the SACROC oilfield since 1947 (Zhang & Huisingh., 2017). This research work is limited to only Carbon capture.

2.4.2. Carbon Capture

Before CO_2 is transported and stored it needs to be captured from different point sources. CO_2 capture is the first stage. In power plants, flue gas is the CO_2 containing gas mixture produced during electricity generation. CO_2 must be separated from this gas mixture before it is stored or utilized. CO_2 capture is the most expensive stage, approximately about two thirds of the total cost of CCS process (Li *et al*., 2011). In addition CO_2 capture can reduce the efficiency of the plant by about 14% and it increases the amount of electricity used in the plant by 30-70% depending on the type of capture technology used, plant type and fuel used (Cebrucean *et al*, 2014). As such, there are various technologies that have been developed and investigated.

CCS can be performed using three different methodological routes for capturing CO_2: pre-combustion, oxy-combustion and post-combustion. In all three methodologies CO_2 must be efficiently separated from other gases before storage.

2.4.2.1. Techniques used to capture carbon dioxide

2.4.2.1.1. Pre-combustion

In this capture method, CO_2 is removed from process before combustion. Pre-combustion is primarily applicable to gasification plants where fuel (coal or biomass) mixed with oxygen is converted to mainly CO and H_2 (Li *et al*., 2011). The CO formed is reacted with steam in a catalytic convertor to produce CO_2 and more H_2 (Li *et al*., 2011). CO_2 is then separated from H_2 by a number of technologies such as absorption, adsorption or membrane separation (Li *et al*., 2011). Pure hydrogen is combusted with air in the power plant. The advantage of this method over post-combustion is that it achieves higher CO_2 concentration and pressure at outlet stream, which makes CO_2 capture much more efficient, it also requires lower energy requirements (Li *et al*., 2011). However this method is disadvantaged by high investment costs and public resistance to new technology (Thorbjornsson *et al*, 2015; Li *et al*, 2011). Figure 2.5 depicts an overview of a process for CO_2 capture by pre-combustion.

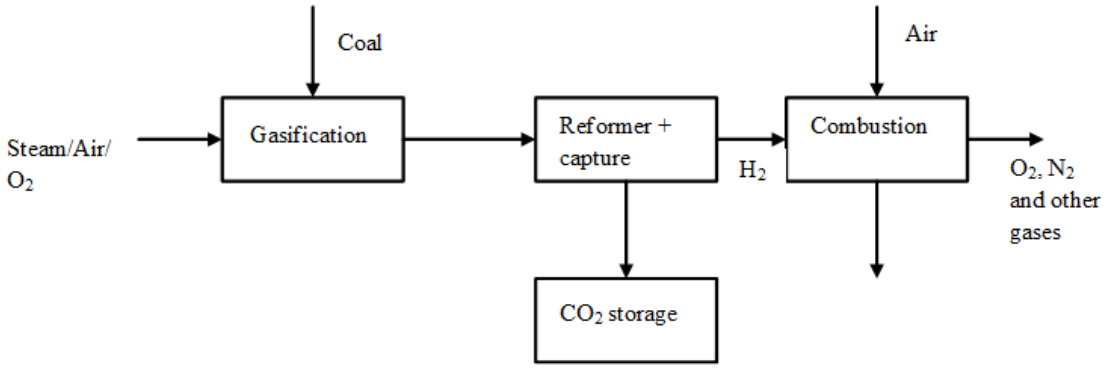

Figure 2.5: Overview of pre-combustion capture (Adapted from Lee and Park, 2015)

2.4.2.1.2. Oxy-combustion

Oxy-combustion is done using pure oxygen produced using a cryogenic air separation or membranes (Perrin *et al*., 2015). Combustion with pure oxygen is associated with high temperature when compared with combustion with air. CO_2 is captured after the combustion stage. Combustion products are CO_2 and water (H_2O). The two are separated by condensing water. CO_2 rich gas is recycled to reduced temperatures. The CO_2 recovery in the output stream is relatively high with values exceeding 95% and produces CO_2 with purity of about 99.999 % (Perrin *et al*., 2015). A major advantage of oxy-combustion over post-combustion is that no nitrogen oxides are formed when using the former technology (Perrin *et al*., 2015). However, oxy-combustion is relatively expensive due to costs associated with obtaining pure oxygen from air. The cryogenic distillation process is quite expensive and is energy intensive. Figure 2.6 depicts the process of CO_2 capture using oxy-combustion.

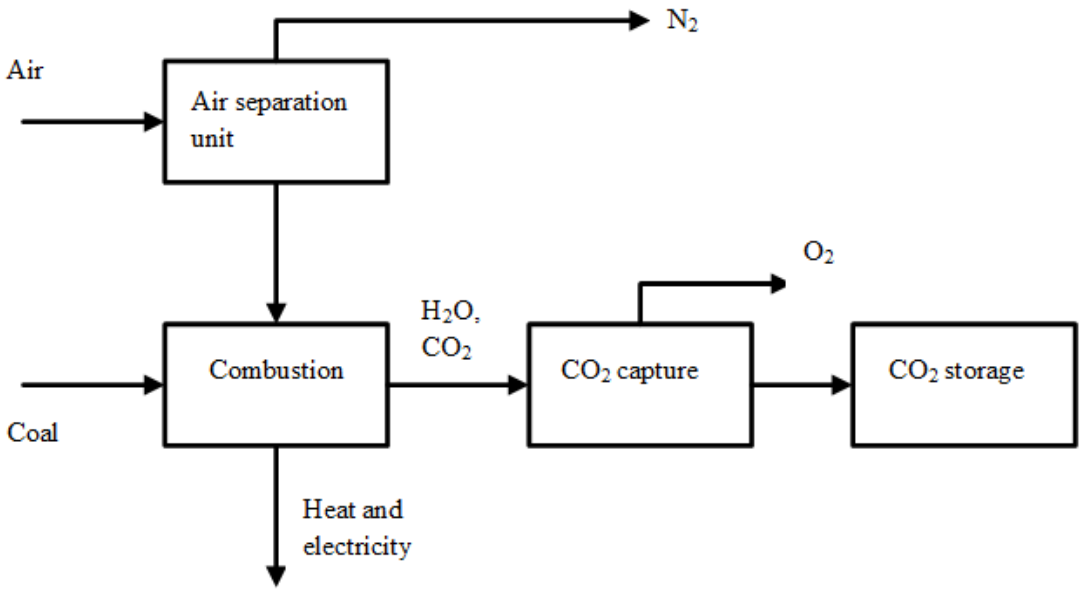

Figure 2:6. Overview of Oxy-combustion capture (Adapted from (Lee & Park, 2015)

2.4.2.1.3. Post-combustion

Like oxy-combustion, CO_2 is removed after combustion of coal. The major difference from oxy-combustion is that for post-combustion air is used during the combustion stage. This technology is applied to fossil fuel burning power plants. Example of such plants is coal fired and oil fired power plants (NETL, 2015). In this coal fired power plants, CO_2 is captured from flue gas after combustion of fossil fuel. This capturing method can be used when gas contains low concentration of CO_2. Main advantage of post-combustion is that it can be easily integrated into existing power plants with few modifications of the combustion process compared to pre-combustion and oxy-combustion (Wang *et al*., 2011). Post-combustion produces CO_2 which can be applied in enhanced oil recovery, urea production and food/beverage industry (Garðarsdóttir *et al*, 2015). In this study, post-combustion method was investigated for CO_2 capture. Figure 2.7 depicts the process of CO_2 capture using post-combustion method.

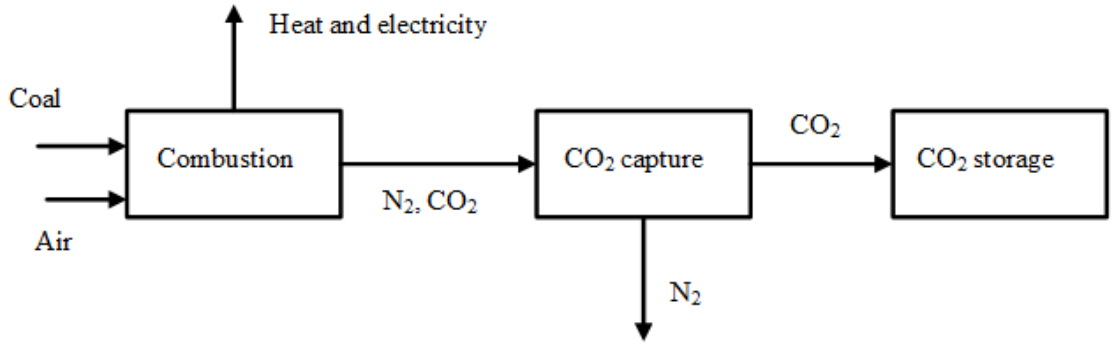

Figure 2.7: Overview of Post-combustion capture (Adapted from Lee & Park, 2015)

2.4.3. Conversional technologies used in capturing CO_2

There are a lot of technologies that have been developed and investigated for capturing CO_2. These technologies include absorption, cryogenic distillation, membranes and adsorption and are discussed in detail in this section.

2.4.3.1. Absorption

Absorption is a process in which molecules dissolve in liquid solvent (Keller & Staudt, 2005). The liquid solvent in which molecules dissolve in is called an absorbent. Molecules undergoing absorption are taken up by a volume of the bulk phase (liquid solvents). Using of liquid solvents as absorbents has practical advantages for large scale gas separation. Advantages include technical maturity and ability to treat large volume of gas (Li *et al.*, 2017). Absorption is accompanied by desorption where the dissolved molecules are separated from the solvent. This is known as stripping. Figure 2.8 depicts the process of adsorption and stripping.

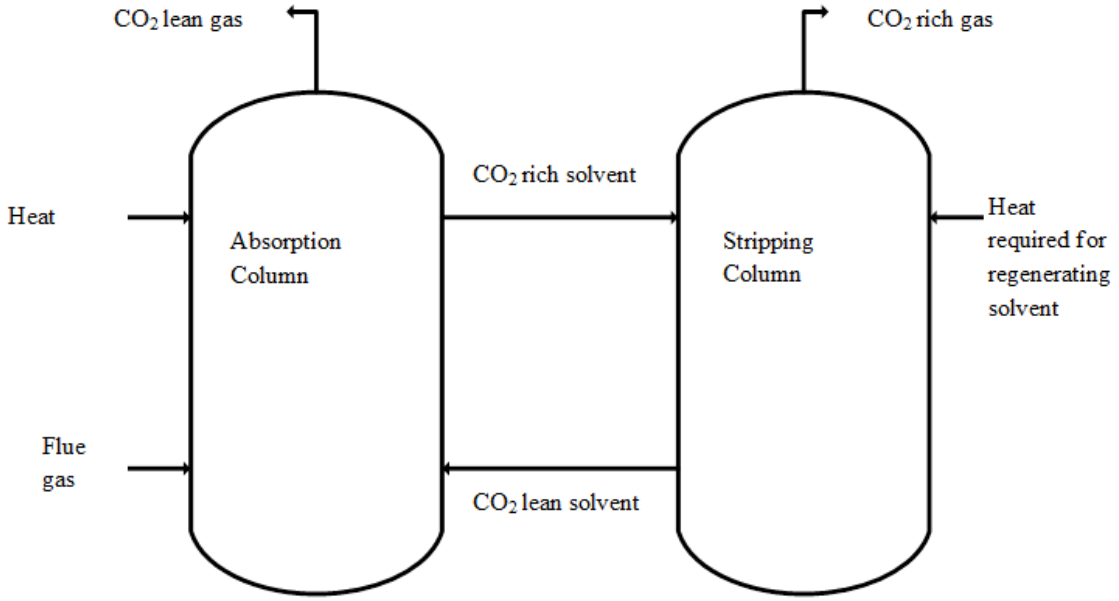

Figure 2.8: Absorption/ regeneration process

Absorption process can be physical or chemical depending on the type of absorbents used. In physical absorption, CO_2 is absorbed at high pressure and low temperature and desorbed at low pressure and high temperature (Yu *et a*l, 2012). The absorbents used are non-reacting. Absorbents used influence separation through of interaction between target gas and absorbents. Physical absorption is more effective when separating gases across large pressure difference or with high concentration of targeted gas (Yu *et al*, 2012).The advantages of physical absorption are low toxicity, low vapor pressure and less corrosion solvent as compared to chemical adsorption. In chemical absorption, absorbents used are reactive. Absorbents effect separation through some type of chemical reaction between the targeted gas and absorbent. Chemical absorption is effective for smaller pressure difference situations that require larger binding energies (Yu *et al.*, 2012). Yu *et al* reported that chemical absorption is usually operated at a pressure of 1 bar. Absorption and desorption temperatures vary at ranges of 40-60 ℃ and 120-140 ℃ respectively (Yu *et al.*, 2012)

There are a number of different solvents that have studied and investigated for CO_2 capture. However the absorption process with amines is the most commonly used process in industry for post-combustion CO_2 capture (Khan *et al*, 2016).) Monoethanolamine (MEA) is the most common and is a commercial solvent due to its low cost, high CO_2 selectivity and availability

(Khan *et al*, 2016). In coal fired power plants, flue gas containing CO_2 gas from combustion stage is contacted with an amine in an absorber column at relatively low temperatures. The CO_2 is absorbed by dissolving in the amine. The CO_2 -loaded amine solvent is pumped into a stripping column, where it is heated to regenerate the solvent and release CO_2 (Yu *et al*., 2012). The hot solvent is then recycled back to the absorber column through a heat exchanger. The heat exchanger cools the hot solvent to the absorption column temperature and preheats the loaded MEA going to the stripper (Yu et al., 2012).

Several studies have been conducted where amine and amine blended solvents were investigated for CO_2 capture. Khan *et al* (2016) did a comparative study of four different amine solvents for CO_2 absorption. The solvents investigated were MEA, 2-amino-2-methyl-1-propanol, methyldiethanolamine (MDEA) and piperazine (PZ) (Khan *et al*, 2016). CO_2 absorption study was conducted in a packed column at temperature range of 298-313 K and CO_2 partial pressure ranging from 10 to 15 kPa. Khan *et al* (2016) investigated the influence of solvent concentration, gas flowrate and solvent flowrate on CO_2 absorption. Three different mass compositions (10, 20 and 30 wt. %) were investigated for each of the four solvents. The authors observed that the specific rate of absorption increased with increase in amine concentration and CO_2 partial pressure for each solvent. CO_2 loading also increased with increase in mass concentration of amine in aqueous solution (Khan *et al*, 2016). CO_2 absorption performance of the investigated solvents followed the trend: PZ>MEA>AMP>MDEA and in terms of specific absorption rate and regeneration performance the following trend was observed: AMP>MDEA>PZ>MEA (Khan *et al*, 2016).

Nwaoha *et al* (2016) reported on the CO_2 absorption using a highly concentrated tri-solvent blend containing 2-amino-2-methyl-1-propanol (AMP), piperazine (PZ) and (MEA). The authors varied individual concentrations of AMP and PZ but the total concentrations of two solvents remained constant in the mixture (Nwaoha *et al*, 2016). This was done to minimize the possibility of precipitation. AMP-PZ-MEA tri solvent blends showed slightly higher equilibrium CO_2 loading compared to that of standard 5 $Kmol/m^3$ MEA (Nwaoha *et al*, 2016). All blends showed improved CO_2 adsorption capacity of about 29.1% - 38% higher as compared to that of just standard MEA (Nwaoha *et al*, 2016).

The advantage of using amine technology is that it is a mature process and has been commercialized for decades (Yu *et al.*, 2012). In spite of this advantage, CO_2 absorption

using amine solvents has several drawbacks. Inefficiencies with amine based absorbent include:

- Loss of amine

Due to their volatility, amines can be lost through emissions. Amine solvent is lost through vaporization, entrainment and chemical degradation (Luis *et al.*, 2012). Even though traps are typically used to minimize amine loss, amine emissions in a form of aerosols are still a major challenge (Dutcher *et al*., 2015).Aerosols can escape these traps causing concern to the environment and resulting in increased amine required to make up for the lost amine(Dutcher *et al*., 2015).

- Amine degradation

Amine degradation is a very serious concern that generally occurs in two methods (Dutcher *et al*., 2015). The first one is oxidative degradation where amines are generally fragmented into toxic compounds such as amides, organic acid and ammonia (Dutcher *et al*., 2015). The second method is thermal degradation that usually occurs in the stripper column where high temperature conditions tend to produce larger amine chain molecules (Dutcher *et al*., 2015). Both methods of degradation results in the formation of compounds with poor CO_2 capture properties, lower capacities and slower kinetics than the original amine (Dutcher *et al*., 2015). The degradation products also have effect on the operating of equipment as they cause corrosion of equipment (Dutcher *et al*., 2015).

- Equipment corrosion

The main problem that industries face with this technology is corrosion as amine solvents especially MEA is more corrosive than most secondary and tertiary amines (Pires *et al*, 2011). In coal fired power stations, CO_2 is separated from flue gas. Flue gas contains oxygen that reacts with amine to produce corrosive degradation products (Pires *et al*, 2012).

- Cost of regeneration

The Regeneration step can increase the operating cost of capture plant by about 70% (Ziobrowski *et al*, 2015). CO_2 absorption using aqueous amine based absorbents results in formation of ammonium salts such as ammonium bicarbonate and ammonium carbonate (Tu *et al.*, 2012). CO_2 needs to be separated from the ammonium salts before it is transported and stored (Dutcher *et al*., 2015). The process of separating CO_2 from ammonium salts is called

striping. The main purpose of striping is to regenerate amine solvents so it can be recycled and reused for absorption again. Absorption products (ammonium salts) are thermally decomposed in order to regenerate and separate solvent from CO_2 (Dutcher *et al*., 2015). Ammonium salts are heated in order to liberate CO_2. Ramdin *et al* (2012) reported that the heat input to remove 1 ton of CO_2 by using 30% MEA aqueous solution is about 2.5 to 3.6 GJ. Yu *et al* (2012) reported that regeneration of CO_2 using 30 wt% to 40 wt% MEA aqueous solution is about 3.3 to 3.01 GJ/ ton CO_2. Favre (2011) reported that about 3.5 GJ/ton is required to regenerate CO_2 from amine solvent.

Other drawbacks of this absorption using amines are low CO_2 loading capacity and large equipment size (Yu et al, 2012). In an effort to overcome these drawbacks, researchers look into improving absorbents and operations (Yu *et al.,* 2012) by combining amines and developing new absorbents. Ionic liquids (IL) are one of the new solvents that researchers develop to absorb CO_2. IL can be applied in both physical and chemical absorption. However the major drawback of using ILs for CO_2 absorption is their high viscosity (Yu *et al.,* 2012).

2.4.3.2. Cryogenic distillation process

Cryogenic distillation is a gas separation technique that uses distillation at extremely low temperatures and high pressure (Leung *et al*., 2014). The difference between this technology and the conventional distillation is that cryogenic distillation separates gaseous mixtures instead of liquid mixture (Leung *et al*., 2014). For CO_2 capture, flue gas is cooled to sublimation temperatures and CO_2 in its solid state is separated from other light gases present in flue gas and then compressed at high pressures of about 100-200 atmosphere (Leung *et al*., 2014).Cryogenic distillation can recover about 90-95% CO_2 from flue gas (Leung *et al*., 2014). This CO_2 separation method is reported to be energy intensive as it operates at low temperature and high pressures (Leung *et al*., 2014). Figure 2.9 depicts an overview of separation by cryogenic distillation

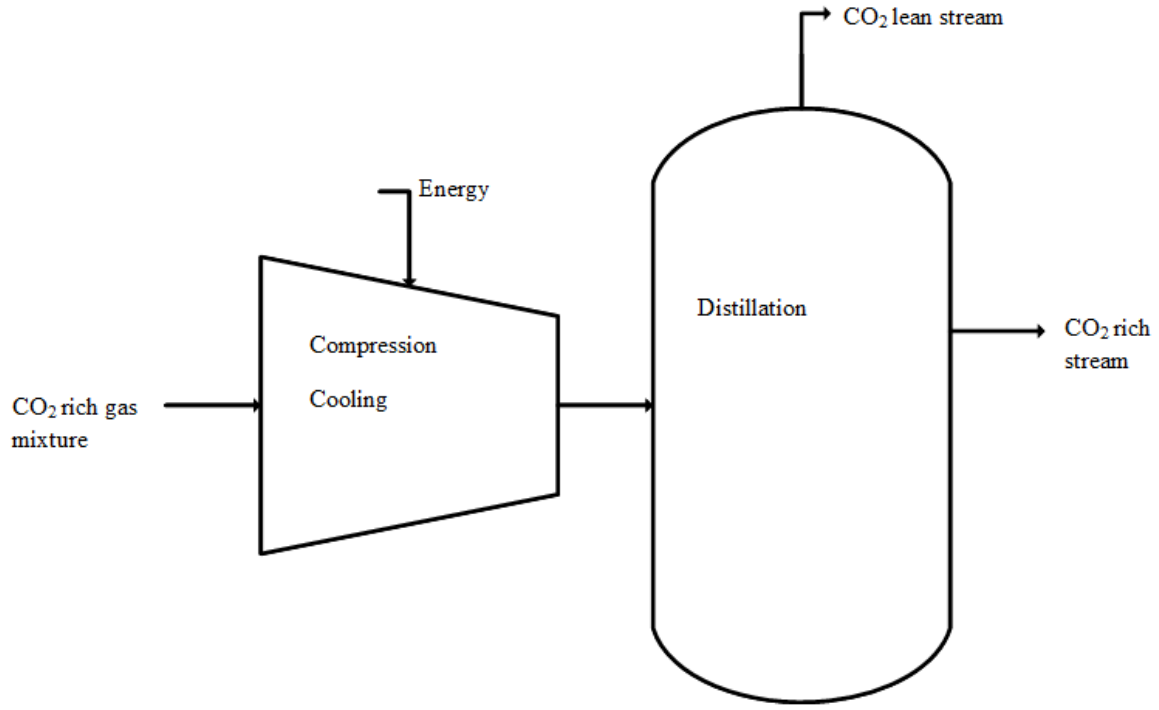

Figure 2.9: Separation by cryogenic distillation

Cryogenic distillation can be applied in post-combustion CO_2 capture where CO_2 and water (H_2O) are separated from gas on a basis of dew and sublimation points. The main advantage of cryogenic method is the simultaneous separation of CO_2 and H_2O from flue gas in the absence of using solvents and high pressures. The main concern with using this method is that the water content in feed stream of cooling units should be minimized or reduced to prevent plugging by ice or high pressure drop during operation (Pires *et al*, 2011). The advantage of cryogenic distillation is that no absorbents are required and CO_2 can be captured at atmospheric pressure (song *et al.*, 2012). According to Song *et al* (2012), the major challenge with cryogenic distillation is the expected high cost of cooling.

Song *et al* (2012) developed a novel system of cryogenic distillation for CO_2 capture. The authors investigated the influence of temperature and flowrate on CO_2 recovery and process performance. Their research was based on the stirring cooler technology. This technology presents several advantages including high reliability and high efficiency (Song *et al*., 2012). Song *et al* (2012) demonstrated that the stirring cooler system can separate CO_2 efficiently. A CO_2 recovery of 96% with 1.5 MJ/Kg CO_2 energy consumption was achieved by song *et al* (2012) using the cryogenic distillation technology.

Song *et al* (2014) optimised the novel cryogenic CO_2 capture process discussed above using response surface methodology (RSM). The authors used three levels and variable central composite design to investigate the influence of capture conditions on performance focusing on CO_2 recovery and energy consumption (Song *et al.*, 2014). Investigated parameters were idle operating time (range of 3-5 h), flowrate (range 1-3 L/min) and FPSC temperature (range 30-10℃). Optimization results showed that these parameters had significant effect on CO_2 recovery and energy consumption (Song *et al.*, 2014). The optimum conditions were found to be idle operating time of 3.9 h, gas flowrate of 2.16 L/min and FPSC temperature of -18℃. Song *et al* (2014) found that the CO2 recovery of 95.2 % and energy consumption of 0.52 MJ/captured CO_2 at the aforementioned operating conditions. The energy consumption was reduced after optimization.

2.4.3.3. Membrane

Membranes separate species by selectively permeating certain components of a mixture faster over others through a thin barrier (Leung *et al.*, 2014). Flue gas enters the membrane and the membrane only allows CO_2 gas molecules to pass through while retaining other gases (Anantharaman *et al*, 2016; Leung *et al*., 2014). The CO_2 rich stream is called permeate and the CO_2 lean stream is called the retentate. Figure 2.10 depicts a flow diagram of CO_2 separation by membrane. The driving force behind membrane separation could be concentration, pressure and chemical potential gradient. Several types of membranes have been developed and investigated; these include metallic, ceramic and polymeric membranes (Hofs *et al*, 2015).

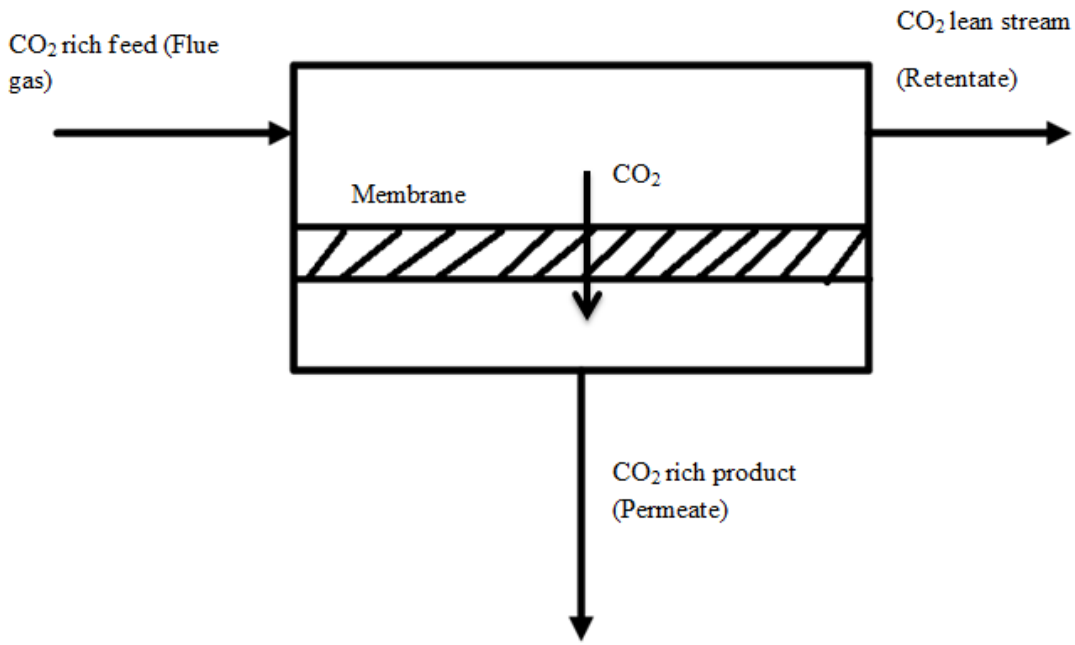

Figure 2.10: Separation of CO_2 using membrane

Membrane separation is advantageous over other method of separating gases. Their advantages include (Quan *et al*., 2017; Leung *et al*., 2014):

- It is a simple and passive operation with no moving parts.
- It is an environmentally friendly method without the use of toxic chemicals
- Less energy intensive because separation of gases do not require phase change
- It has higher separation efficiency as compared to equilibrium based processes

In membrane separation, molecules move or permeate through the membrane through variety of transport driving forces. The type of transport is largely dependent on sizes of pores or free volume elements in the membrane and the size of molecules to be separated. Table 2.2 gives the common types of membrane transport mechanism.

Table 2.2: Membrane transport mechanisms (Adapted from carbon capture: beyond 2020, 2010)

Pore size ($\dot{A}$)	**Transport mechanism**	**Application**
>200	Convective flow	No separation-typical gas filter
$\lambda/_D$ >1 (20-1000)	Knudsen flow	Very low separation
5-10	Surface flow	An example of this is micro porous carbon with 5-7$\dot{A}$ pore size for separation of H_2 from hydrocarbons
<5	Molecular sieving	Carbon membranes with < 5$\dot{A}$ pore. It is very selective
Dense no permanent pores	Solution diffusion	Commercial polymeric gas separation membranes. Used mainly for H_2 separation, Air separation, CO_2 separation from natural gas.
Dense	Ion transport ceramic	Under development for ultrapure H_2, O_2

For gas separation applications such as capturing CO_2 from flue gas, solution diffusion transport mechanism is of interest. An example of membranes with such mechanism is polymeric membrane. Polymeric membranes are typically limited to the relationship between selectivity and permeability. Polymeric membranes present several advantages such as low cost, high performance separation, easy to synthesis and mechanically stable (Pires *et al*, 2011). For CO_2 capture using post-combustion, polymeric membranes cannot be applied without cooling the flue gas. This is because high temperatures rapidly destroy the membrane (Pires *et al*, 2011). Polymeric membrane can also be applied in pre combustion in steam reforming reaction to separate CO_2 from H_2. In oxy-combustion, polymeric membranes can be applied to produce oxygen rich streams from air (Pires *et al*, 2011). The application of polymeric membranes in pre combustion and oxy combustion is an attempt to increase amount of CO_2 captured in outlet stream (Pires *et al*, 2011).

Major drawbacks of polymeric membranes such as thermal stability resulted in the development of ceramic membranes (Nwogu *et al*, 2015). Unlike polymeric membranes, ceramic membranes can capture CO_2 at high temperature (Lackner & West, 2007). Other

advantages of ceramic membranes are mechanical stability and higher chemical stability which results to longer lifespan of membrane (Hofs *et al*, 2015). Several studies have been done where ceramics membranes have been applied for CO_2 capture. Nwogu *et al* (2015) reported on the performance evaluation of inorganic ceramic membranes for CO_2 gas separation. Daramola *et al* (2016) reported on the successful synthesis and characterisation of Nano composite Sodalite ceramic membrane via pore plugging hydrothermal synthesis for pre-combustion CO_2 capture.

In spite of the many advantages of membrane separation technology for CO_2 capture, there are several disadvantages presented by this technology. The main problem is that treatment of large flowrate of flue gas emitted from coal fired power stations requires large membrane area which results in increased costs of the membrane capture technology (Pires *et al*, 2011). Another major problem with this technology is that it requires large energy compensation and expensive compression equipment for post-combustion capture, thus making the technology expensive (Pires *et al*, 2011). The membrane technology is still under development (Leung *et al*., 2014).

2.4.3.4. Adsorption

This process is believed to be the most suitable for post-combustion capture (Yu *et al*, 2012). Adsorption is a process where molecules (liquid, gas or solid) adhere to the surface of a material (Keller & Staudt, 2005). In the case of gas adsorption, when a gas makes contact with a solid; it can be taken up by the solid. The solid that takes up the gas is referred to as the adsorbent and the gas adsorbed to the solid as the adsorbate (Keller & Staudt, 2005). The reverse of adsorption where the gas detaches from the adsorbent is called desorption (Keller & Staudt, 2005). Adsorption is considered advantageous over other capture methods because it requires low energy for regeneration, fast kinetics, increased loading capacity and it can operate at low temperature as well as pressure (Saxenaa *et al*, 2014). Adsorption process requires for molecules to make strong contact with solid surface. Depending on the interaction energy and strength between adsorbate and adsorbent, adsorption can either be physisorption (physical) or chemisorption (chemical) (Keller & Staudt, 2005).

Physisorption and chemisorption

Physisorption is also known as physical adsorption. If the interaction between the adsorbent and adsorbate is weak, then physisorption is taking place (Dutta, 2009). In this process there

is weak binding between the adsorbent and adsorbate. Forces of physisorption are van der Waal forces and for electrostatic force between adsorbate and surface of adsorbent (Dutta, 2009; Suzuki, 1990). The main advantage of physisorption is that it requires lower energy to separate the gas molecules from the adsorbent (Dutta, 2009). Examples of adsorbents used in physical adsorption include activated carbon and zeolites.

Chemisorption process is also chemical adsorption. Where binding between the solid adsorbent and adsorbate is strong chemical bond (Dutta, 2009). Chemisorption requires high energy to regenerate adsorbent as compared to physisorption (Dutta, 2009). The increased energy required to release gas from adsorbent contributes to energy costs. Table 2.3 provides some of the difference between chemical and physical adsorption.

Table 2.3: comparison of physisorption and chemisorption (Dutta, 2009; Keller & Staudt, 2005; Lowell & Shields, 1998)

Physical adsorption	**Chemical adsorption**
Small heat of adsorption	Large heat of adsorption
Usually occurs at low temperature and adsorption decreases with increase in temperature	Occurs at high temperature and adsorption increases with increase in temperature
Caused by intermolecular forces	Caused by chemical bond
Results in multimolecular layer	Results in unimolecular layer.
Reversible	Irreversible
Fast kinetics	Slow kinetics

Adsorption Isotherms

When an adsorbent comes in contact with adsorbate, adsorption process occurs, after some time equilibrium will be established between amount of adsorbate adsorbed and amount of adsorbate remaining (not adsorbed). The relationship that occurs in equilibrium is described by adsorption isotherms. Equilibrium is usually described in terms of partial pressure (gas) or concentration (liquid) and amount adsorbed (Donohue & Aranovich, 1998). Therefore adsorption isotherm is a graph that represents the relationship between the amounts of adsorbate adsorbed on the surface of adsorbent with changing pressure at constant temperature. Adsorption isotherms are significant because they are used to calculate the specific surface area and pore size of adsorbents.

There are different types of adsorption isotherms and there are 6 main adsorption isotherms (type I to type VI). Figure 2.11 depicts an illustration of these adsorption isotherms. Type I isotherms also known as Langmuir isotherm is representative of micro-porous adsorbents (Balbuena & Gubbins, 1993; Donohue & Aranovich, 1998). Type II and type III isotherms are representative for non-porous adsorbents with weak and strong adsorbate-adsorbent attractive forces respectively (Balbuena & Gubbins, 1993; Donohue & Aranovich, 1998). Type VI and V isotherms is representative of meso-porous adsorbents with strong and weak adsorbate-adsorbent attractive forces respectively (Balbuena & Gubbins, 1993). Type V is generated when adsorbate condenses in mesopores of solid adsorbents. Type VI is a rare isotherm which is generated for strong adsorbate-adsorbent attractive forces, it occurs usually when the temperature of the adsorbate (gas) is close to melting point (Balbuena & Gubbins, 1993).

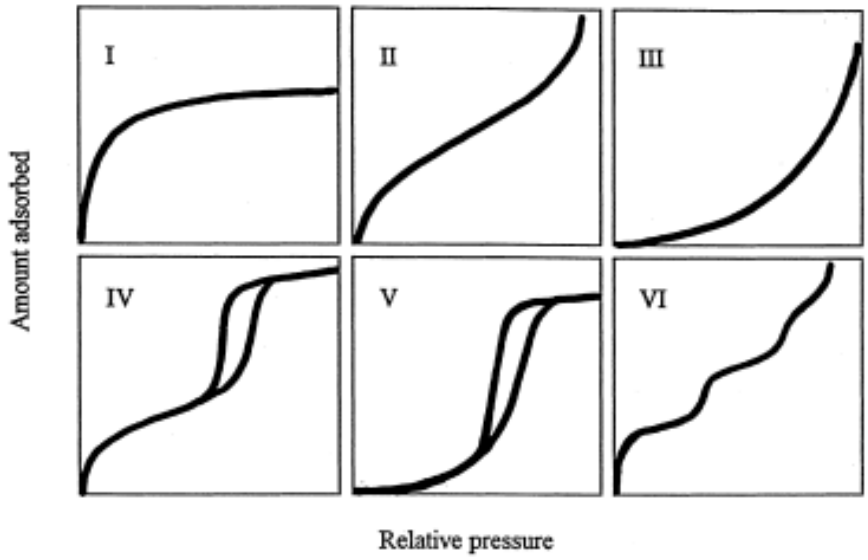

Figure 2.11: Classification of adsorption isotherms (Taken from Donohue & Aranovich, 1998)

Adsorption Mechanism

Adsorption process occurs due to the presence of unbalanced forces on the surface of the adsorbent. These unbalanced forces have a tendency to attract and adsorb molecules that come in contact with the adsorbent surface. This is explained by attractive forces that exist between the adsorbent and the molecules they adsorb (adsorbate). Figure 2.12 illustrates a clear demonstration of the adsorption mechanism of CO_2 from flue gas. As depicted by

Figure 2.12, a flue gas stream is passed through an adsorbent. The adsorbent attracts and adsorbs CO_2 molecules while other gas molecules pass. After CO_2 molecules are adsorbed, the adsorbent is subjected to either pressure change or temperature change in order to desorb CO_2 and regenerate the adsorbent so it is recycled.

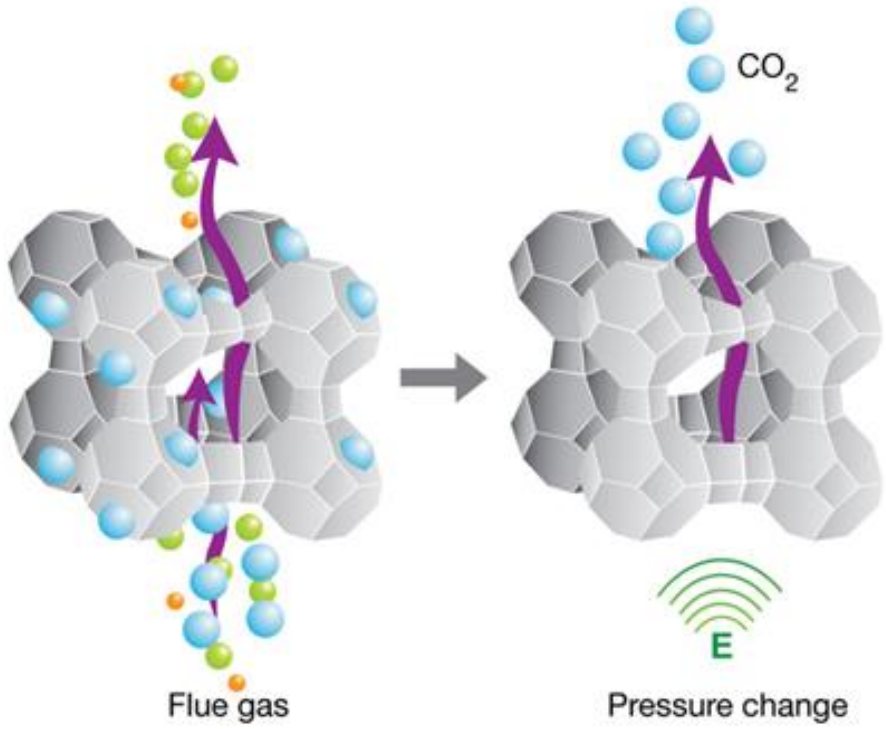

Figure 2.12: Adsorption Mechanism of carbon dioxide (taken from CO2CR2, 2015)

When adsorbent is regenerated by changes in temperature, the process is known as temperature swing adsorption (TSA). The column is usually heated by hot gas such as nitrogen in order to remove impurities from the adsorbent (Tlili *et al*, 2009). TSA is an attractive adsorption mechanism because it is potentially less energy intensive due to the moderate heat of adsorption, there is no volatility of solid adsorbents and moderate temperature of regeneration is required (Joss *et al*, 2017). Figure 2.13 depicts a diagram of the overview of how TSA works.

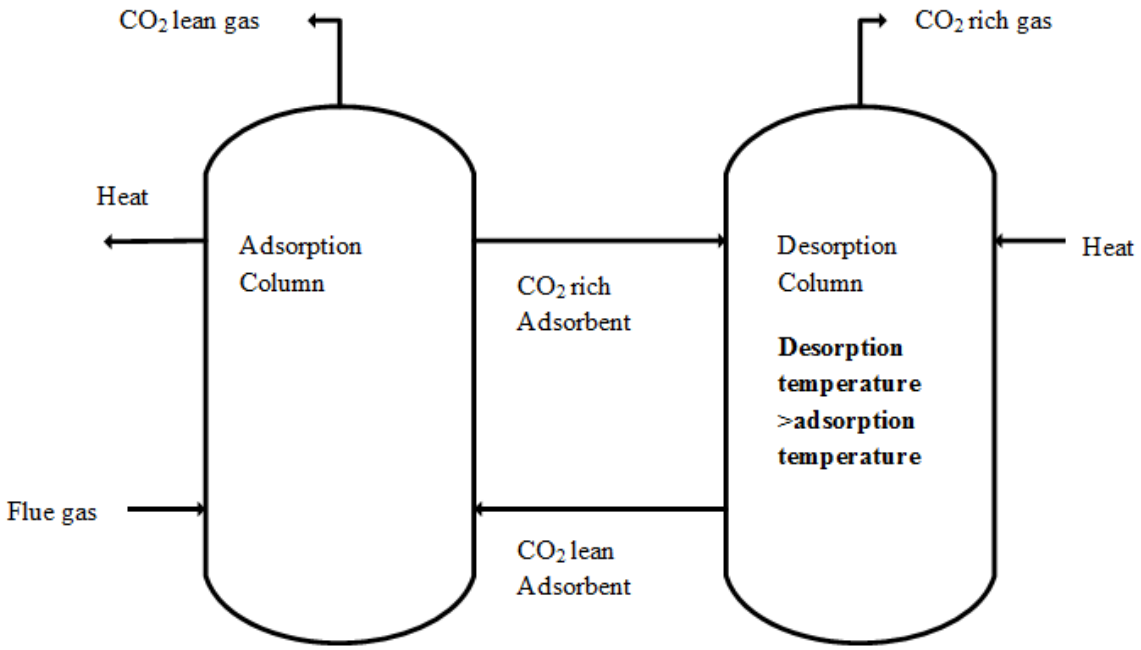

Figure 2.13: Overview of TSA process

When adsorbent is regenerated through change in pressure, the process is called pressure swing adsorption (PSA). PSA is a cyclic process where adsorption is carried out in relatively high pressures while desorption occurs at lower pressure (Gomes & Yee, 2002). When PSA is used adsorption is done at pressures higher than atmospheric (Tlili *et al*, 2009). The major advantage of PSA is the absence of high energy associated with regeneration stage (Riboldi & Bolland, 2015). Several studies have been done on CO_2 capture using PSA (Gomes & Yee, 2002; Tlili *et al*, 2009; Riboldi & Bolland, 2015). Figure 2.14 depicts a diagram of the overview of how PSA works

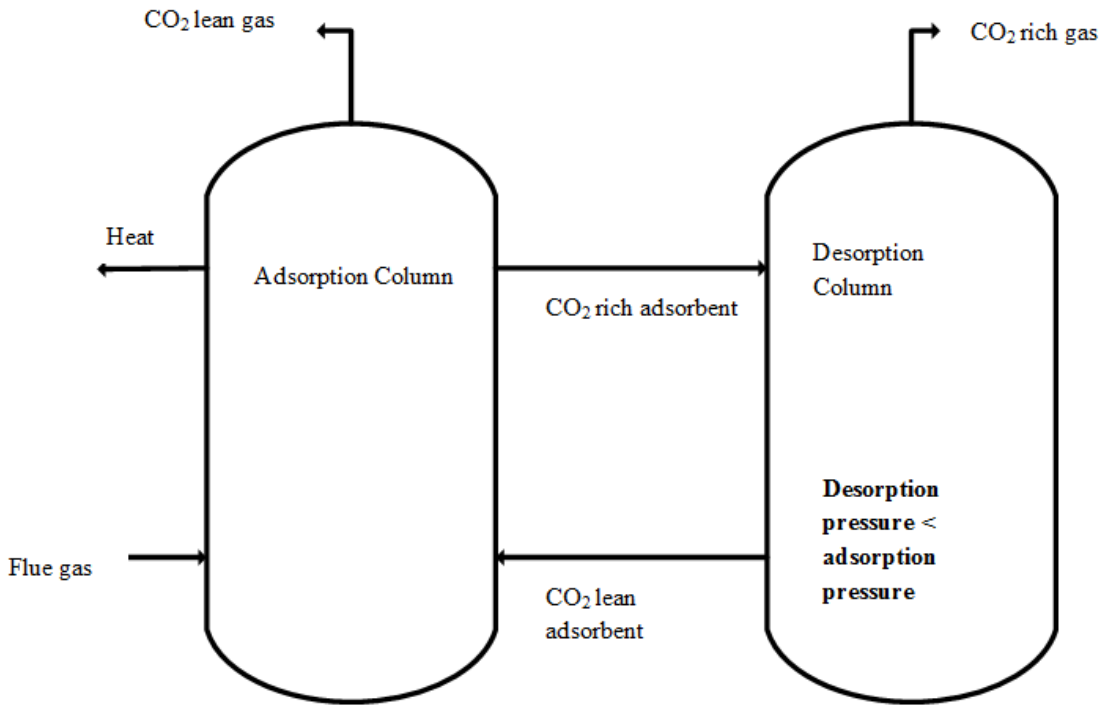

Figure 2.14: Overview of PSA process

The desorbed CO_2 by TSA, PSA or other desorption methods can be utilized in other processes that require CO_2 or stored in ways that will not affect the environment. The adsorbent is regenerated and used again to capture more CO_2. The process of adsorption and desorption continues for a number of cycles depending on the type of adsorbent. Figure 2.15 depicts process flow diagram of adsorption and desorption by either TSA or PSA.

Modes of adsorption operation

Adsorption can be operated in either a batch flow or continuous flow system. In a batch flow system the quantity of adsorbent is mixed with specific amount of mixture containing the adsorbate. Mixing is continued until the adsorbate in the mixture is reduced to a desired level. The adsorbent is then removed and either discarded or regenerated. Batch flow systems are usually used for small volume of adsorbate.

In Continuous adsorption operation there is continuous contact between adsorbate and adsorbent. There are three types of continuous adsorption systems which are fixed/packed-bed, moving bed and fluidized bed. This study investigates adsorption using a fixed/packed-bed adsorption system. In a fixed/packed-bed adsorption column, adsorbent is loaded inside

the column and the gas mixture containing CO_2 enters the column at bottom. As the gas moves through the column it gets adsorbed. After adsorption is complete the saturated adsorbent is then passed to a regeneration column where CO_2 is separated from the adsorbent using either temperature or pressure changes as discussed. Figure 2.15 depicts a schematic diagram of a fixed/packed-bed adsorption system.

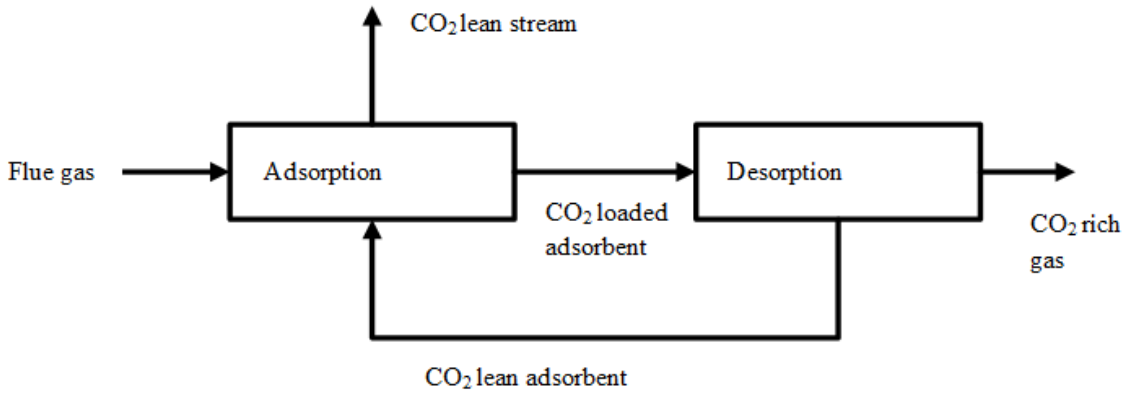

Figure 2.15: Overview of fixed/packed-bed adsorption system (Adapted from Rashidi & Yusup, 2016)

Adsorbents materials

Adsorbents are materials used to adsorb or capture other substance from a mixture. There are important factors for solid adsorbents used in the adsorption process should have so adsorption can be effective.

Selectivity is a very important characteristic and property. Adsorbents should be designed in a way that it is selective to adsorbate of interest from mixtures. A selective adsorbent allows its pores to be filled with adsorbate of interest, which is then released for adsorbent to be reused. Selectivity of the adsorbent could be governed by the difference in affinity, rate of diffusion and particle size. These may determine the selectivity of the adsorbent individually or collectively (Dutta, 2009).

Where selectivity is governed by rate of diffusion; different component in the mixture are likely to diffuse into the pallet of the adsorbent at different rates and this gives rise to selectivity for gas molecules that diffuse faster to be adsorbed quickly (Dutta, 2009). This kind of selectivity is also called kinetic selectivity (Dutta, 2009).

Selectivity can also be governed by molecule size and shape of different components in the mixture as this may vary (Dutta, 2009). Hence molecules that have molecular size greater than the pore size of the adsorbent will not be able to enter the pores of the adsorbent (Dutta, 2009). Only molecules that have a molecular size smaller than the pore size of the adsorbent will enter the pores (Dutta, 2009).

Other factors include adsorption capacity, amount of energy required to regenerate the adsorbent. Adsorbent should be designed in a way to minimize the energy required for regeneration. Particle size, porosity, structural strength and stability are also factors to be considered for a good adsorbent (Dutta, 2009). A good adsorbent must be highly porous and have a narrow particle distribution (Dutta, 2009). Good adsorbent should have large number of adsorption sites that the adsorbate can bind in which is achieved by high surface area of adsorbent. High surface area made possible by designing small particles of adsorbents (Dutta, 2009).

Adsorbents commonly used for CO_2 capture

Adsorption process provides an alternative to CO_2 capture over the above aforementioned methods. This is because adsorption method for gas removal is less energy intensive, process has the ability to operate at low to moderate temperature and pressure. Most importantly, adsorption process is more economic due to versatility of adsorbents (Ackley *et al*, 2003).

An effective CO_2 adsorbent is one that has cheap raw materials, fast kinetics, high CO_2 adsorption capacity, high selectivity towards CO_2, low heat capacity and has thermal as well as mechanical stability (Yu *et al*, 2012). A lot of adsorbents have been proposed and investigated for CO_2 capture. The most common of these adsorbents are discussed.

Zeolites

Zeolites, three dimensional materials, are crystalline aluminosilicates structures which are porous (Lee & park, 2015). Mostly due to presence of aluminium in the silicate structure, CO2 can be adsorbed by zeolites. Zeolite materials can be natural or synthetic. Synthetic zeolites are synthesized by hydrothermal reaction in an autoclave (Lee & Park, 2015). Examples of synthetic zeolites that are commercially used are type A and type X zeolites (Suzuki, 1990).This material consists of metal ions such as Li, Na and Al that are surrounded by four oxygens in tetrahedron geometry (Lee & Park, 2015). These metal ions influence the heat of adsorption (Lee & park, 2015). The shape and size of zeolites can be tuned to specific dimensions that allow selective passage of different gases. The tuning of the shape and size of

zeolites depends on the atoms and structures used for the material (Carbon Capture: Beyond 2020, 2010). There are number of different zeolites that vary with chemical and physical properties. Properties such as molecular pore size, strength, selectivity and cation are not the same for different zeolites (Lenntech, 2015). Zeolites are currently the largest class of commercially available adsorbents.

There three main applications of zeolites in industry. These applications include catalysis, ion exchange and gas separation (Lenntech, 2015). In catalysis, zeolites are used as catalysts for several reactions. An important example is isomerization, cracking and hydrocarbon synthesis. Hydrated cations within zeolite pores are loosely bounded to zeolite framework. These cations can be exchanged with other cations in aqueous media. An example of this application is where zeolite-like metal organic framework is ion exchanged with alkali metals.

Due to their ability to adsorb polar compounds, zeolites have long been considered as best candidates for separation and purification of gases (Ackley *et al*, 2003). Here the porous structure of zeolites is used to sieve molecules according and size. Molecules of particular size are allowed to enter the pores of the zeolite.

Zeolites are one of the most widely investigated adsorbents for CO_2 capture. Hefti *et al* (2015) investigated zeolites 13X and ZSM-5 for Adsorption equilibrium of binary mixtures of carbon dioxide and nitrogen. The aforementioned authors first investigated single component adsorption isotherms of CO_2 and N_2 over a range of temperatures from 25 ℃ to 140℃. Hefti *et al* (2015) then investigated binary adsorption equilibrium measurements at temperatures of 25℃ and 45℃ on both zeolite 13X and ZSM-5. The measured equilibrium was compared with predictions by adsorption models and application of ideal adsorbed solution theory and real adsorbed solution theory for non-ideal behaviour (Hefti *et al*., 2015). This work was limited in the description and interpretation of the behaviour of adsorption on the aforementioned zeolites. The authors found that zeolite ZSM-5 behaves close to ideal over the entire temperature and pressure investigated, while zeolite 13X demonstrated non-ideal behaviour with increased pressure which motivated the use of real adsorbed solution theory to describe the binary mixture adsorption data (Hefti *et al*., 2015).

The disadvantages of using zeolites as adsorbents for CO_2 capture are that the CO_2 adsorption capacity and CO_2/N_2 selectivity are very low. Another drawback of zeolites is that in the presence of moisture CO_2 adsorption capacity declines because of the hydrophilic nature of

zeolites. This then results in high regeneration temperatures thus large energy required (Yu *et al*, 2012). A major disadvantage is that the design and tunability of zeolites restricts the aforementioned zeolite to a particular pore size which results to less molecule application (Eddaoudi *et al*, 2014).

Silica materials

Pure silica is naturally a material that is inactively non-polar, however once it has a hydroxyl functional group its surface becomes polar and hydrophilic (Suziki, 1990). In literature, work has been reported on synthesis and modification of silica materials for CO_2 capture. In most studies, silica supports are incorporated with amine functional groups or metal nanoparticles in order to enhance CO_2 adsorption capacity (Lee & park, 2014). Silica materials are cheap, have large micro and meso pores and can CO_2 adsorption can be done at medium of low temperature and pressure (Lee & Park, 2014). However in spite this advantages, silica materials adsorb moisture easily which results in poor performance for CO_2 adsorption. Another drawback is that this material requires high energy during desorption (Lee & Park, 2014).

Xu *et al* (2002) reported on Polyethylenimine-modified mesoporous molecular Sieve of MCM-41 (MCM-41-PEI) by loading PEI onto MCM-41 as silica adsorbent for CO_2 capture.CO_2 adsorption-desorption runs were measured in a flow system using a microbalance that measures weight change. MCM-41-PEI had an adsorption capacity of 215 mg CO_2 / PEI at 348 K and 1 bar which were 24 times that of MCM-41 and 2 times that of PEI alone (Xu *et al*, 2002). Adsorbent could adsorb CO_2 at very low concentrations and was found to be stable when cyclic operations were conducted (Xu *et al*, 2002).

Hung *et al* (2017) investigated CO_2 capture using polyamine-immobilized mesostructured silica. The authors investigated the role of amine modification and the existence of poly (ethylene oxide) surfactant molecules on surface properties of mesoporous silica on CO_2 uptake using 2 dimensional heteronuclear correlations (HETCOR) solid-state NMR technique. The investigated silica materials showed a CO_2 adsorption uptake of 4.43 mmol CO_2/ g adsorbent (Hung *et al*., 2017).

Activated carbon

This is a non-graphite form of carbon from natural raw materials such as wood, saw dust, nut shell, coal and lignite (Dutta, 2009; Suzuki, 1990). In order to produce activated carbon, the

aforementioned raw materials are mixed with alkali metals and heated at temperatures of 500-900 ℃ (Dutta, 2009). The product is washed, filtered and dried (Dutta, 2009).

This adsorbent is widely used to purify gases, remove impurities from drinking water and also absorbs poisons from digestive systems in medical application (Carbon Capture: Beyond 2020, 2010). Commercially available activated carbons are produced in two forms; powder form or granular form (Dutta, 2009; Suzuki, 1990).

Activated carbon is suitable post-combustion capture due to their properties such as low cost, wide availability, high porosity, high thermal stability, low sensitivity to moisture and stability in adsorption-desorption cycles (Yu *et al*, 2014, Rashidi & Yusup, 2016). Activated carbon is considered more superior for post-combustion capture than zeolites because of its hydrophobic property that prevents an additional step of moisture removal prior to CO_2 adsorption (Rashidi & Yusup, 2016). Activated carbon are physical adsorbents and have weak interaction with CO_2, thus they have a lower heat of adsorption compared to zeolites (Rashidi & Yusup, 2016; Montagnaro *et al.,* 2015)

Montagnaro *et al* (2015) investigated post-combustion CO_2 capture on two commercial activated carbons which are filtrasorb 400 (F600–900) and nuchar RGC 30 (RGC30). The aforementioned activated carbons were studied at temperatures 303, 323 and 353 K. Montagnaro *et al* (2015) carried equilibrium and kinetic CO_2 adsorption tests in fixed bed apparatuses on filtrasorb 400 and nuchar RGC 30 at different temperatures and CO_2 inlet concentrations in order to provide insights on the role played by microstructure features of activated carbon on CO_2 adsorption capacity. F600–900 exhibited high CO_2 adsorption capacity under typical flue gas conditions which the authors explained by narrower pore size distribution.

Sexenaa *et al* (2014) investigated activated carbon as adsorbents for CO_2 capture and results showed that activated carbon has potential to be used for capturing CO_2. In spite of its advantages, there are several drawbacks associated with using activated carbon to capture carbon dioxide. The major drawback is that activated carbon is negatively affected by NO_X, SO_X and H_2O. This is a major disadvantage because the flue gas produced from post-combustion contains these compounds. Other disadvantages are low CO_2 adsorption capacity at mild conditions and wide variety of raw materials (Spigarelli & Kawatra, 2013).

Metal Organic Frameworks (MOFs)

MOFs are organic-inorganic porous solids that contain metal ions linked to organic ligands which assembles together to form an extended framework through coordination bonds. According to Rowsell and Yaghi (2004), a porous solid is called a metal organic structure when it displays a geometrically well-defined structure, strong bonding that provides robustness, linking units that are available for modification by organic synthesis. The solid should be highly crystalline as this allows precise structural characterization by diffraction methods (Rowsell & Yaghi, 2004). MOFs are advantageous over the aforementioned adsorbents due to higher large surface area, Regular pore distribution, pore size can be enlarged by increasing the size of linker while keeping the same structure type and finally; properties of MOFs can be modified by the possibility of modifying the linker with various organic groups while keeping the same structure (Devic & Serre, 2009).

MOFs synthesis

Synthesis of various MOFs

They are several methods that have been investigated for MOFs synthesis. These methods include hydrothermal, electrochemical, solvent free, ionothermal, solvothermal and microwave synthesis. The standard method for synthesizing of MOFs is the solvothermal reaction starting from metal precursor and organic ligand at temperatures between room temperatures and 400 degrees. This is better illustrated by the Equation 2.2

Metal precursor + organic linker = metal organic framework **(2.2)**

Metal source can be a metal salt such as halide, nitrate or hydroxide. Also metal source can also be metal which is further oxidized during reaction by adding oxidizing agents such as ad nitric acid or perchloric acid in reaction vessel. In this case the inorganic subunit will form in original place during the course of the reaction.

Reactants are mixed in high boiling polar solvents such as water, amides and alcohol. Water is usually the solvent of choice but amides, alcohols or their mixture is commonly used (Devic & Serre, 2009). Products produced are either one, two or three dimensional metal organic structures. The metal organic structure needs to be filtered and dried from this wet process. This needs to be done carefully because, due to high surface areas and porosity of MOFs, they may easily carry 50 to 150 weight percent of the occluded solvent (Czaja *et al*,

2009). It is therefore advisable to first remove the adsorbed solvent under gentle conditions in terms of temperature and pressure before high thermal activation (Czaja *et al*, 2009). Synthesis of MOFs is affected by many important parameters including temperature, concentration of metal salt and organic ligand, the extent of solubility of reactants on solvent as well as the PH of the solution.

Structure of MOFs and characterization

Structure of MOFs

MOFs are both crystalline and highly porous materials. Choice of building blocks (metal and organic linker) determines the structure and properties of MOFs. Figure 2.16 depicts a structural picture of MOF. As can be seen in Figure 2.16, the structural picture of MOF where the structure contains metal centres as well as organic linkers.

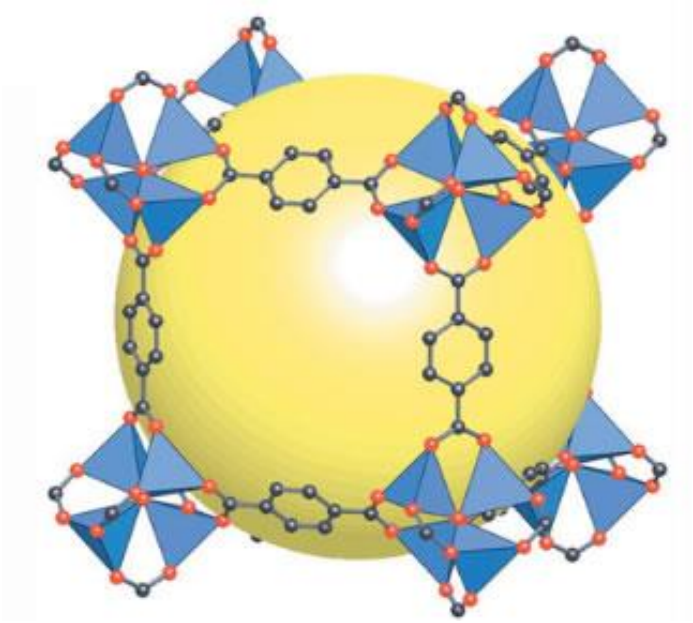

Figure 2.16: Overview of metal organic framework (taken from University of Crete, 2001)

Characterization of MOFs

After synthesis, MOFs are characterized in order to identify their different properties such as textual properties, the morphology, surface chemistry, pore volume, pore size and surface area. Different techniques are used for different properties. These techniques are summarized below include X-Ray diffraction (XRD), Scanning electron microscope (SEM), Thermal gravimetric analysis (TGA), Fourier Transform Infrared spectrum (FTIR) and Brunauer-Emmett-Teller method (BET).

XRD is one of the most important tools used in solid state chemistry characterization. This characterization technique is used for two main purposes; for determination of textual properties and also for determination of whether powder is crystalline or amorphous. XRD is based on the constructive interference of monochromatic x-rays and the crystalline sample (Practical Analytical, 2015).

TGA provides thermal stability of sample by measuring the change in chemical and physical properties of materials. It measures this as a function of increasing temperature or as a function of weight or time. TGA also measures thermal decomposition patterns.

FTIR Identifies unknown materials in the sample and determines the amount of components in a mixture

BET is a standard method of determining surface area of materials from standard nitrogen adsorption isotherms. The surface area of the material is determined by the physical adsorption of the nitrogen gas on the surface of the solid.

Applications of MOFs in CO_2 capture

MOFs can be applied in many different areas. A few of these areas include gas purification, gas storage, and catalysis and gas separation. In this study MOFs are applied for gas separation.

In gas separation the gas mixture usually contains components having concentrations in the same order of magnitude. Currently industrial technologies for gas separation are cryogenic, membrane, absorption and adsorption techniques. Absorption using monoethanolamine is the commonly used method in industry, however this process possess drawback with the major one being that regeneration of solvent is quite expensive as explained in previous sections. Adsorption using porous materials such as activated carbon, zeolites, carbon nanotubes, silica

gel, molecular sieves and MOFs is a promising alternative (Kupple *et al.*, 2009). These materials are chosen based on adsorption capacity of adsorbent as well as selectivity of the material to adsorbate than the aforementioned materials (Kupple *et al.*, 2009). MOFs are very promising for gas separation because of their large surface area, adjustable pore sizes, open metal sites and less energy for regeneration (Chen *et al.*, 2011). One example of MOFs application in gas separation is carbon dioxide separation from gases such as hydrogen, nitrogen and methane by adsorption where MOFs are considered as CO_2 adsorbents. There are a number of different MOFs that have been investigated for capturing CO_2. The next Section below discusses some of the types of MOFs that have been applied for gas separation in CO_2 capture.

MOFs for CO_2 capture

Since the discovery of MOFs, researchers have synthesized various types of MOFs for the purpose of capturing CO_2. This includes fluorinated metal organic frameworks (F-MOFs), MOF-505 and HKUST-1 MOF, Mg-based MOF-74 and ZMOFs (Lee & Park, 2017). Other MOFs for Carbon dioxide capture are amino functionalized metal organic framework, light weight metal organic framework and nitrogen containing metal organic framework. According to Saha *et al* (2012) F-MOFs are synthesized using perfluorinated polycarboxylate ligands with porous surface and exposed to fluorine atoms for carbon capacity storage.

Saha *et al* (2012) investigated all the aforementioned MOFs and found that they can physically adsorb CO_2 at ambient temperatures and pressure. The CO_2 adsorbed by these MOFs can be removed at room temperatures and materials can be reused as an adsorbent again. The drawback of the aforementioned materials is that the CO_2 loading capacity is not very high and considerable efforts must be made for better carbon dioxide storage (Saha *et al*, 2012).

Millward & Yaghi (2005) reported on MOFs with exceptionally high capacity for CO_2 storage at room temperature. Table 2.4 depicts the nine MOFs with their surface areas reported by Millward & Yaghi (2005). The MOFs reported by Millward & Yaghi (2005) have exceptionally high surface area. MOF-177 was reported to have a CO_2 adsorption capacity of 33.5 mmol CO_2 / g adsorbent at room temperature and 35 bars which is much greater than adsorption capacity to that of zeolite 13X (Millward & Yaghi, 2005).

Table 2.4: MOFs examined for CO_2 storage capacity (Millward & Yaghi, 2005)

Type of MOF	Surface area (m^2/g)
MOF-2	345
IRMOF-11	2096
MOF-505	1547
IRMOF-3	2160
MOF-74	816
IRMOF-6	2516
$CU_3(BTC)_2$	1781
IRMOF-1	2833

Llewellyn *et al* (2008) reported on the CO_2 uptake of Metals Organic Frameworks MIL-100 and MIL-101. The maximum CO_2 loading of MIL-100 and MIL-101 obtained by Llewellyn *et al* (2008) was 18 and 40 mmol CO_2 / g adsorbent respectively at a temperature of 304 K and a pressure of 5 Mpa.

Bao *et al* (2011) reported on a magnesium-based metal organic framework, also known as Mg-based MOF-74 for CO_2 capture. A volumetric adsorption unit was used to measure the CO_2 adsorption equilibra and kinetics on Mg-based MOF (Boa *et al*., 2011). Mg-based MOF-74 synthesized by Boa *et al* (2011) had a surface area of 1174 m^2/g and CO_2 adsorption capacity of 8.61 mmol CO_2/g adsorbent at 298 K and 1 bar. The CO_2 adsorption capacity of Mg-based MOF-74 was significantly high compared to that of zeolite 13X under the same operating conditions.

Zeolite metal organic framework (ZMOFs)

ZMOFs are a unique subset of MOFs with zeolite like framework topologies impressive properties like tunability and rational design for a number of applications (Eddaoudi *et al.,* 2007). According to Chen *et al* (2011), the main difference is that in ZMOFs, organic linkers replace oxygen and metal ions replace tetrahedral coordinated Si or Al atoms found in zeolites. ZMOFs are negatively charged frameworks and because of this allows for tuning of pore through extra-framework cations exchange. Thus ZMOFs have the potential to be tuned and enhance host (interaction with specific guest molecules) (Al-Maythalony *et al*, 2014). ZMOFs can be mesoporous, however unlike mesoporous silica they exhibit crystalline framework (Devic & Serre, 2009). ZMOFs exhibit distinctive properties including: accessible

extra-large cavities, exceptional chemical stability and potential to be applied in many fields (Al-Maythalony *et al*, 2014). There is a diverse nature of ZMOFs due to the conditions of synthesis as well as what is known as structure directing agents (SDA) which is basically a template. Different types of ZMOF are produced depending of the type of SDA used. Examples of this include SOD-ZMOF and rho-ZMOF where SOD and rho refers to the topology of the ZMOF.

Synthesis of ZMOFs

The easiest way to describe the synthesis of ZMOF is a solvothermal reaction given by:

Indium nitrate hydrate + 4, 5- Imidazoledicarboxylic acid = ZMOF **(2.3)**

The two reactants in equation 2.2 are mixed with a SDA in order to yield a type of ZMOF. The SDA used to yield SOD-ZMOF is imidazole and 1, 3, 4, 6, 7, 8-hexahydro-2H-pyrimidine [1, 2-α] pyrimidine (HPP) yields rho-ZMOF. In Figure 2.17, different SDAs were added to reaction 2 to yield different ZMOFs with different templates. SOD-ZMOF has a diameter of approximately 9.6 angstroms ($\dot{A}$) (Eddaoudi *et al*, 2014). This diameter is large enough to allow CO_2 molecules with a diameter of 3.3$\dot{A}$ to penetrate (Eddaoudi *et al*, 2014).

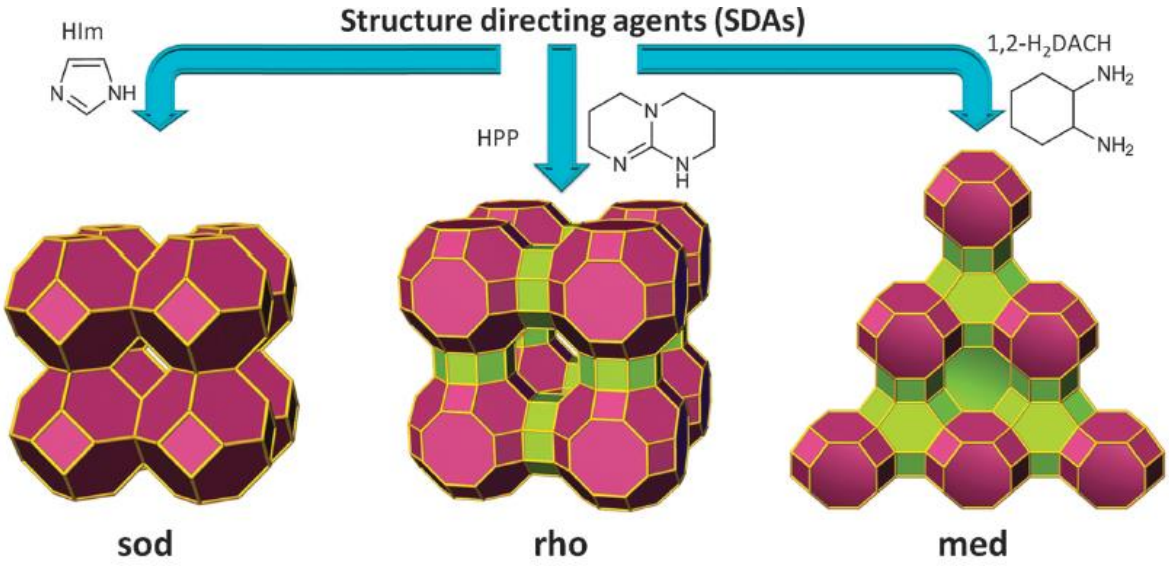

Figure 2.17: Formation of different ZMOFs due to the use of different SDA's

Carbon dioxide capture by Zeolite like metal organic frameworks (ZMOFs)

Chen *et al* (2011) investigated ZMOFs, rho-ZMOF and SOD-ZMOFs as CO_2 adsorbents. They investigated the effect of ion exchange on SOD-ZMOFs adsorption capacity. SOD-ZMOF was ion exchanged with group 1 metals (Li^+, Cs^+, Na^+, and K^+) cations. SOD-ZMOF showed no significant changes in textual properties after ion exchange (table 2.5). The carbon dioxide adsorption capacity of SOD-ZMOF was compared to that of most commonly investigated material ZIF (ZIF-8) and the CO_2 adsorption capacity of ZIF-8 was far less compared (30mg/g adsorbent) to SOD-ZMOF (53mg/g adsorbent). Although the surface area of SOD-ZMOF was smaller than that of ZIF-8 (table 2.5), the former has a much superior adsorption capacity. All ion exchanged alkali cations exhibited improved CO_2 adsorption capacity than the prepared sample without ion exchange alkali metals. The K^+-SOD ZMOF exhibited the highest CO_2 capacity which was 15% higher than the as prepared SOD-ZMOF followed by Na^+ and then Li^+ (Chen *et al*, 2011).

Table 2.5: Textual properties of ZMOFs (adapted from Chen *et al* (2011))

Sample	Surface area (m^2/g)	Volume of pore (cm^3/g)
Li^+ ion-exchanged SOD-ZMOF	345	0.16
K^+ ion-exchanged SOD-ZMOF	363	0.16
Na^+ ion-exchanged SOD-ZMOF	373	0.17
SOD-ZMOF	375	0.16
Rho-ZMOF	816	0.34
ZIF-8	1450	0.5

Composite MOFs for CO_2 capture

In order to improve adsorption capacity and selectivity, adsorbents are chemically modified on the surface of solid. As mentioned in the previous section, MOFs are very promising adsorbents due to their unique chemical and physical properties. Their properties can be further improved or enhanced by various means. This includes grafting, change in organic

linkers, ion exchange and impregnation of suitable active material (Imteaz & Sung, 2014). Imteaz and Sung (2014) defines composite adsorbents as porous materials with multiple phases which have at least one continuous phase. MOFs composites have large improvements in synthesis kinetics, morphology, stability, physiochemical properties and potential applications (Imteaz & Sung, 2014). MOFs composites have been receiving attention due to various applications including CO_2 adsorption.

- **Ionic liquid based adsorbents**

Ionic liquids (IL) are environmentally friendly solvents which exhibits great potential for CO_2 capture (Dai *et al*, 2015). IL have great potential for CO_2 capture due to their many unique advantages such as high thermal stability, strong soluble capacity for CO_2, non-flammable, high CO_2 solubility, non-volatile, negligible vapour pressure and wide liquid range. Aki *et al* (2007) found that CO_2 solubility is affected by type of anion and various alkyl in the cation, but solubility is strongly influenced by anion (Gupta *et al*., 2012). Muldoon *et al.* (2007) expanded the investigation and found that IL containing fluoroalkayl chain as either cation or anion have improved CO_2 solubility compared to less fluorinated IL (Gupta et al, 2012). IL investigated for CO_2 capture are room temperature ionic liquids (RTIL), task specific ionic liquid (TSIL) and supported ionic liquid (SIL) (Dai *et al*., 2015).

In SIL, IL impregnate the pores of porous supports (adsorbents). The two most concerns when it comes to the use of IL are cost and viscosity. SIL reduce the cost and viscosity of IL used because the amount of IL is less compared to RTIL and TSIL. This provides an important economic benefit for the application of SIL.

For SIL, IL can be supported by different types of porous materials. Since the discovery of SIL for CO_2 capture; a lot of experimental and theoretical work has been done on different IL supported by various types of porous materials.

Simulation studies have been done to establish the potential of ionic liquid impregnated MOFs for CO_2 capture. Molecular and atomistic simulations were done by Chen *et al.* (2011) and Gupta *et al.* (2012) to investigate CO_2 capture on MOF supported IL adsorbents. Both authors used IRMOF-1 as support but they used different types of IL. Results of this studies showed that the anion MOF supported IL adsorbents selectively adsorbs CO_2 from a N_2/CO_2 mixture, the selectively of the composite adsorbent is generally higher and might be potentially useful for CO_2 capture (Chen *et al*, 2011). Atomistic simulation was done to

investigate CO_2 capture in IL supported by MOFs (ZIF-71 and Na-rho-ZMOF) in order to investigate how hydrophobic and hydrophilic framework can affect CO_2 adsorption capacity. Gupta *et al.* (2013) observed that at a particular pressure CO_2 was more adsorbed than N_2 in both membranes.

IL based adsorbents are very good for CO_2 capture. In spite all the advantages associated with ionic liquids, their major disadvantage is that they are very expensive. So far, from most literature only simulation work has been done in investigating MOF supported IL for CO_2 capture. Experimental work still needs to be done so as to validate the simulation work.

- **Amines based adsorbents**

Amine based adsorbents solids that are chemically modified by adding amine to the solid support. These adsorbents have been widely studied and they exhibit an advantage due to high CO_2 adsorption capacity. This is based on the fact that CO_2 is acidic and amine is basic, so the two reacts with one another. Other advantages of amine based adsorbents include high rate of adsorption and desorption, high ability to tolerate moisture and high selectivity for CO_2 in a mixture of gases (Yu *et al,* 2012). According to the type of amine and solid support, amine based adsorbents can be categorized as amine impregnated or amine grafted adsorbents (Yu *et al*, 2012).

Chitsiga *et al* (2015) reported synthesis and performance evaluation of amine grafted poly-succinimide (PSI) adsorbent referred to as polyaspartamide (PAA) for post-combustion CO_2 capture. The authors investigated the effect of grafting water soluble amines on PSI. TGA was used to measure the adsorption capacity of the synthesized adsorbent. Grafting water soluble amine on PSI resulted in an increase in adsorption capacity. PAA showed a highest adsorption capacity of 44 mg CO_2/ g adsorbent at 40℃ and 1 bar.

Chen *et al* (2013) did an experimental investigation on SOD-ZMOF grafted with ethylenediamine (ED) for CO_2 capture. The authors' grafted SOD-ZMOF with ED. Chen *et al* (2013) characterized SOD-ZMOF before and after amine grafting using XRD, FTIR, elemental analysis and BET. The surface area and pore volume of the grafted SOD-ZMOF decreased from 375 m^2/g to 347 m^2/g and 0.16 cm^3/g to 014 cm^3/g respectively. This showed that the grafting of ED was successful. Grafting SOD-ZMOF with ED resulted in a 30% increase in adsorption capacity. The work done by Chen *et al* (2013) also showed high CO_2

selectivity with nitrogen (N_2) and the grafted SOD-ZMOF showed outstanding stability of CO_2 adsorption desorption measurements than the original SOD-ZMOF (Chen *et al.*, 2013).

Amines based adsorbents are strong potential for CO_2 capture due to the acid-base interaction between the weak acidic CO_2 gas and weak basic amines. However amine based adsorbents have drawbacks such as high cost and the environmental impact associated with synthetic amines; making it challenging for this adsorbents to commercialize (Liu *et al.*, 2013). This calls for an alternative material that has strong affinity for CO_2 but which is also less expensive and has less impact on the environment. This work proposes the use of a material called chitosan to replace synthetic liquid amines.

- **Chitosan based adsorbents**

Ma *et al.* (2015) defined chitosan defined as a natural occurring bio-compatible, bio-degradable, bio-renewable and non-toxic co-polymer composed of glucosamine and acetyl glucosamine. This polymer is derived from chitin which is the second most plentiful natural polysaccharide (Shukla *et al.*, 2013). Chitin which is a biopolymer produced by many different living organisms (Rinaudo, 2006). It produced from sources from nature such as insects, shellfish, crabs, fungi, arthropods and crustacean shells (Rinaudo, 2006). Naturally chitin occurs as three types (α, β *and* $\gamma - structures$). The third type ($\gamma - chitin$) seems to just be a combination of the $\alpha -$ structure and $\beta -$structure rather than a third allomorph. $\alpha -$chitin is the most abundant and it is found in walls of yeast and fungal cells, shrimp cells, crab tendons and cells as well as insect cuticle. $\beta -$chitin is rare and is found in association with proteins in squid pens (Rinaudo, 2006). The structure of chitin illustrated in Figure 2.18 is compact and this disallows it to be soluble in most solvents. Therefore there is a need for chitin to be transformed into chitosan (Rinaudo, 2006).

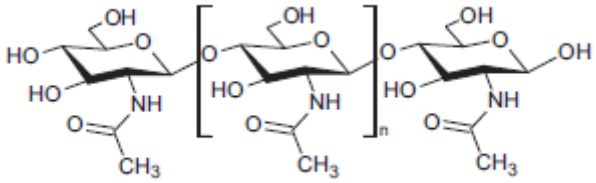

Figure 2.18: Structure of chitin (Taken from Shukla *et al*, 2013)

Chitosans are advantageous due to the fact that they are produced from plentiful renewable resource (chitin). Properties of chitosan include viscosity, solubility in various media, ability to form films and capability to bind with various metal ions (metal chelation) (Shukla *et al*, 2013). Chitosan is produced from chitin under alkaline conditions or by enzymatic hydrolysis. Acetate moiety is removed from chitin under alkaline conditions through hydration in order to produce chitosan (Shukla *et al*, 2013). Chitosan is a polymer that consists of amine and hydroxyl functional groups (See Figure 2.19). Due to the presence of these functional groups, chitosan can be applied in many fields as well as be incorporated with other materials to improve performance.

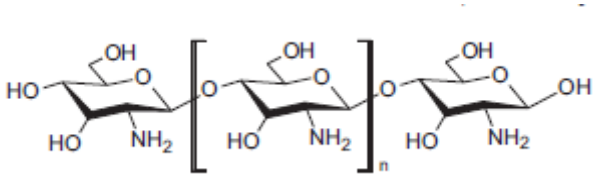

Figure 2.19: Structure of chitosan (Taken from Shukla *et al*, 2013)

Due to its unique properties, chitosan has been applied to industries such as wastewater treatment, food industry, cosmetics, and agriculture and biomedical. In the biomedical industry, chitosan has been found to be a good candidate for gene therapy, cell culture and tissue engineering due to its excellent properties.

The presence of functionalities such as amine ($-NH_2$) and hydroxyl (-OH) in the chitosan molecules provides basis for interaction with other materials. Therefore, the recent chitosan has been receiving great attention to be used as novel functional composite material. Chitosan composite can be produces either by chemical modification or physical modification. Physical modification is the easiest way and is mostly done by physically mixing (Shukla *et al*, 2012).

Chitosan composite materials have received interest in the wastewater industry. Recently in 2013, Xie *et al* (2013) studied on chitosan modified zeolite as an adsorbent for the removal of different wastewater pollutants. Xie et al (2013) synthesized a zeolite (ZFA) from coal fly ash and modified it by chitosan. Results obtained by Xie *et al* (2013) showed that the chitosan modified zeolite enhanced the adsorption performance of zeolite ZFA. Ngah *et al* (2012) did a study on chitosan-zeolite composite as an adsorbent to remove copper from aqueous solution.

Work has been done where MOFs (ZIFs in particular) have been impregnated with chitosan for different applications. Kang *et al* (2013) investigated ZIF-7/chitosan mixed –matrix membranes for separation of mixtures of water and ethanol in a pervaporation process (Kang *et al*, 2013). Casado-Coterillo *et al* (2015) successfully synthesized and characterized MOF/ionic liquid/chitosan mixed-matrix membrane for separation of CO_2 and nitrogen (Casado-Coterillo *et al*, 2015). The aforementioned authors used ZIF-8 as MOF. Chitosan has high potential for the removal of metal ion; this is because chitosan has amine and hydroxyl groups that serve as active sites for metal ions (Ngah *et al*, 2012). Therefore chitosan and MOFs have potential to be used as composite adsorbent.

Sneddon *et al*, (2015) reported on a family of chitosan/mesoporous silica composite materials with a simple deposition method for CO_2 capture. The materials had a maximum CO_2 adsorption capacity of 0.98 mmol/g at a temperature of 25℃ and pressure of 1 atm and they could be regenerated at a low temperature of 75℃. Chitosan/mesoporous silica retained about 85% capacity after 4 cycles.

CO_2 adsorption can take place on the free amine groups of glucosamine found in chitosan through cooperative adsorption of one CO_2 molecule with two adjacent amine group the same way to amine based adsorbents (Sneddon *et al*, 2015). Chitin from which chitosan is produced is a major food waste from the sea food industry (Sneddon *et al*, 2015).This provides an opportunity for mass scale production of chitosan for CO_2 capture (Sneddon *et al*, 2015). By doing so, chitosan would be used to tackle another environmental problem.

As far as could be ascertained, no work has been reported on the study where chitosan is impregnated on MOFs and applied for CO_2 capture. Therefore this work investigated impregnation of chitosan on MOFs (SOD-ZMOF in particular). The presence of amine groups on chitosan can enhance the adsorption capacity of SOD-ZMOF as amines are basic while CO_2 is acidic. Amine is known to react easily with carbon dioxide to form carbamates.

Factors affecting adsorption process

They are several factors that influence adsorption of CO_2. Adsorbents are first characterized by surface properties such as polarity and surface area. During the adsorption process, there are several factors that affect adsorption. These are factors such as temperature, pressure, nature of adsorbate and concentration of adsorbate.

Generally temperature increase results in decrease in adsorption since adsorption is an exothermic process (Dhawan & Dhawan, 2011). At constant temperature, the rate adsorption of a gas increases with increase in pressure (Dhawan & Dhawan, 2011). At the same temperature, the degree at which different gases are adsorbed by the same adsorbent is not the same. Nature of adsorbent also affects adsorption. An adsorbent with a rough surface will have greater number of pores than an adsorbent with a smooth surface. Thus a rough surface adsorbent can adsorb greater number of molecules than a smooth surface adsorbent (Dhawan & Dhawan, 2011). Extent at which adsorption occurs is affected by surface area of adsorbent. Greater the surface area of adsorbent means the greater the extent of adsorption. Specific surface area is the surface area of adsorption per gram of adsorbent (Dhawan & Dhawan, 2011).

2.5. Summary

CCS allows the continuous used of coal for energy generation while reducing CO_2 being released to the atmosphere. Post-combustion capture is the most advantageous technology as it is easy to retrofit in power plants. Adsorption is the best capture method because it requires less energy as compared to other capture methods.

From the previous sections it can be observed that much work has been reported since MOFs were developed over the last decade. From literature a lot of investigation of CO_2 capture using MOFs as adsorbents has been reported. Researchers have also modified MOFs by impregnation and grafting with liquids like amines and ionic liquid. Chen *et al* (2011) developed SOD-ZMOFs and investigated these materials for CO_2 capture. The aforementioned authors also grafted the SOD-ZMOFs with an amine group and the results from their work showed that the SOD-ZMOF and modified SOD-ZMOF are excellent adsorbents for CO_2 capture. Gupta *et al* (2012) did a simulation study on impregnating ionic liquid ([SCN] [BIMM]) on rho-ZMOF and results did show that the material had a good CO_2 adsorption capacity.

As far as could be ascertained, no work has been reported in capturing CO_2 using SOD-ZMOF-chitosan composite. Chitosan has been applied as a composite with other materials in industries such water treatment as explained above. Not much work has been reported in using chitosan composite materials for CO_2 capture. Past studies have shown the possibility of incorporating chitosan in zeolite materials for removal of pollutants in water. In the same manner, the presence of functional groups such as (-NH_2-) and (OH) in chitosan may be

useful in making ZMOF-chitosan composite adsorbent for CO_2 capture. The presence of amine group in chitosan can promote the adsorption of CO_2. On this basis, this study aims to design a composite adsorbent for CO_2 capture by incorporating chitosan on SOD-ZMOFs.

References

1. Ackley M, Rege S, Saxena H. Application of natural zeolites in purification and separation of gases. *Microporous and mesoporous materials*. 2003; 25:42
2. Aki SNVK, Mellein BR., Saurer EM, Brennecke JF. High-pressure phase behaviour of carbon dioxide with imidazolium-based ionic liquids. *The Journal of Physical Chemistry B.* 2004; 20355:20365, 2004
3. Al-Maythalony B, Shekhah O, Swaidan R, Belmabkhout Y, Pinnau I, Eddaoudi, M. Quest for Anionic MOF Membranes: Continuous SOD-ZMOF Membrane with CO_2 Adsorption-Driven Selectivity . *Journal of the American chemical society*. 2014; 1754:1757.
4. Anantharaman R, Peters T, Xing W, Fontaine M, Bredesen R. Dual phase high-temperature membranes for CO_2 separation – performance assessment in post- and pre-combustion processes. *Royal society of chemistry*. 2016; , 251:269
5. Anderson TR , Hawkins E , Jones PD. CO_2, the greenhouse effect and global warming: from the pioneering work of Arrhenius and Callendar to today's Earth System Models. *Science Direct*. 2016; 178:197
6. Bachu, S. CO_2 storage in geological media: Role, means, status and barriers to deployment. *Progress in energy and combustion science*. 2008; 254:273
7. Balbuena P, Gubbins K. Theoretical Interpretation of Adsorption Behavior of Simple Fluids in Slit Pores. *ACS Publications* (1993); *9*(7).
8. Bao Z, Yu L , Ren Q , Lu X , Deng S. Adsorption of CO_2 and CH_4 on a magnesium-based metal organic framework. *Journal of Colloid and Interface Science*. 2011; 549: 556
9. Carbon Capture: Beyond 2020. *Basic Research needs for Carbon capture: Beyond 2020.* Ridge National Laboratory. 2010
10. Casado-Coterillo C, Fern´andez-Barqu´ın A, Zornoza B, T´ellez, C, Coronas J, Irabien, A. Synthesis and characterisation of MOF/ionic liquid/chitosan mixed matrix membranes for CO_2/N_2 separation. *Royal Society of Chemistry*. 2015; 102350–102361

11. Cebrucean D, Cebrucean V, Ionel I. CO_2 Capture and Storage from Fossil Fuel Power Plants. *Energy Procedia*. 2014; 18:26
12. Chemistry Desk. (2016, March 10). Types of Adsorption. Retrieved October 24, 2012, from Types of Adsorption: http://chemistry-desk.blogspot.co.za/2012/10/types-of-adsorption.html
13. Chen C, Kim J, Park, D, & Ahn, W. Ethylenediamine grafting on zeolite like metal organic frameworks (ZMOF) for CO_2 capture. *Materials letters*. 2013; 344:347.
14. Chen C, Kim J, Yang D, Ahn, W. Carbon dioxide adsorption over zeolite-like metal organic frameworks (ZMOFs) having a SOD topology: structure and ion exchange effect. *Chemical Engineering Journal*. 2011; 1134:1139
15. Chen Y, Hu Z, Gupta K, Jiang J. Ionic Liquid/Metal-organic Framework Composite for CO_2 Capture: A Computational Investigation. *American Chemical Society*. 2011; 21736: 21742.
16. CO2CRC. (2015). About *CCS*. (CO2CRC Limited) Retrieved January 21, 2016, from CO_2 capture/ separation techniques.
17. Czaja A, Trukhan N, Muller U. Industrial applications of metal organic frameworks. *Chem Sov Rev*. 2009; 1284:1293
18. Dai C, Wei W, Zhigang L, Li C, Chen, B. Absorption of CO_2 with methanol and ionic liquid mixture at low temperatures. *Fluid phase equilibra,* 2015; 9:17.
19. Daramola MO, Oloye O, Yaya A. Nanocomposite Sodalite/ceramic membrane for pre-combustion CO_2 capture: synthesis and morphological characterization. *International Journal of Coal Science and Technology*. 2016
20. Devic T, Serre C. Porous Metal Organic Frameworks: From Synthesis to Applications. *25th European Crystallographic Meeting, ECM 25*. 2009; 100
21. Dhawan P, Dhawan V. Target 2011: Chemistry. *Tata Mc-Graw-Hill*. 2011; 181:183
22. Donohue MD, Aranovich GL. Classification of Gibbs adsorption isotherms. *Advances in Colloid and Interface Science.* 1998; 137:152
23. Dutcher B, Fan M, Russell AG. Amine-Based CO_2 Capture Technology Development from the Beginning of 2013: A Review. *Applied materials and interfaces*. 2015; 2137:2148
24. Dutta, BK. Principle of mass transfer and separation processes. *PHI learning private limited*. 2009; 609:617
25. Eddaoudi M, Eubank JF, Liua, Y, Kravtsov C, Larsen RW, Branta JA. Zeolites embrace metal-organic frameworks: building block approach to the design and

synthesis of zeolite-like metal-organic frameworks (ZMOFs). *Studies in surface science and catalysis*. 2007; 2021:2029

26. Eddaoudi M, Sava D, Eubank J, Adila K, Guillerma V. Zeolite-like metal–organic frameworks (ZMOFs): design, synthesis, and properties. *Royal society of chemistry*. 2014; 228:249.
27. Eddaoudi M, Sava D, Eubank J, Adila K, Guillerma V. Zeolite-like metal–organic frameworks (ZMOFs): Design, synthesis, and properties. *Royal society of chemistry*. 2014; 228:249.
28. Favre E. Membrane processes and post-combustion carbon dioxide capture:
29. Freije AM, Hussain T, Salman EA. Global warming awareness among the University of Bahrain science students. *Journal of the Association of Arab Universities for Basic and Applied Sciences*. 2016; 1:8
30. Garðarsdóttir S, Normann F, Andersson K, Prölß K, Emilsdóttir S, Johnsson F. Post-combustion CO_2 capture applied to a state-of-the-art coal-fired power plant-The influence of dynamic process conditions. *International Journal of Greenhouse Gas Control*. 2015; 51:62
31. Gomes VG, Yee KWK. Pressure swing adsorption for carbon dioxide sequestration from exhaust gases. *Separation and Purification Technology*. 2002; 161:171
32. Gupta K, Chen Y, Hu Z, Jiang J. Metal–organic framework supported ionic liquid membranes for CO_2 capture: anion effects. *Phys.Chem*. 2012; 5785:5794.
33. Hefti M, Marx D, Joss L, Mazzotti M. Adsorption equilibrium of binary mixtures of carbon dioxide and nitrogen on zeolites ZSM-5 and 13X. *Microporous and Mesoporous Materials.* 2015; 215:228
34. Hofs B, Ogier J, Vries D, Beerendonk EF, Cornelissen ER. Comparison of ceramic and polymeric membrane permeability and fouling using surface water. *Separation and purification technology*. 2015; 365:374

35 Hung C, Yang C, Lin J, Huang S, Chang Y, Liu S. Capture of carbon dioxide by polyamine-immobilized mesostructured silica: A solid-state NMR study. *Microporous and Mesoporous Materials*. 2017; 2:13

36 Imteaz A, Sung H. Composite of metal organic framework: Preparation and Application in adsorption. *Materials today*. 2014; 136:146.

37 International Energy Agency (IEA). Energy Technology Perspectives 2014. 2014

38 International Energy agency. CO_2 emissions from Fuel combustions highlights. *IEA Publications*. 2015; 1:139

39 Kang, C., Lin, Y., Haung, Y., Tung, K., Chang, K., Chen, J. Synthesis of ZIF-7/chitosan mixed matrix membranes with improved separation performance of water/ethanol mixtures. *Journal of membrane science*. 2013; 105–111

40 Keller J, Staudt R. Gas Adsorption Equilibria experimental methods and Adsorptive isotherms. *Springer*. 2005; 2:4

41 Khan A, Haldera GN, Saha AK. Comparing CO_2 removal characteristics of aqueous solutions of monoethanolamine, 2-amino-2-methyl-1-propanol, methyldiethanolamine and piperazine through absorption process. *International Journal of Greenhouse Gas Control*. 2016; 179:189

42 Laboratory Testing inc. (2015). *SEM Analysis with EDS capabilities*. Retrieved April 5, 2015, from Inverse Paradox: http://www.labtesting.com/services/materials-testing/metallurgical-testing/sem-analysis/

43 Lackner KS, West AC. Carbon dioxide separation at high temperatures with ceramic membrane. *Columbia technology ventures*. 2007; 27:28

44 Le Quéré, C,. Jain AK, Raupach MR , Schwinger J, Sitch S, Stocker BD, Viovy N, Zaehle S, Huntingford C, Friedlingstein P,. Andres RJ, Boden T, Jourdain C, Conway T, Houghton RA, House JI, Marland G, Peters GP, Van Der Werf G, Ahlström A, Andrew RM, Bopp L, Canadell JG, Kato E, Ciais P, Doney SC, Enright C, Zeng N, Keeling RF, Klein Goldewijk K, Levis S, LevyP, Lomas M, Poulter B. The global carbon budget 1959–2011.*Earth System Science Data Discussions* 5. 2012; 1107:1157.

45 Lee S, Park S. A review on solid adsorbents for carbon dioxide capture. *Journal of Industrial and Engineering Chemistry*. 2015; 1;11

46 Lenntech. (2015). *Water treatment solutions*. Retrieved March 12, 2015, from Zeolite Applications: http://www.lenntech.pl/zeolites-applications.htm

47 Leung DYC, Caramanna G, Maroto-Valer MC. An overview of current status of carbon dioxide capture and storage technologies. *Renewable and Sustainable Energy Reviews.* 2014; 426:443

48 Li J, Ma Y, McCarthy MC, Sculley J, Yu J, Jeong H, Balbuena P, Zhou H. Carbon dioxide capture-related gas adsorption and separation in metal-organic frameworks. Coordination Chemistry Reviews. 2011; 1791:1823

49 Li L, Conway C, Burns R, Maeder M , Puxty G, Clifford S, Yu H. Investigation of metal ion additives on the suppression of ammonia loss and CO_2 absorption kinetics

of aqueous ammonia-based CO_2 capture. *International Journal of Greenhouse Gas Control*. 2017;165:172

50 Liu D, Xia Q , Li Z , Xi H. Experimental and molecular simulation studies of CO_2 adsorption on zeolitic imidazolate frameworks: ZIF-8 and amine-modified ZIF-8. *Springer Science and Business Media*. 2013; 19:25–37

51 Llewellyn PL, Bourrelly S, Serre C, Vimont A, Daturi M, Hamon L, De Weireld G, Chang J, Hong D, Hwang Y, Jhung S, Fe´rey G. High Uptakes of CO_2 and CH_4 in Mesoporous MetalsOrganic Frameworks MIL-100 and MIL-101. *American Chemical Society*. 2008; 7245:7250

52 Lowell S, Shields J. Powder Surface Area and Porosity. *Chapman & Hall*. 1998; 210;215

53 Luis P, Van Gerven T, Van der Bruggen B. Recent developments in membrane-based technologies for CO_2 capture. *Progress in Energy and Combustion Science*. 2012; 419;448

54 Ma J, Xin C, Tan C. Preparation, physicochemical and pharmaceutical characterization of chitosan from Catharsius molossus residue Jiahua. *International Journal of Biological Macromolecules.* 2015; 547:556

55 Millward A, Yaghi OM. Metal-Organic Frameworks with Exceptionally High Capacity for Storage of Carbon Dioxide at Room Temperature. *Journal of American Chemical society*. 2005; 17998:17999

56 Montagnaro F, Silvestre-Albero, A, Silvestre-Albero, J, Rodríguez-Reinoso F, Erto A, Lancia A, Balsamo M. Post-combustion CO2 adsorption on activated carbons with different textural properties. *Microporous and Mesoporous Materials*. 2015; 157:164

57 Muldoon MJ, Aki SNVK, Anderson JL, Dixon JK, Brennecke JF. Improving carbon dioxide solubility in ionic liquids. *The Journal of Physical Chemistry B*. 2007; 9001:9009

58 NETL. (2015). *CO_2 capture processes*. Retrieved August 6, 2015, From CO_2 capture processes: http://www.netl.doe.gov/research/coal/carbon-storage/carbon-storage-faqs/co2-capture-proces

59 Ngah W, Teong L, Toh R, Hanafiah M. Utilization of chitosan-zeolite composite in the removal of Cu (II) from aqueous solution: Adsorption, desorption and fixed bed column studies. *Chemical Engineering Journal*. 2012; 46:53.

60 Nwogu N, Kajama M, Gobina E. Performance Evaluation of an Inventive CO_2 Gas Separation Inorganic Ceramic Membrane. *International Journal of Chemical, Molecular, Nuclear, Materials and Metallurgical Engineering*. 2015; 674:677

61 Nwaoha C, Saiwan C, Tontiwachwuthikul P, Supap T, Rongwong W , Idem R, AL-Marri MJ. Carbon dioxide (CO_2) capture: Absorption-desorption capabilities of 2-amino-2-methyl-1-propanol (AMP), piperazine (PZ) and monoethanolamine (MEA) tri-solvent blends. *Journal of Natural Gas Science and Engineering*. 2016; 742:750

62 Perrin N, Dubettier R, Lockwood F, Court P, Tranier J, Bourhy-Weber C, Devaux M. Oxy-combustion for carbon capture on coal power plants and industrial processes: advantages, innovative solution and key projects. *Energy Procedia*. 2013; 1389 : 1404

63 Pires J, Martins F, Aliuim-Ferraz M, Simoes, M. Recent developments on carbon capture and storage: An overview. *Chemical Engineering Research and Design*. 2011; 1446:1460

64 Practical Analytical. (2015). *X-Ray Difraction*. Retrieved April 10, 2015, from Practical Analytical: http://particle.dk/methods-analytical-laboratory/xrd-analysis/

65 Quana S,∗, Wei Li S , Xiao Y, Shao L. CO_2-selective mixed matrix membranes (MMMs) containing graphene oxide (GO) for enhancing sustainable CO_2 capture. *International Journal of Greenhouse Gas Control*. 2017); 22:29

66 Ramdin M, Loos T, Vlugt T. State-of-the-Art of CO_2 Capture with Ionic Liquids. *Industrial and engineering chemistry research*. 2012; 8149:8177

67 Rashidi N, Yusup M. An overview of activated carbons utilization for the post-combustion carbon dioxide capture. *Journal of CO_2 Utilization*. 2016; 1:16

68 Riboldi L, Bolland O. Evaluating Pressure Swing Adsorption as a CO_2 separation technique in coal-fired power plants. *International Journal of Greenhouse Gas Control*. 2015; 1:16

69 Rinaudo M. Chitin and chitosan: Properties and applications. *Progress in polymer science*. 2006; 603:632

70 Rowsell J, Yaghi O. Metal-organic frameworks: a new class of porous materials. *Microporous and Mesoporous Materials*. 2004; 3:14.

71 Saha S, Chandra S, Gurai B, Banerjee R. Carbon dioxide capture by metal organic frameworks. *Indian Journal of chemistry*. 2012; 1223:1230.

72 Saxenaa R, Singha V, Kumar E. Carbon Dioxide Capture and Sequestration by Adsorption on Activated Carbon. *Energy Procedia*. 2014; 320 : 329

73 Shukla S, Mishra A, Arotiba O, Mamba B. Chitosan-based nanomaterials: A state-of the-art review. *International Journal of Biological Macromolecules*. 2013; 46:58.

74 Song C, Kitamura Y, Li S, Ogasawara K. Design of a cryogenic CO_2 capture system based on Stirling coolers. *International Journal of Greenhouse Gas Control*. 2012; 107:114

75 Song C, Kitamura Y, Li S. Optimization of a novel cryogenic CO_2 capture process by response surface methodology (RSM). *Journal of the Taiwan Institute of Chemical Engineers.* 2014;1666:1676

76 Spigarelli BP, Kawatra SK. Opportunities and challenges in carbon dioxide capture. *Journal of CO_2 Utilization.* 2013; 69:87

77 Stanley M. Carbon Capture and Storage: A Realistic Solution? Executive Summary. *Morgan Stanley & Co. LLC*. 2014

78 Susarla N, Haghpanah R, Karimi IA, Farooq S, Rajendran, Tan LSC, Lim JST. Energy and cost estimates for capturing CO_2 from a dry flue gas using pressure/vacuum swing adsorption. *Chemical Engineering Research and Design*. 2015; 354:367

79 Suzuki M. Adsorption Engineering. Amsterdam: *Elsevier Science publishing company*. 1990

80 Thorbjornsson A, Wachtmeister H, Wang J, Hook M. Carbon capture and coal consumption: Implications of energy penalties and large scale deployment. *Energy Strategy Reviews*. 2015;18:28

81 Tlili N, Grevillot G, Vallieres C. Carbon dioxide capture and recovery by means of TSA and/or VSA. *International Journal of Greenhouse Gas Control*. 2009; 519:527

82 University of Crete- Chemistry group. (2001). Retrieved may 14, 2015, from materials modeling and design group: http://www.chemistry.uoc.gr/frudakis

83 Venkataramanan M, Smitha. Causes and effects of global warming. *Indian Journal of Science and Technology*. 2011; 226:229

84 Wang J, Chameides B. Global Warming's Increasingly Visible Impacts. *Environmental Defense*. 2005; 1:27

85 Wang M, Lawal A, Stephenson P, Sidders J, Ramshaw C. Post-combustion CO_2 capture with chemical absorption: A state-of-the-art review. *Chemical Engineering Research and Design*. 2 0 1 1: 1609;1624

86 Xie J, Li C, Chi L, Wu D. Chitosan modified zeolite as a versatile adsorbent for the removal of different pollutants from water. *Fuel*. 2013; 480:485

87 Xu X, Song C, Andresen JM, Miller BG, Scaroni AW. Novel Polyethylenimine-Modified Mesoporous Molecular Sieve of MCM-41 Type as High-Capacity Adsorbent for CO_2 Capture. *American Chemical Society.*2005; 1463:1469

88 Yu C, Huang C, Tan C. A Review of CO_2 Capture by Absorption and Adsorption. *Taiwan Association for Aerosol Research*. 2012; 745:769.

89 Zhang Z, Huisingh D. Carbon dioxide storage schemes: Technology, assessment and deployment. *Journal of Cleaner Production.* 2017; 1055:1064

90 Ziobrowski Z, Krupiczka R, Rotkegel A. Carbon dioxide absorption in a packed column using imidazolium based ionic liquids and MEA solution. *International Journal of Greenhouse Gas Control*. 2016; 8:16

CHAPTER 3: EXPERIMENTAL PROCEDURE

This chapter reports on the materials and procedure employed in the synthesis, characterization and performance evaluation of SOD-ZMOF-chitosan adsorbent. Section 3.1 reports on the materials used Section 3.2 reports on the synthesis of the adsorbent, Section 3.3 reports on the characterisation and lastly Section 3.4 describes how the synthesized adsorbent was evaluated for CO_2 capture. Figure 3.1 depicts an overview of the experimental methodology used in this work.

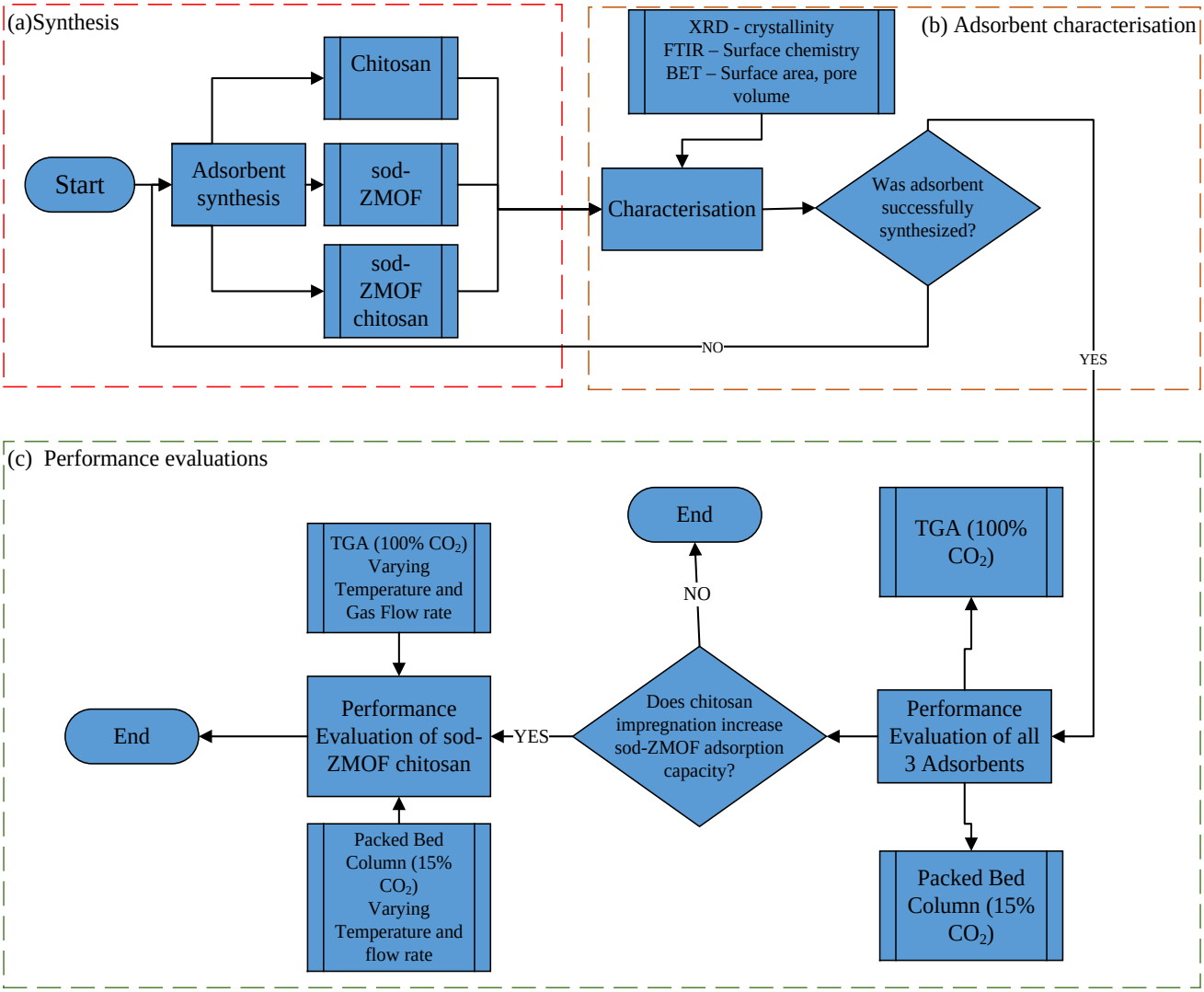

Figure 3.1: Summary of research methodology

3.1. Materials and Adsorption equipment

3.1.1. Materials

The chemicals used in the study: 98 % 4, 5 Imidazoledicarboxylic acid, 99 % imidazole, 99.99% indium (III) nitrate hydrate, hydrochloric acid, 99.8 % N, N-dimethylformamide(DMF) , 70% sodium hydroxide (NaOH), 70 % nitric acid, 99.8 % acetonitrile, 99.8% methanol and 99.98 % acetic acid were all purchased from Sigma Aldrich, South Africa. The chitin was obtained from the shell of crabs (usually a waste material from restaurants). The gas mixture, 15%-85% CO_2-N_2, 100% CO_2 and nitrogen baseline were obtained from Afrox, South Africa.

3.1.2. Description of Adsorption equipment

Adsorption experiments were performed using a thermogravimetric analyser (TGA) of type TA-Q600 as well as adsorption equipment which contain a packed-bed adsorption column (Figure 3.2). Both TGA and adsorption equipment are connected to a gas flow panel and the flowrate of the influent gas was controlled using a mass flow controller. Adsorption is shown through weight changes of the adsorbent for the TGA, while for the adsorption equipment adsorption is shown through changes in concentration of effluent gas stream.

3.2. Synthesis of SOD-ZMOF-chitosan composite

3.2.1. Synthesis of SOD-ZMOF

The method used to synthesize SOD-ZMOF in this study was adapted from the work reported elsewhere (Chen *et al*, 2011). About 0.84 g 4.5-imidazoledicarboxylic acid, 0.6 g indium (III) nitrate hydrate ($In(NO_3)_3.2H_2O$), 60 mL N, N-dimethylformamide (DMF), 20 mL acetonitrile (CH_3CN), 0.82 g imidazole in 8 mL DMF and 1.8 mL nitric acid (HNO_3) in 12 mL DMF were added into a 100 mL flask. The solution was mixed thoroughly until a clear solution was obtained. The solution was heated up to 85℃ under reflux for 12 h. after 12 h, the temperature was increased to 105℃ and continued heating for 23 hours. Polyhedral crystals formed where collected by filtration; washed with methanol to remove any DMF from the pores and surface and then dried in an oven at 100 ℃ for 2 h. The dried poly crystals obtained were SOD-ZMOF.

3.2.2. Production of chitosan

The crabs flesh was removed, the exoskeletons thoroughly washed and sundry. The dried exoskeletons were then chopped into smaller sizes, pulverized to a particle size of < 74 nm.

For preparation of chitosan, chitin was sieved and subjected to demineralization, deproteinization and decolonization.

Chitin was added to 10 % (v/v) hydrochloric acid (HCl) with a solvent to solid ratio of 1:10. The reaction was carried out at 65 ℃ for 2 h with continuous stirring, after which the obtained material was filtered and washed with distilled water until filtrate pH was neutral. The resulting sample was dried in an oven at 50 ℃ for 24 h.

The demineralized chitin was added to 4 % (w/v) Sodium hydroxide (NaOH) with a solvent to solid ratio of 1:10 and heated at 65 ℃ for two h with continuous stirring. The resultant product was then filtered and washed with distilled water to a neutral pH. The sample was dried in an oven at 50 ℃ for 24 h.

About 50 g of Deproteinized chitin was added to 50% (w/v) of Sodium hydroxide (NaOH) at 90 ℃ for 5 h with continuous stirring. The resultant product was filtered, washed with distilled water to a neutral pH and dried in an oven at 50 ℃ for 24 h.

3.2.3. Development of SOD-ZMOF-chitosan composite adsorbent

The procedure used for impregnation of chitosan was adapted from the work reported elsewhere (Sun *et al, 2008*). Chitosan was dissolved in 2 wt. % acetic acid and stirred at 80 ℃ for 1 h to obtain 2 wt. % chitosan solution. 1 g of SOD-ZMOF was added into the solution under stirring for 1 h. The suspension mixture was filtered and the obtained product dried in an oven at 50 ℃ for about 2 h.

3.3. Characterisation techniques

Characterization of SOD-ZMOF-chitosan was done before and after chitosan impregnation. It is important to understand the changes in SOD-ZMOF after chitosan was impregnated. X-ray diffraction (XRD) was done in order to determine the crystallinity of the synthesized adsorbent. The XRD patterns in this study were obtained using a cobalt ($CoK\propto$) radiation with wavelength (λ) of 1.79$\dot{A}$. Fourier Transform Infrared Spectroscopy (FTIR) was used to check the surface chemistry of the synthesized adsorbents. N_2 physisorption at 77 K was carried out to determine the BET surface area, pore volume and the pore size of the synthesized adsorbent.

3.4. Performance evaluation

3.4.1. TGA performance evaluation

Thermal galvanic analysis was first used to evaluate the adsorption capacity of SOD-ZMOF, chitosan and SOD-ZMOF-chitosan at an adsorption temperature of 25℃, pressure of 1 bar and flowrate of 60 ml/min. 100 % CO_2 was used to evaluate the aforementioned adsorbents. About 11 mg of adsorbent was used. Only 11 mg was used because this was the maximum mass that could be loaded on the TGA. First nitrogen is passed through the adsorbent at a sweeping temperature of 110 ℃ for 30 minutes in order to remove any impurities in the adsorbent. At constant pressure, a traditional method was used to investigate the effect of adsorption temperature and influent gas flowrate at a temperature range and gas flowrate range listed in Table 3.1. Amount of CO_2 adsorbed during the experiment was obtained using the CO_2 concentration before and after adsorption:

$$\%\, CO_2\ adsorbed = \frac{Weight\ of\ adsorbent\ after\ adsorption - Weight\ of\ adsorbent\ before\ adsorbent}{Weight\ of\ adsorbent\ before\ adsorption}$$

(3.1)

Table 3.1: Operating conditions investigated

Operating Conditions	Value (range)
Adsorption temperature range	25 -85 ℃
Influent gas flowrate range	15- 90 ml/min
Operating pressure	1 bar

3.4.2. Packed-bed column evaluation

Adsorption set-up depleted in Figure 3.2 was used to evaluate the CO_2 adsorption performance of the synthesized SOD-ZMOF-chitosan. The set-up consists of a packed-bed column connected to a CO_2 detector in order to read the CO_2 concentration before, during and after adsorption. About 0.05 g of the adsorbent was packed in the column. The sample in the column was then heated from room temperature to 110℃ under the continuous flow of nitrogen through the sample and held for another 30 minutes at 110^{o}C for sweeping impurities such as moisture from the adsorbent. Then the temperature was dropped to the 25 ^{o}C. A influent gas mixture of about 15% CO_2 (balance being nitrogen) at a flowrate of 25 ml/min and a pressure of 1 bar was passed through the sample for about 1 h., which contains

about 15% CO_2. Amount of CO_2 adsorbed during the experiment was obtained using CO_2 mass balance as a mathematical relationship below Equation 3.2:

$$q = \frac{P \times M_r}{R \times T \times m_{adsorbent}} \left(Q(y_{i-} y_f) \right) \times t \quad \textbf{(3.2)}$$

Where q is the amount of CO_2 adsorbed in mol/g adsorbent (to express the amount in mg CO_2/ g adsorbent, q was multiplied by the molar mass of CO_2 (M_r)), y_i and y_f is the mole fractions of CO_2 in the influent and effluent gas streams, respectively, Q is the volumetric flowrate of the feed stream. P and T are the adsorption pressure and temperature, respectively. R is the universal gas constant; $m_{adsorbent}$ is the mass of the adsorbent, M_r is the molar mass of CO_2, and t is the adsorption time. The aforementioned procedure was repeated at adsorption temperatures of 40 ^oC, and 55 ^oC with constant influent gas flowrate and then repeated for varying influent gas flowrate keeping adsorption temperature and pressure constant at 25 ^oC and at 1 bar, respectively. The gas mixture employed in the study was used to mimic the composition of flue gas expected from a typical coal-fired power plant. A packed-bed column with diameter of 4 mm, bed height of 12 mm and operated at a pressure of 1 bar was utilized in this work.

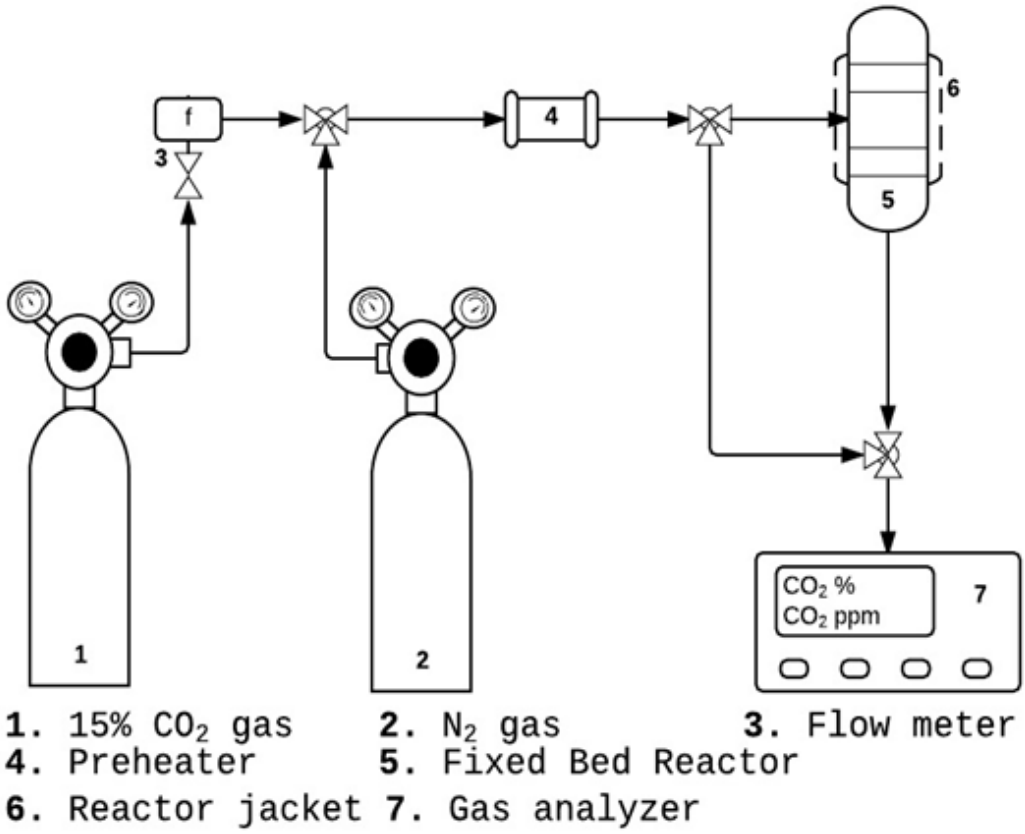

Figure 3.2: Process flow diagram of the adsorption set-up

References

1. Chen C, Kim J, Yang D, Ahn, W. Carbon dioxide adsorption over zeolite-like metal organic frameworks (ZMOFs) having a SOD topology: structure and ion exchange effect. Chemical Engineering Journal. 2011; 1134:1139
2. Sun H, Lu L, Chen X, Jiang Z. Surface modified zeolite-filled chitosan membranes for pervaporation dehydration of ethanol. *Applied surface science*, 2008; 5367:5374.

CHAPTER 4: SYNTHESIS AND CHARATERISATION OF SOD-ZMOF-CHITOSAN COMPOSITE ADSORBENT

4.1. Introduction

The first objective of this work was to synthesise SOD-ZMOF and compare results with literature. The first part of the second objective was to impregnate chitosan on SOD-ZMOF. This chapter reports on these objectives. After synthesis it is important to characterize the sample for comparison with literature as well as to identify the properties of the synthesized material. This section discusses the characterisation results of SOD-ZMOF, chitosan and SOD-ZMOF-Chitosan. Characterisation techniques used in this study were XRD for phase identification and crystallinity, FTIR for surface chemistry and N_2 physisorption at 77 K for surface area and pore volume.

4.2. Experimental

4.2.1. Synthesis

SOD-ZMOF and SOD-ZMOF-chitosan were synthesized using the methodology discussed in chapter 3. To recap, SOD-ZMOF was first synthesized using the method adapted from Chen *et al* (2011). Chitosan was then derived from chitin of crabs purchased from a beach in Lagos, Nigeria. Finally chitosan was impregnated on the synthesised SOD-ZMOF using a method adapted from Sun *et al* (2008).

4.2.2. Characterisation techniques for SOD-ZMOF and SOD-ZMOF-chitosan

Figure 4.1 depicts an overview of the characterisation techniques used in this study as well as what they were used for. After synthesis, SOD-ZMOF and SOD-ZMOF-chitosan were characterized. First, SOD-ZMOF characterisation results were compared to those obtained from literature (Chen *et al*, 2011). This was done to confirm if the properties of the synthesized SOD-ZMOF was similar to that reported in literature. After it was confirmed that the synthesized material was SOD-ZMOF, SOD-ZMOF and SOD-ZMOF chitosan were compared in order to observe the changes in properties before and after chitosan impregnation.

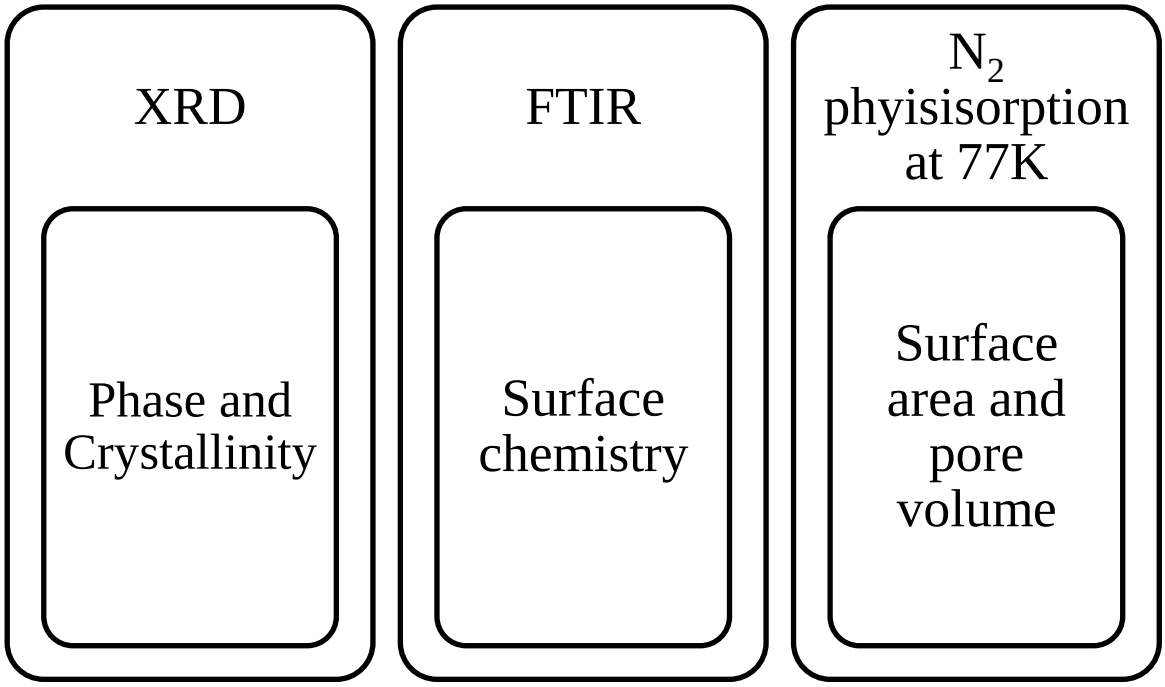

Figure 4.1: Characterisation methods used to analyse SOD-ZMOF, chitosan and SOD-ZMOF

4.3. Results and Discussion

4.3.1. Physicochemical characterization

Figure 4.2 depicts the XRD pattern of SOD-ZMOF before and after chitosan impregnation. XRD was characterized to determine the crystallinity of SOD-ZMOF is crystalline because MOFs are highly crystalline materials. XRD patterns of the SOD-ZMOF and chitosan-impregnated SOD-ZMOF were obtained using cobalt (CoK∝) radiation with a wavelength of (λ) of 1.79$\dot{A}$. In literature, XRD patterns of SOD-ZMOF were obtained using copper radiation (CuK∝) radiation with wavelength of 1.54 $\dot{A}$. In order to compare XRD patterns from this work with that from literature values obtained from CoK∝ radiation were corrected to expected values of CuK∝ (refer to Appendix A). The sharpness of the XRD peaks is important in identifying the crystallinity of SOD-ZMOF. The sharp peaks depicted in Figure 4.2 represent that the synthesized material is crystalline; this was expected as metal organic frameworks are highly crystalline materials. SOD-ZMOF showed a XRD pattern that is similar to that reported in literature (Chen *et al*, 2011; Calleja *et al*, 2010), confirming that SOD-ZMOF material were synthesised in this study.

The XRD pattern of chitosan impregnated SOD-ZMOF shows a comparable pattern to that of SOD-ZMOF indicating that the structure of SOD-ZMOF was still conserved after chitosan impregnation. At a 2-theta of about 30 degree, there is a drastic decrease in the intensity on

the XRD pattern of SOD-ZMOF-chitosan as compared to that of SOD-ZMOF. The decrease could be as a result of the impregnated chitosan in SOD-ZMOF. Thus chitosan was successfully impregnated on SOD-ZMOF to produce SOD-ZMOF-chitosan.

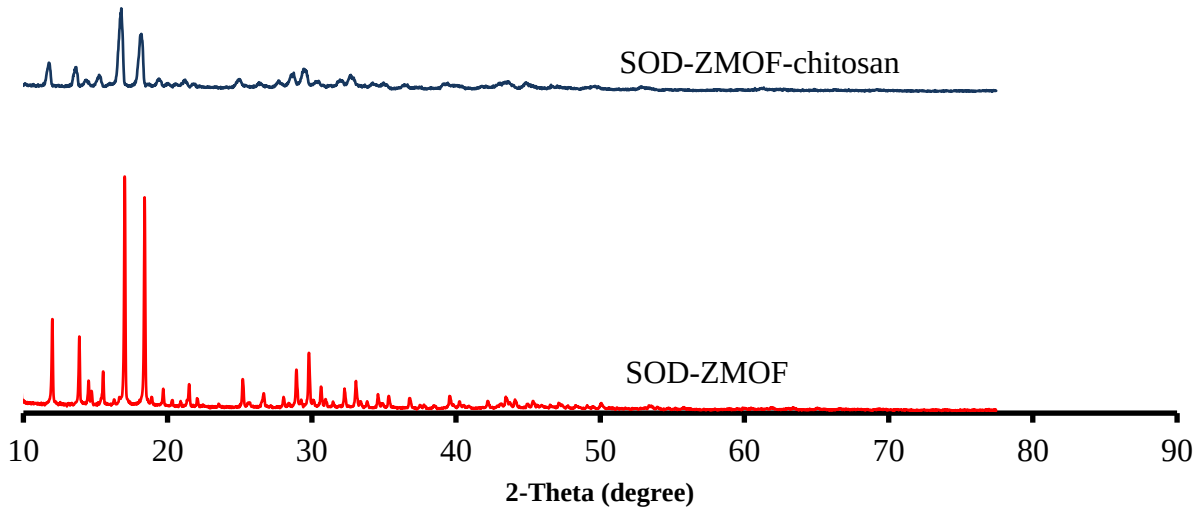

Figure 4.2: XRD pattern of SOD-ZMOF before and after impregnation

The FTIR spectra of SOD-ZMOF and SOD-ZMOF-chitosan are depicted in Figure 4.2. The organic linker in SOD-ZMOF is 4.5-Imidazoledicarboxylic acid and as such it is expected that SOD-ZMOF and this organic linker have similar functional groups. The functional groups present in 4.5-Imidazoledicarboxylic acid are amine (N-H), carboxylic acid (COOH), aromatics (C-C (in ring)), aromatic amine (CN) and (C=O). The FTIR analysis of SOD-ZMOF in Figure 4.3 shows the presence of COOH at a wavelength of 3178 cm^{-1}, C-C (in ring) at a wavelength of 1476 cm^{-1}, C-N at a wavelength of 1105 cm^{-1}, N-H at a wavelength of 779 cm^{-1} and C=O at a wavelength of 1700 cm^{-1}, which therefore confirms the successful synthesis of SOD-ZMOF. Table 4.1 contains defined explanation of the FTIR.

Figure 4.3 also shows FTIR spectrum for SOD-ZMOF-chitosan. The FTIR spectrum of SOD-ZMOF-chitosan showed functional groups similar to those found in SOD-ZMOF. However, there is a drastic decrease in the intensity of the COOH (carboxylic acid) band in the spectrum for SOD-ZMOF-chitosan as compared to that of SOD-ZMOF. When Chen *et al.* (2013) grafted SOD-ZMOF with ethylenediamine (EDA), the FTIR also showed a decrease in COOH band after grafting. Chen *et al.* speculated that the decrease in COOH band could be attributed to the transformation of the carboxylic acids to amide groups. In this work, the decrease in the COOH band could also be due to the impregnation of chitosan containing

amine which then confirms the presence of chitosan (amine group) in SOD-ZMOF chitosan. The expected functional group present in chitosan are amines (N-H), aliphatic amines (C-N) and alcohol (O-H) (Refer to Figure 2.13 for structure of chitosan). N-H is present at a wavelength of 876 cm^{-1}, C-N is present at a wavelength of 1046 cm^{-1} and O-H is present at a wavelength of 3649 cm^{-1}.

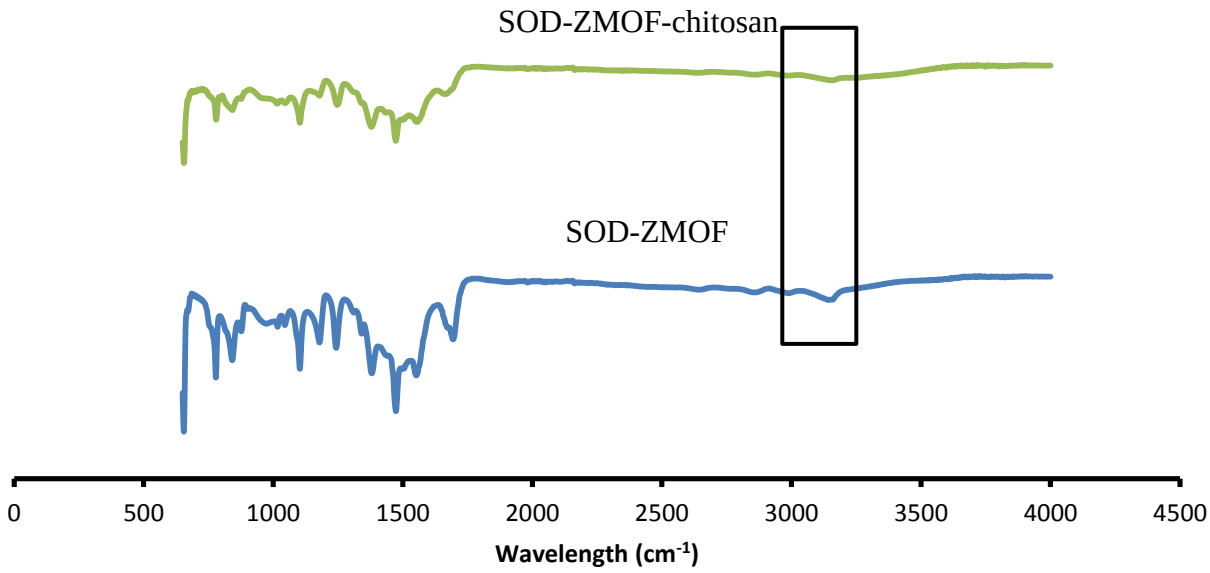

Figure 4.3: FTIR spectra of SOD-ZMOF before and after chitosan impregnation

Table 4.1: Interpretation of characteristics of IR absorption

Wavelength (cm^{-1})	**Functional group**	**Interpretation**
3640–3610	O-H	Alcohol
3300–2500	COOH	Carboxylic group
1710–1665	C=O	Unsaturated aldehydes
1500–1400	C-C (in ring)	aromatics
1250–1020	C-N	aromatic amines
910–665	N-H	1°, 2° amines

4.3.2. Surface area and pore volume

Nitrogen physisorption at 77 K was conducted on SOD-ZMOF before and after chitosan impregnation in order to determine the pore volume, pore size and BET surface area. Table 4.3 depicts a summary of the BET results obtained in this study. From work done in literature, SOD-ZMOF has a pore volume and BET surface area greater than the one obtained in this study.

Table 4.2: Comparison of textual properties

Adsorbent	**Surface area (m^2/g)**	**Pore volume (cm^3/g)**	**Pore size (nm)**	**Reference**
SOD-ZMOF	375	0.16		Chen *et al* (2011)
SOD-ZMOF	361	0.13		Calleja *et al* (2010)
SOD-ZMOF	52.40	0.0445	3.40	This work
Chitosan	17.1	0.119	27.0	This work
SOD-ZMOF–chitosan	0.527	0.0265	201.2	This work

In this study, SOD-ZMOF had a pore volume, pore size and BET surface which were much less than that obtained from the work of Chen *et al*. (2011) and Calleja *et al* (2010). In this work, the total volume of the reactant species solution was up - scaled compared to those of Chen *et al* (2011) and Calleja *et al* (2010). However, the reaction conditions were identical to that of Chen *et al* (2011) and Calleja *et al* (2010). Rubio-Martinez *et al* (2016) reported that synthesis of MOFs that proceed satisfactory in a small scale vessel may not always proceed well when scaled up using a bigger vessel at the identical process conditions as in a small vessel. According to Rubio-Martinez *et al* (2016), up scaling of MOFs synthesis bring a challenge that affect product quality such as reduction of surface area. The aforementioned challenge was encountered in this work. McKinstry *et al* (2016) encountered a reduction in surface area per unit mass when the authors up - scaled the synthesis of MOF-5 by increasing the concentration of reactant species which caused interpenetration. Prasad & Suh (2012) observed a drastic reduction in surface area from 5290 m^2/g to 1770 m^2/g of a MOF with similar framework but differ only in degree of interpenetration**.** In MOFs synthesis, Interpenetration is when the pore size of material is reduced without blockage of available

adsorptive sites (Jiang *et al*, 2013). Interpenetration is a phenomenon which negatively affects the porous nature of MOFs by reducing the size of pores (Jiang *et al*, 2013). Han *et al* (2012) reported that interpenetration can sometimes create new CO_2 adsorption sites with high affinity at low pressures thus enhancing CO_2 uptake of material. However, this phenomenon decreases CO_2 uptake at high pressures of about 50 bar (Han *et al.*, 2012)

One of the causes of interpenetration in MOFs is temperature and concentration conditions (Zhang *et al*, 2009; Prasad & Suh, 2012; Jiang *et al*, 2013). For this work, the amount of reactants species was increased while still maintaining the same molar ratio. A high volume of reactants species in a larger vessel (100 ml) was heated at the same temperature and same reaction time as a low volume of reactants in a small vessel (20 ml) reported in literature (Chen *et al.*, 2011). Increasing the volume from 20 ml to 100 ml could have resulted in materials such as Structure Direction Agent (SDA) and solvent being occluded in the SOD-ZMOF structure thus occupying the available pores resulting to interpenetration.

In an attempt to remove the occluded material from the SOD-ZMOF, drying temperature was increased from 100℃ to 150℃. However this resulted in the structure of SOD-ZMOF being affected as the FTIR spectra in Figure 4.4 illustrates the FTIR spectra of the SOD-ZMOF where drying occurred at 100℃ and 150℃ are different. The carboxylic acid at a wavelength of about 3116 cm^{-1} completely disappeared for the SOD-ZMOF that was dried at 150℃ as compared to the one dried at 100℃. This shows that the structure of SOD-ZMOF was affected. This is expected as metal organic frameworks are unstable at high temperatures (Lee & Park, 2015).

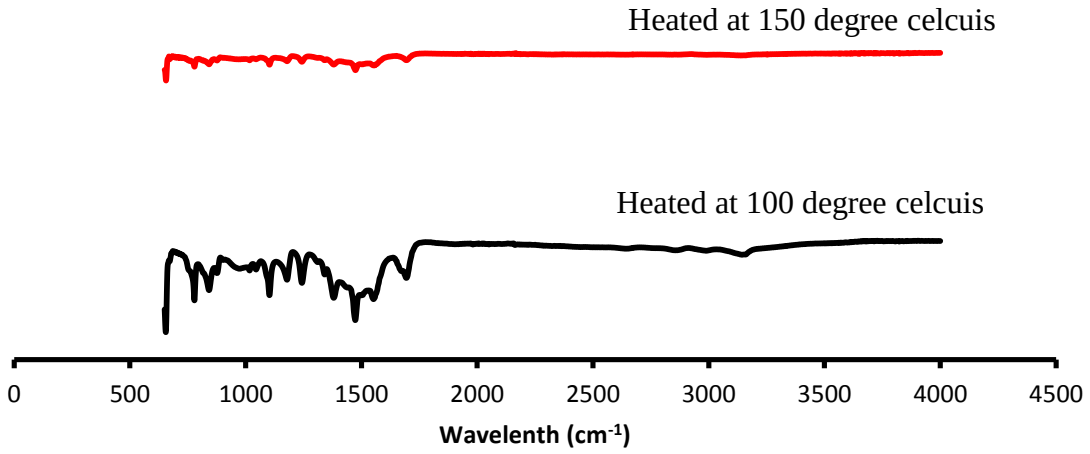

Figure 4.4: FTIR spectra of SOD-ZMOF dried at different temperatures

In addition, impregnation of chitosan on SOD-ZMOF resulted in a decrease in surface area and pore volume. The decrease in surface area and pore volume is expected as chitosan impregnated occupies the surface area and pore volume in SOD-ZMOF. The decrease in surface area and pore volume is a significant indication of the successful impregnation of chitosan. Chen *et al* (2011) also observed a decrease in surface area and pore volume when they grafted amine onto SOD-ZMOF.

4.4. Summary

The first objective of this study was to synthesize SOD-ZMOF and compare results with literature and the second objective to impregnate chitosan on SOD-ZMOF. SOD-ZMOF was successfully synthesized and their physiochemical properties with textual properties with the exception of BET are comparable with those reported literature. BET analysis results showed a reduction in surface area compared to that reported by Chen *et al* (2011). The decrease in surface area could be as a result of interpenetration. After chitosan impregnation there was a decrease in surface area per unit mass. SOD-ZMOF crystal structure was still maintained after chitosan impregnation. Thus chitosan was successfully impregnated onto SOD-ZMOF

References

1. Ayşe K, Çiğdem A, Ahmet S., Birgül T. SOD-ZMOF/Matrimids mixed matrix membranes for CO_2 separation. *Journal of Membrane Science*. 2015; 81:89
2. Calleja G, Botas JA, Sa´nchez-Sa´nchez M, Orcajo, MG. Hydrogen adsorption over Zeolite-like MOF materials modified by ion exchange. International. *Journal of Hydrogen Energy*. 2010; 9916:9923
3. Chen C, Kim J, Park D, Ahn, W. Ethylenediamine grafting on zeolite like metal organic frameworks (ZMOF) for CO_2 capture. *Materials letters*. 2013; 344:347
4. Chen C, Kim J, Yang D, Ahn, W. Carbon dioxide adsorption over zeolite-like metal organic frameworks (ZMOFs) having a SOD topology: structure and ion exchange effect. *Chemical Engineering Journal*. 2011; 1134:1139
5. Han S, Jung D, Heo J. Interpenetration of Metal Organic Frameworks for Carbon Dioxide Capture and Hydrogen Purification: Good or Bad?. *The Journal of Physical Chemistry*. 2012; 71:77
6. Jiang H, Makala T, Zhou H. Interpenetration control in metal–organic frameworks for functional applications. *Coordination Chemistry Reviews*. 2013;2232:2249

7. Lee S, Park S. A review on solid adsorbents for carbon dioxide capture. *Journal of Industrial and Engineering Chemistry*. 2015; 1:11
8. McKinstry C, Cathcart RJ, Cussen EJ, Fletcher AJ, Patwardhan SV, Sefcik J. Scalable continuous solvothermal synthesis of metal organic framework (MOF-5) crystals. *Chemical Engineering Journal*. 2016; 718:725
9. Prasad TK, Suh MK. Control of Interpenetration and Gas-Sorption Properties of Metal–Organic Frameworks by a Simple Change in Ligand Design. *Chemistry: A European Journal*. 2012; 8673 : 8680
10. Rubio-Martinez M, Hadley TD, Batten MP, Constanti-Carey K, Barton T, Marley D, Mçnch A, Lim K, Hill MR. Scalability of Continuous Flow Production of Metal–Organic Frameworks. *ChemSusChem Communications*. 2016; 938 : 941
11. Zhang J, Wojtas L, Larsen RW, Eddaoudi M, Zaworotko MJ. Temperature and Concentration Control over Interpenetration in a Metal-Organic Material. Journal of American Chemistry Society. 2009; 17040–17041

CHAPTER 5: PERFORMANCE EVALUATION OF SOD-ZMOF-CHITOSAN COMPOSITE ADSORBENT FOR CO_2 CAPTURE

5.1. Introduction

After characterising the synthesised adsorbents (SOD-ZMOF, SOD-ZMOF-chitosan and chitosan), they were evaluated for CO_2 capture. The second objective of this work was to study the performance of SOD-ZMOF, chitosan and SOD-ZMOF-chitosan during CO_2 capture. Performance evaluation is significant as it shows if the synthesized adsorbent can capture CO_2. This Chapter reports on results of the evaluation of SOD-ZMOF, chitosan and SOD-ZMOF-chitosan adsorbents for CO_2 adsorption. SOD-ZMOF was impregnated with chitosan to produce SOD-ZMOF-chitosan composite. Thermal gravimetric analysis and packed-bed column were used to evaluate the performance of the aforementioned adsorbents. CO_2 adsorption using 100% CO_2 with TGA was carried out to evaluate if the synthesised adsorbents can adsorb CO_2 without the influence of impurities like N_2. Then the CO_2 adsorption was carried out using a gas mixture containing 15% CO_2 and 85% N_2 in a packed bed column. This was done because flue gas from post-combustion capture has a maximum concentration of 15% CO_2 with N_2 as one of the impurities.

5.2. Experimental

Experimental procedure described in section 3.2 was used. SOD-ZMOF, chitosan and SOD-ZMOF-chitosan were all evaluated for CO_2 adsorption using the TGA as well as the adsorption equipment depicted in Figure 3.1. The aforementioned adsorbents were investigated at 25℃, pressure of 1 bar and influent gas flowrate of 25 ml/min for packed-bed column and 25℃, 1 bar and 30 ml/min for the TGA.

5.3. Results and discussion

5.3.1. TGA performance evaluation

Adsorption of CO_2 using SOD-ZMOF, chitosan and SOD-ZMOF-chitosan was first investigated using the TGA as it is the equipment mostly used in literature. Figure 5.1 depicts a profile of how adsorption occurs when a TGA is used (Refer to appendix C for the TGA profile of individual samples). The TGA measures the weight percentage of the adsorbent as a function of time. First when nitrogen is passed through the adsorbent for sweeping, the weight percentage of the adsorbent decreases with adsorption time. This indicates that

something (in this case, impurities) is being removed from the adsorbents. When CO_2 is passed through the adsorbent the weight percentage increases indicating that CO_2 is attaching on the surface of the adsorbent. The weight percentage of the adsorbent of CO_2 increases until adsorbent is saturated and adsorption is complete. When adsorption is complete the weight percentage of the adsorbent remains constant with further increase in time. The reason for this is that the gas will just be passing over the adsorbent because the pores of the adsorbent are saturated.

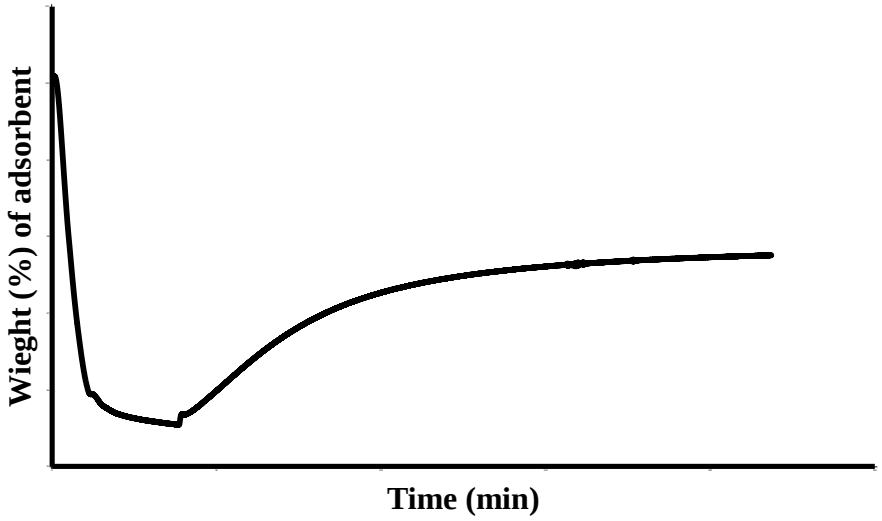

Figure 5.1: Profile of TGA adsorption profile

At an adsorption temperature of 25℃, pressure of 1 bar and influent gas flowrate of 30 ml/ min, SOD-ZMOF-chitosan displayed the highest adsorption capacity followed by SOD-ZMOF, and chitosan displayed the lowest adsorption capacity (refer to Figure 5.2). This is expected as impregnated chitosan contains amine group. Amines have high affinity for CO_2 through acid base interaction between the slightly acid CO_2 and basic amines. In addition, the SOD-ZMOF provided a larger surface area for the adsorption of CO_2 in the chitosan impregnated SOD-ZMOF. There was a 39% increase in CO_2 adsorption capacity of SOD-ZMOF after chitosan impregnation.

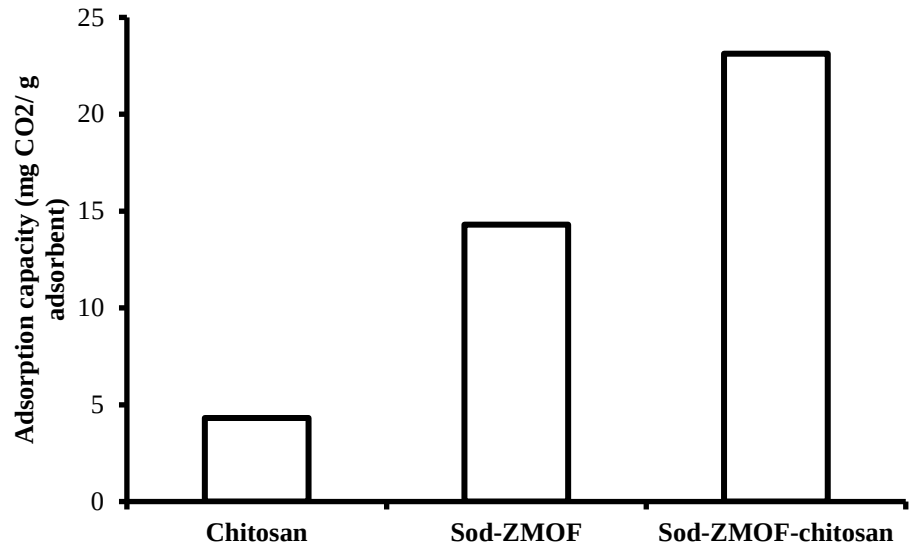

Figure 5.2: CO_2 adsorption capacity of SOD-ZMOF and chitosan using TGA

5.3.2. CO_2 adsorption capacity in packed-bed column

After it was determined that synthesized adsorbents can adsorb 100% CO_2, CO_2 adsorption performance of SOD-ZMOF, chitosan and SOD-ZMOF-chitosan was then evaluated using the adsorption set-up depicted in Figure 3.2. The performance evaluation of the adsorbents was determined using a gas mixture containing CO_2 (15%) and N_2 (85%). Unlike with TGA, the packed-bed column is connected to a CO_2 gas analyser which records the concentration of CO_2 in the effluent gas mixture and not the weight percentage of the adsorbent. During the indication of the CO_2 adsorption by the gas analyser, the CO_2 concentration reading in the effluent gas stream starts to decrease with adsorption time indicating that some of the CO_2 was adsorbed onto the adsorbent from the influent stream. After a certain time, the gas analyser displayed an increase in the CO_2 concentration and continued to increase until it reached the initial concentration in the influent stream, indicating the completeness of the adsorption process. Figure 5.3 depicts the CO_2 concentration profile of the adsorption process as obtained from the CO_2 gas analyser.

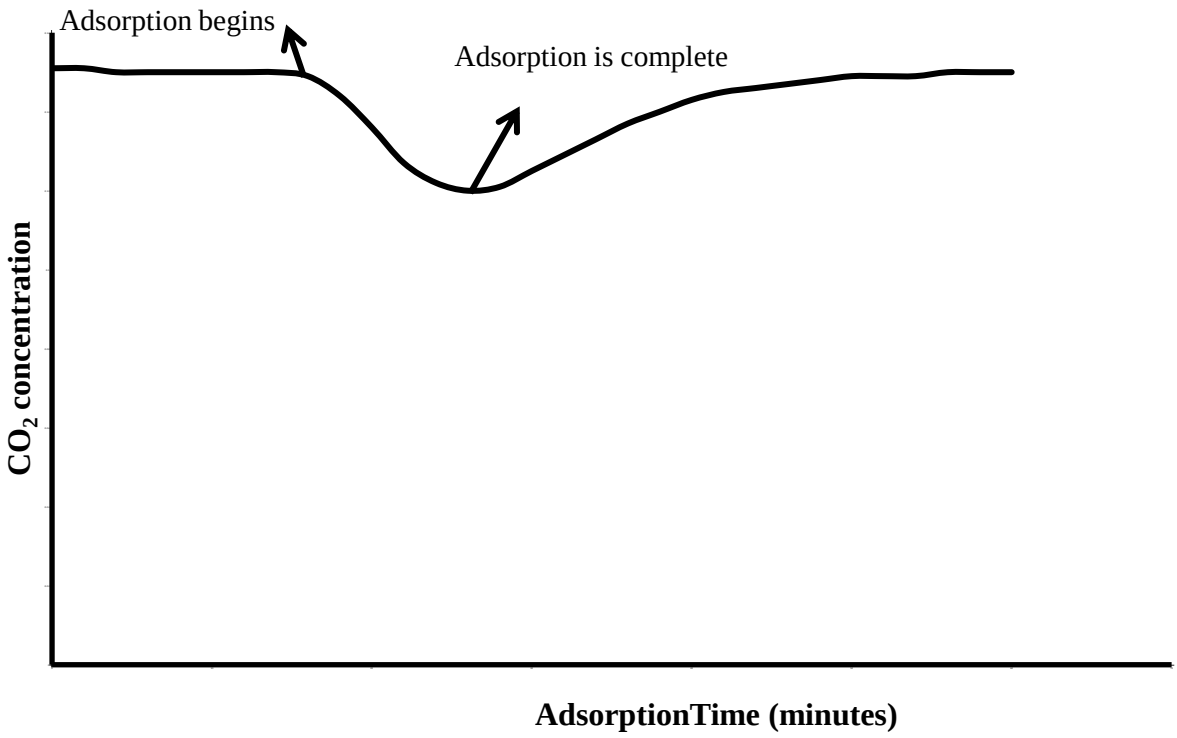

Figure 5.3: **Concentration profile of Adsorption equipment depicted in figure 3.1**

SOD-ZMOF-chitosan, chitosan and SOD-ZMOF were evaluated for CO_2 adsorption using the adsorption set-up in Figure 3.1. Operating conditions were temperature of 25℃, pressure of 1 bar and influent gas flowrate of 25 ml/min. After chitosan was impregnated on SOD-ZMOF, there was a huge reduction in surface area. However, as depicted in Figures 5.2 and 5.4, the CO_2 adsorption capacity increased after chitosan impregnation. The increase in the adsorption capacity after chitosan impregnation could be attributed to the role played by impregnated amine present in chitosan on the SOD-ZMOF. The interaction between slightly acidic CO_2 and slightly basic impregnated amines in chitosan facilitates CO_2 adsorption through formation of carbamate covalent bonds. With SOD-ZMOF adsorption mechanism is physisorption. When CO_2 comes in contact with SOD-ZMOF, CO_2 molecules attaches on the available adsorption sites on the surface of SOD-ZMOF. For SOD-ZMOF-chitosan, adsorption mechanism is chemisorption where CO_2 and amine present in chitosan form a carbamate covalent bond. When Chen *et al* (2013) impregnated EDA on SOD-ZMOF, its adsorption capacity increased by 30% and the authors speculated that it was due to the introduction of amine groups which interacts specifically with CO_2 through formation of carbamate-like complexes (Chen *et al*, 2013). In this study, similar observation occurred and

16% increase in CO_2 adsorption capacity was obtained for the SOD-ZMOF-chitosan adsorbent.

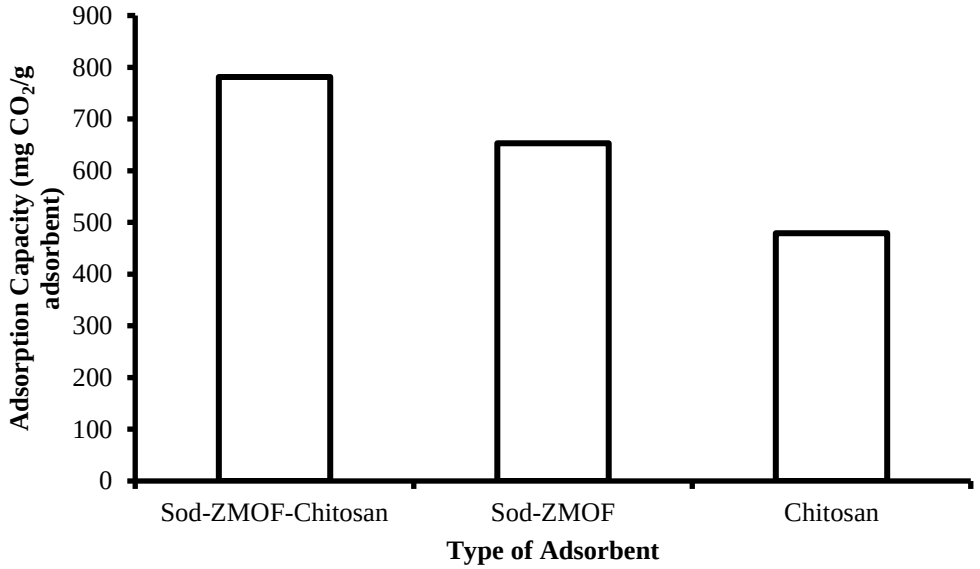

Figure 5.4: CO_2 adsorption capacity of MOFs and chitosan using packed-bed column

Both the TGA and packed-bed column showed an increase in adsorption capacity of SOD-ZMOF after chitosan impregnation. However the values of the adsorption capacity obtained using the packed-bed column is higher than those obtained using TGA (Figure 5.2). This could be because the TGA provides less contact between the gas and the adsorbent as compared to the packed-bed column. In a TGA, the gas flows on top of the adsorbent, while in a packed-bed column the gas flows through the bed (refer to Figure 5.5). It is speculated that, for a TGA, the gas only has contact with the top layer of the adsorbent since the gas flows horizontally over the top whereas with the packed-bed column the gas flows vertically through the adsorbent (refer Figure 5.5). As a result, with the packed column, there is greater mass transfer between the gas and the adsorbent because the gas flows directly through the adsorbent. The other reason for the huge difference in adsorption capacity could be the fact that with the TGA the mass of the adsorbent used was 11 mg as the TGA was limited to this mass only whereas 50 mg of adsorbent was used for the packed-bed column and it's almost 4 times greater than the amount in the TGA. Extremely higher adsorption capacity obtained using the packed-bed column could be attributed to the systematic errors from the set-up. However it should be emphasized that the experiments were repeated severally for repeatability and accuracy

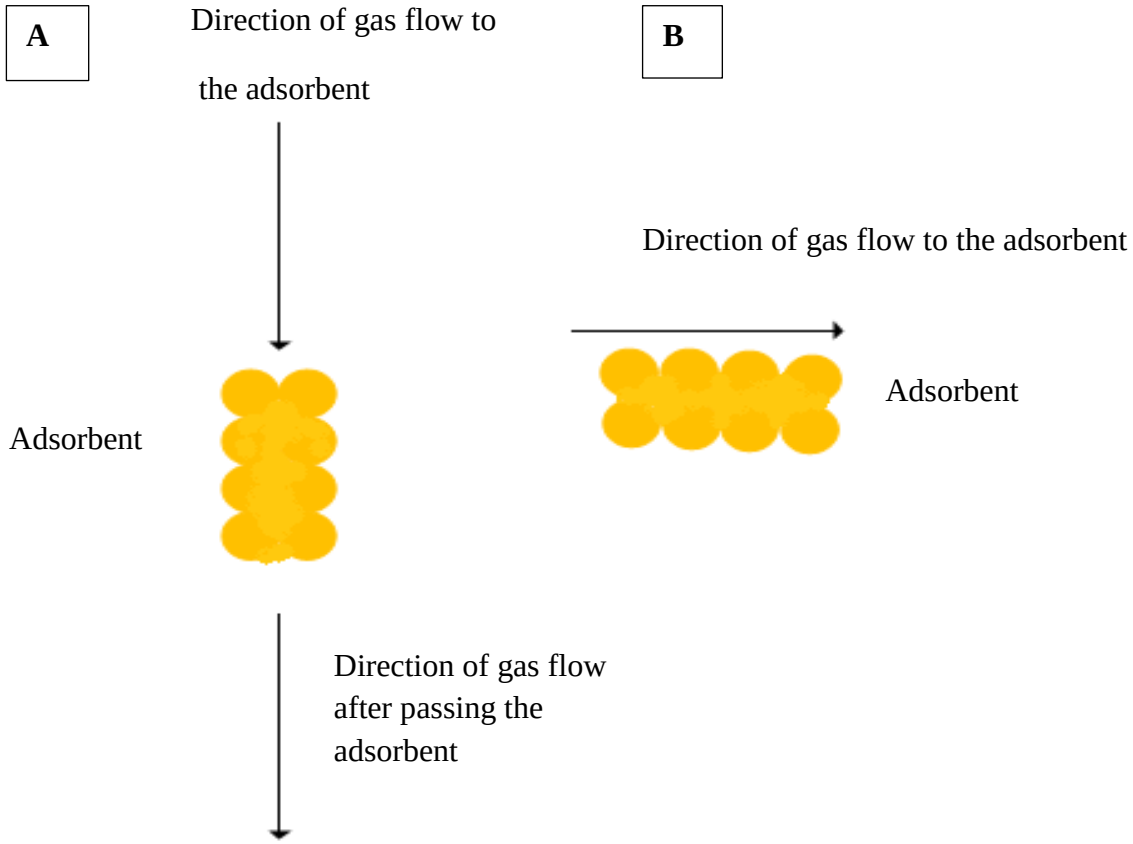

Figure 5.5: Overview of how gas flows in A) Packed-bed column. B) TGA

5.4. Results compared with literature

CO_2 adsorption performance of SOD-ZMOF-chitosan was compared with other adsorbents in literature. It should be noted that conditions and type of equipment at which adsorption was used for adsorption influence the adsorption capacity of adsorbents as discussed in detail in Chapter 2. Table 5.1 depicts different type of adsorbents that were tested for CO_2 capture at different conditions and using different adsorption methods as obtained from literature.

Table 5.1: Comparison of adsorbents and adsorption methods

Adsorbent	Adsorption capacity (mg CO_2/ g adsorbent)	Operating conditions/Equipment	Ref
Zeolite 13X	304	15 bar, 25 ℃/ Integrated gravimetric sorption analyzer	Liang *et al* (2005)
MIL-100	792	50 bar, 31 ℃/ Volumetric adsorption unit	Llewellyn *et al* (2008)
MIL-101	1760	50 bar, 31 ℃/ Volumetric adsorption unit	Llewellyn et al (2008)
MOF-177	1474	35 bar, room temperature/ Volumetric adsorption unit	Millward & Yaghi (2005)
Mg-based MOF-74	379	1 bar, 25 ℃ /Volumetric adsorption unit	Bao *et al* (2011)
Cu-BTC	559	15 bar, 25 ℃/ Integrated gravimetric sorption analyser	Liang *et al* (2005)
ED-SOD-ZMOF	69	1 bar, 25 ℃/ TGA and BEL adsorption instrument	Chen *et al* (2013)
SOD-ZMOF	53	1 bar, 25 ℃/ TGA and BEL adsorption instrument	Chen *et al* (2013)
PAA	44	1 bar, 40 ℃/ TGA	Chitsiga *et al* (2016)
ZIF	30	1 bar, 25 ℃/ TGA and BEL adsorption unit	Chen *et al* (2011)

60 mg of Mg based MOF-74 was evaluated for CO_2 capture using a volumetric adsorption unit. MIL-100 and MIL-101 were evaluated for CO_2 capture using a volumetric (1 g of

adsorbent), gravimetric (0.5 g of adsorbent) and Microcalorimetry (0.3 g of adsorbent) adsorption unit. 15 mg Cu-BTC and zeolite 13X were evaluated for CO_2 adsorption using integrated gravimetric sorption analyser (IGA unit). ED-SOD-ZMOF, SOD-ZMOF ZIF and PAA were evaluated using a TGA, thus their low adsorption capacities compared to other adsorbents in table 5.1. In this work, SOD-ZMOF-chitosan was evaluated using a TGA and a packed-bed column.

Most of the adsorbents in Table 5.1 including, MIL-100, MIL-101, PAA, SOD-ZMOF-ED-SOD-ZMOF, ZIF and Mg-based MOF-74 were evaluated using pure CO_2. In these work 100% CO_2 was used for adsorption tests using the TGA and 15% CO_2 was used for adsorption tests using the packed-bed column. From Table 5.1, MIL-101 showed the highest adsorption capacity, but this at relatively high pressure compared to the conditions at which other adsorbents in table 5.1 were subjected to during adsorption. The reported adsorption capacity of MIL-101 is almost 44% greater than that of SOD-ZMOF-chitosan, however this at different operating conditions and when using different adsorption equipment. SOD-ZMOF-chitosan is comparative with other adsorbents reported in literature.

5.5. Summary

SOD-ZMOF-chitosan composite displayed the highest adsorption capacity followed by SOD-ZMOF and chitosan had the lowest adsorption capacity. SOD-ZMOF-chitosan showed higher adsorption capacity of 781 and 23 mg CO_2/ g adsorbent using the packed-bed column and TGA respectively. Impregnation of chitosan on SOD-ZMOF improved CO_2 adsorption capacity by 16 % for packed-bed column and 39% in a TGA. Adsorption capacity is higher when a packed-bed column was used as compared to when a TGA was used due to enhanced direct contact between the gas and adsorbent. SOD-ZMOF-chitosan is comparative with other adsorbents reviewed in literature.

References

1. Bao Z, Yu L , Ren Q , Lu X , Deng S. Adsorption of CO_2 and CH_4 on a magnesium-based metal organic framework. *Journal of Colloid and Interface Science*. 2011; 549: 556
2. Chen C, Kim J, Park D, Ahn, W. Ethylenediamine grafting on zeolite like metal organic frameworks (ZMOF) for CO_2 capture. *Materials letters*. 2013; 344:347

3. Chen C, Kim J, Yang D, Ahn, W. Carbon dioxide adsorption over zeolite-like metal organic frameworks (ZMOFs) having a SOD topology: structure and ion exchange effect. Chemical Engineering Journal. 2011; 1134:1139
4. Chitsiga T, Daramola MO , Wagner N , Ngoy J. Effect of the presence of water-soluble amines on the carbon dioxide (CO_2) adsorption capacity of amine-grafted polysuccinimide (PSI) adsorbent during CO_2 capture. Energy Procedia. 2016; 90:105
5. Liang Z, Marshall M, Chaffee AL. CO_2 Adsorption-Based Separation by Metal Organic Framework (Cu-BTC) versus Zeolite (13X). *Energy & Fuels.* 2009; 2785:2789
6. Llewellyn PL, Bourrelly S, Serre C, Vimont A, Daturi M, Hamon L, De Weireld G, Chang J, Hong D, Hwang Y, Jhung S, Fe´rey G. High Uptakes of CO2 and CH4 in Mesoporous MetalsOrganic Frameworks MIL-100 and MIL-101. American Chemical Society. 2008; 7245:7250
7. Millward A, Yaghi OM. Metal-Organic Frameworks with Exceptionally High Capacity for Storage of Carbon Dioxide at Room Temperature. Journal of American Chemical society. 2005; 17998:17999

CHAPTER 6: INFLUENCE OF OPERATING CONDITIONS ON CO_2 ADSORPTION CAPACITY OF SOD-ZMOF COMPOSITE

6.1. Introduction

Having understood the CO_2 adsorption performance of the SOD-ZMOF-chitosan as reported in the previous chapter, the adsorbent was then evaluated at different operating conditions to evaluate the effect of adsorption conditions on the CO_2 adsorption capacity of the adsorbent. It is important to know how the behaviour of the synthesized adsorbent changes at different operating conditions. The traditional method approach was one variable is varied at a time and the others kept constant was used. Results of the third objective of this study are hereby presented in this chapter.

6.2. Experimental

Experimental procedure described in Chapter 3 was used. However, adsorption temperature as well as gas mixture flowrate were varied in order to investigate the effect of these operating conditions on the CO_2 adsorption capacity of SOD-ZMOF-chitosan. The temperatures and gas flowrate investigated for the packed-bed column and the TGA are depicted in Table 6.1.

Table 6.1: Investigated operating conditions for packed bed and TGA

Packed-bed column			
Run	**Temperature (℃)**	**Pressure (bar)**	**Gas flowrate (ml/min)**
1	25	1	25
2	40	1	25
3	55	1	25
4	25	1	50
5	25	1	70
TGA			
6	25	1	60
7	40	1	60
8	55	1	60
9	70	1	60
10	85	1	60
11	25	1	30
12	25	1	45
13	25	1	75
14	25	1	90

6.3. Results and discussion

6.3.1. CO_2 adsorption capacity behaviour with time in TGA and packed-bed column

Figure 6.1 depicts a function of adsorption capacity as a function of adsorption time for the TGA at different influent gas flowrates. As the gas attaches to the surface of the adsorbent, the weight of the adsorbent increases and it continues to increase until the available pores are filled up. Thus adsorption capacity increases drastically for the first 100 minutes. Adsorption capacity increases with adsorption time for all gas flowrates investigated until adsorbent was saturated. This is the point where adsorption is complete. This is expected because initially the adsorbent has free adsorption sites and as the gas passes through the adsorbent it fills these free adsorption sites until eventually with adsorption time the adsorption sites are filled. Once the adsorption sites on the adsorbent are filled, the adsorbent becomes saturated and the

gas just passes the adsorbent. Hence the adsorption capacity increased drastically initially and then the curve starts to become flat after about 150 minutes.

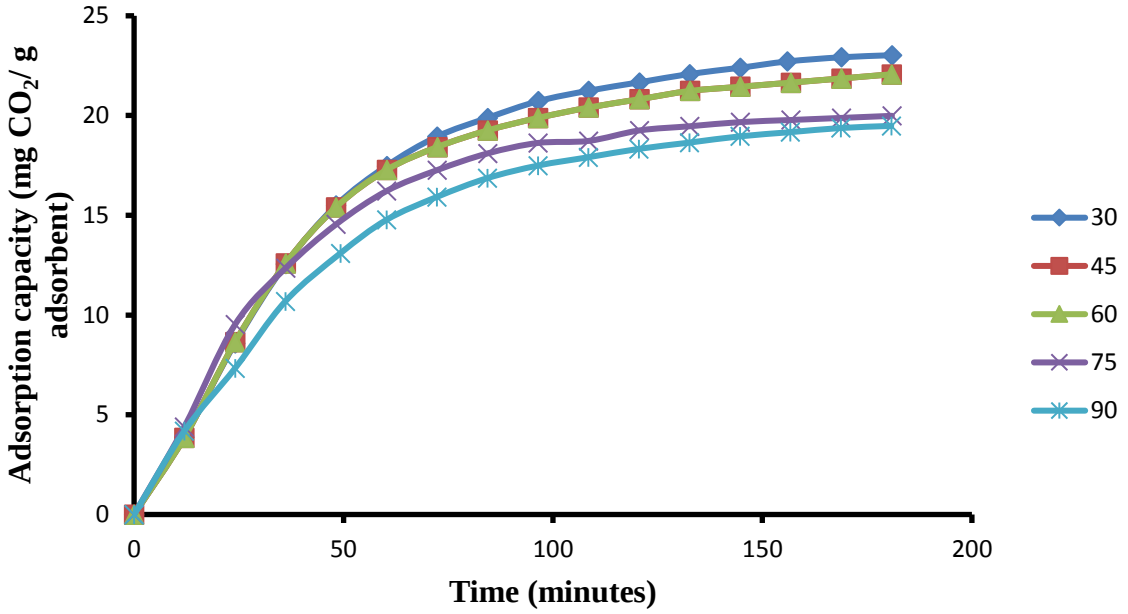

Figure 6.1: Adsorption capacity as a function of time (TGA)

Figure 6.2 depicts adsorption capacity as a function of adsorption time at different temperatures for the packed-bed column used in this study. The influent gas was passed through the packed-bed column for a total of 60 minutes while recording changes in CO_2 concentration of the effluent gas using the gas analyser. Adsorption capacity increased with adsorption time to a point and then starts to decrease. As the influent gas passed through the adsorbent, it fills the available adsorption sites of the adsorbent. Adsorption capacity continued to increase with adsorption time until all the available sites were filled. However once the available sites were filled up, the influent gas passed through the adsorbent with no adsorption occurring and this resulted in the decrease in the adsorption capacity because there was no more decrease in the CO_2 concentration of the effluent gas. Adsorption capacity decreased as the concentration reading of the effluent gas on the analyser increased to the initial concentration. At a temperature of 25℃ , total adsorption time was about 44 minutes while at a temperature of 55℃, adsorption time was about 12 minutes. This shows that the kinetics of CO_2 adsorption was fast at higher adsorption temperature as compared to a low adsorption temperature. Such is expected because at a higher temperature, gas molecules have high kinetic energy than at low temperature. This means that at low temperature

molecules move slower through the adsorbent and can fill up all the adsorption sites, while at high temperature gas molecules move much faster and may not fill up all the adsorption sites.

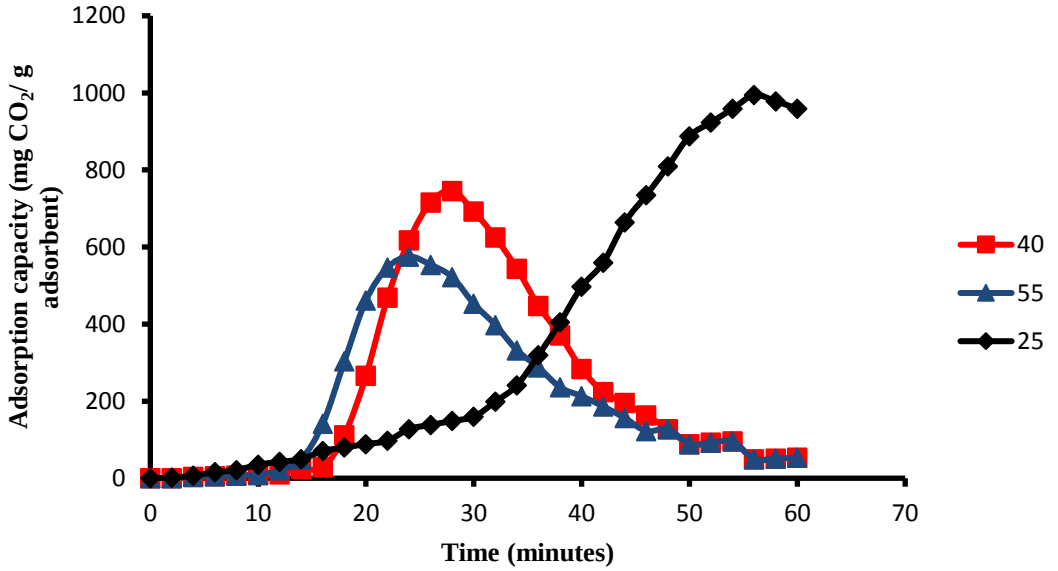

Figure 6.2: Adsorption capacity as a function of time in the Packed-bed column

6.3.2. CO_2 adsorption behaviour with temperature in TGA and packed-bed column

Figures 6.3 and 6.4 depict the adsorption capacity of SOD-ZMOF-chitosan as a function of adsorption temperature for TGA and packed-bed column, respectively. For the TGA, at the lowest adsorption temperature of 25℃, adsorption capacity was 19 mg CO_2/ g adsorbent and reduced to 3 mg CO_2/ g adsorbent at a high temperature of 85℃. Adsorption capacity decreased from 781 mg CO_2/ g adsorbent at 25 ℃ to 314 mg CO_2/ g adsorbent at 55 ℃ for the packed-bed column (see Figure 6.2). For both the TGA and packed-bed column, CO_2 adsorption capacity of SOD-ZMOF-chitosan increased with decreasing adsorption temperature. This is expected as adsorption is an exothermic process (Yu *et al*., 2012). When influent CO_2 gas molecules come into contact with the adsorbent, the gas molecules are adsorbed by the adsorbent and heat is generated (that is heat of adsorption) (Mori &Yamada, 1994). Increasing adsorption temperature increases the kinetic energy of CO_2 gas molecules so at high adsorption temperatures CO_2 molecules have high kinetic energy thus they move faster and results in less adsorption time on the adsorbent surface, resulting thereby in low adsorption capacity at high adsorption temperature.

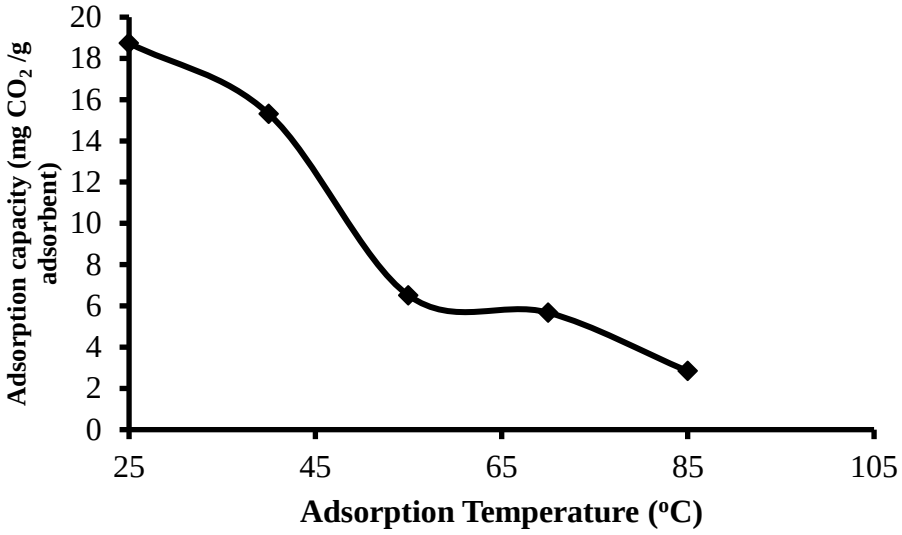

Figure 6.3: Effect of temperature on CO_2 adsorption capacity of SOD-ZMOF-chitosan using TGA

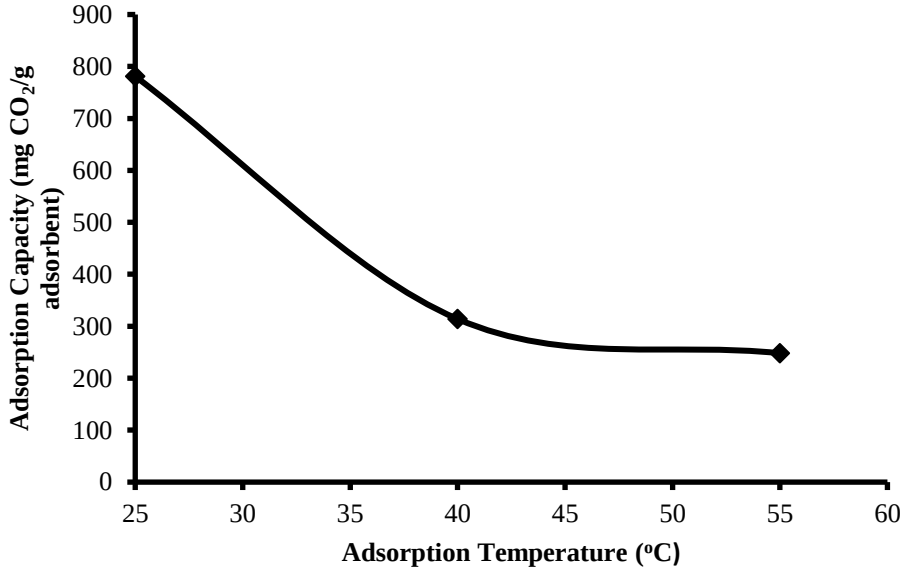

Figure 6.4: Effect of temperature on CO_2 adsorption capacity of SOD-ZMOF-chitosan using packed-bed column

6.3.3. Effect of gas Flowrate on the CO_2 adsorption capacity of SOD-ZMOF-chitosan

SOD-ZMOF-chitosan was evaluated at different adsorption gas mixture flowrates using the TGA and packed-bed column depicted in Figure 3.2. The adsorption capacity of SOD-ZMOF-chitosan was evaluated at flowrates range from 25-70 ml/min and 30-90 ml/min for the packed-bed column and TGA, respectively, at constant temperature and pressure of 25℃

and 1 bar. Figures 6.3 and 6.4 depict the CO_2 adsorption capacity of SOD-ZMOF-chitosan at these varying adsorption flowrates. At the lowest adsorption flowrate of 25 ml/min CO_2 adsorption capacity of SOD-ZMOF-chitosan was 781 mg CO_2/ g adsorbent and at a high adsorption flowrate of 70 ml/ min the adsorption capacity was just 194 mg CO_2/ g adsorbent for the packed-bed column (see Figure 6.4). For the TGA, adsorption capacity of SOD-ZMOF-chitosan at a low adsorption flowrate of 30 ml/min was 23 mg CO_2 / g adsorbent and at a high adsorption flowrate of 90 ml/min it was 20 mg CO_2 / g adsorbent. In both the TGA and packed-bed column, adsorption capacity decreased with increase in adsorption flowrate. This could be because at low adsorption flowrates the CO_2 gas has high superficial velocity which results to less contact time between the CO_2 gas and the adsorbents compared to low adsorption flowrates. Superficial velocity is simply defined as the volumetric flowrate of the gas divided by the cross sectional area thus increase in adsorption gas flowrate results in increase in superficial velocity. Less contact time means there is adsorption time at the surface of the adsorbent resulting in the adsorption of fewer gas molecules at higher adsorption flowrates.

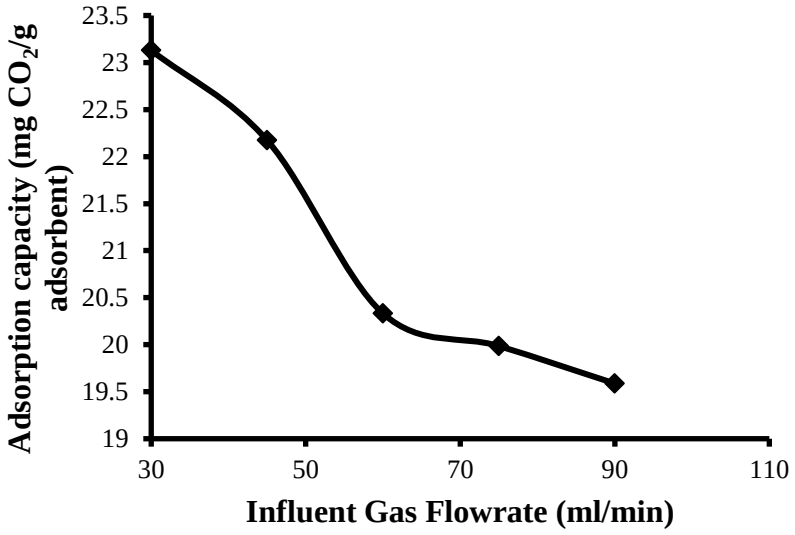

Figure 6.5: Effect of gas flowrate on CO_2 adsorption capacity of SOD-ZMOF-chitosan using TGA

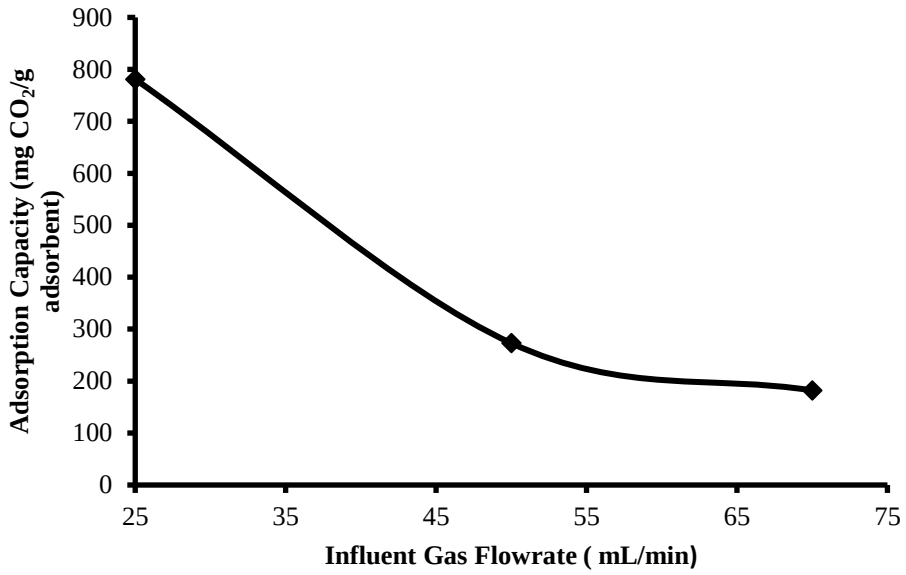

Figure 6.6: Effect of gas Flowrate on CO_2 adsorption capacity of SOD-ZMOF-chitosan using packed bed column

In literature, several researchers usually use TGA to investigate CO_2 adsorption capacity of their adsorbents. In this study CO_2 was evaluated using the TGA and packed-bed column at different temperatures and gas flowrates. However similar trend regarding the influence of operating conditions on CO_2 adsorption capacity of the synthesised adsorbent was displayed with the TGA (see Figures 6.3-6.6). However the adsorption capacity obtained when a packed-bed column is higher than that obtained using a TGA in spite of using 100% CO_2 was used for the TGA and 15% CO_2/85% N_2 for the packed column. In the packed-bed column, there is greater mass transfer between the adsorbent and adsorbate (CO_2). Extremely higher adsorption capacity obtained using the packed-bed column could be attributed to the systematic errors from the set-up. However it should be emphasized that the experiments were repeated severally for repeatability and accuracy as explained in Chapter 5.

6.4. Summary

The final objective of this study was to investigate the effect of operating conditions on the CO_2 adsorption capacity of SOD-ZMOF-chitosan. Two operating conditions (adsorption temperature and flowrate) were investigated using the traditional approach. CO_2 adsorption capacity of SOD-ZMOF-chitosan increased with decrease in adsorption temperatures and flowrates. At the 25℃, CO_2 adsorption capacity was high as compared to the highest adsorption temperature investigated. CO_2 adsorption capacity was highest at low adsorption

flowrates as compared to high adsorption flowrates for both the TGA and the packed-bed column. The highest adsorption capacity of 781 mg CO_2/ g adsorbent was obtained at 25℃, 1 bar and 25 ml/ min for the packed-bed column. With the TGA, the highest adsorption capacity was 23 mg CO_2/ g adsorbent at 25℃, 1 bar and 30 ml/ min. The significant difference in adsorption capacity when the packed-bed column and the TGA were used has been discussed in detail in chapter 5.

References

1. Mori Y, Yamada A. Dynamic behaviour of an adsorption column heat exchanger. Proceedings of the tenth international heat transfer conference. Brighton, UK.1994; 161:166
2. Yu C, Huang C, Tan C. A Review of CO_2 Capture by Absorption and Adsorption. Taiwan Association for Aerosol Research. 2012; 745:769-12

CHAPTER 7: CONCLUSIONS AND RECOMMENDATIONS

7.1. Conclusions

Climate change is a major challenge that the whole world is facing due to the increase in atmospheric concentration of GHG, especially CO_2. Increase in atmospheric concentrations of CO_2 has resulted in the capture of CO_2 from point sources such as coal fired power plants in an attempt to reduce the amount of CO_2 being released into the atmosphere. This is the first and most expensive stage of the process called CCS. CCS captures CO_2 from point sources and stores in a way that it would not affect the atmosphere. The high cost of CO_2capture methods has resulted in investment on research and development of capture technologies. Most common and mature capture technology is absorption; however this process has several drawbacks. Adsorption is a promising CO_2 capture alternative due to its ability to operate at medium temperature and pressure and being less energy intensive. For the aforementioned reasons, this work focused on synthesis and performance evaluation of SOD-ZMOF-chitosan for CO_2 capture through adsorption. The main aim of this work was to enhance the CO_2 adsorption capacity of SOD-ZMOF through impregnation of chitosan. The specific objectives were:

i) Can up-scaling synthesis protocol for producing SOD-ZMOF affect physicochemical properties of the synthesized crystals?
ii) Can SOD-ZMOF-chitosan composite adsorbent be synthesized successfully?
iii) What will be the performance of the adsorbent for post-combustion CO_2 capture?
iv) What will be the effect of operating variables on the CO_2 adsorption capacity of the material?

Up-scaling the synthesis protocol of SOD-ZMOF affected the surface area of the material as it had a low surface area compared to that reported in literature. However physiochemical properties (XRD and FTIR) of SOD-ZMOF were not affected. This observation confirms what has been reported in literature.

Effect of impregnation of chitosan on SOD-ZMOF on CO_2 capture by adsorption was investigated. First SOD-ZMOF was synthesized and chitosan was produced from chitin. Chitosan and SOD-ZMOF were then characterized using XRD, FTIR and BET. Then

chitosan was impregnated on SOD-ZMOF to produce SOD-ZMOF-chitosan which was also characterized using the aforementioned characterisation techniques.

XRD showed that SOD-ZMOF is a crystalline material and the XRD pattern obtained in this work was similar to that in literature (Chen *et al*., 2011). The XRD pecks of SOD-ZMOF-chitosan decreased but maintained a similar shape to that of just SOD-ZMOF meaning that chitosan was successfully impregnated and SOD-ZMOF maintained its crystallinity after chitosan impregnation.

FTIR spectra of SOD-ZMOF showed presence of functional groups that are also present in organic linker used to synthesize SOD-ZMOF meaning that SOD-ZMOF was successfully synthesized. FTIR spectra of SOD-ZMOF-chitosan showed a drastic decrease in the carboxylic acid band. It was speculated that this was due to the impregnation of chitosan which is a source of amine.

N_2 physisorption for BET surface area and pore volume was also conducted for SOD-ZMOF before and after chitosan impregnation. BET surface area, pore volume and pore size obtained in this work were lower than those obtained for SOD-ZMOF in literature and this could be due to interpenetration during up scaling the synthesis protocol in which total volume of the starting materials have been increased. Reports in literature show that up - scaling the synthesis of MOFs can lead to a reduction in surface area of the final product. In addition a drastic decrease in surface area, pore volume and pore size of SOD-ZMOF after chitosan impregnation was observed indicating a successful impregnation of chitosan on SOD-ZMOF.

SOD-ZMOF before and after chitosan impregnation were then evaluated for CO_2 capture using TGA and packed-bed column. First 100% CO_2 was used for CO_2 adsorption in a TGA and after determining that the synthesized adsorbent can capture pure CO_2, adsorbents were then evaluated in a packed-bed column using 15% CO_2. This was used in order to mimic flue gas conditions. In both TGA and packed-bed column, chitosan impregnated SOD-ZMOF had a high CO_2 adsorption capacity as compared to just SOD-ZMOF. This is due to the presence of amine groups on chitosan which have high affinity for CO_2. Packed-bed column displayed higher adsorption capacities than those of the TGA. This could be attributed to the enhanced direct contact between the gas and the adsorbent in the packed-bed column was used.

Effect of adsorption temperature as well as influent gas flowrate were investigated on the CO_2 adsorption capacity of SOD-ZMOF-chitosan. CO_2 adsorption capacity of SOD-ZMOF-chitosan increased with a decrease in temperature and inlet gas flowrate. This is expected as adsorption is an exothermic process, and an increase in flowrate increases the superficial velocity of the gas and thereby decreasing contact time between the gas and the adsorbent. Consequently, the maximum CO_2 adsorption capacity obtained at 25 ℃, 1 bar and inlet CO_2 flowrate of 60 ml/min was 23 mg CO_2/ g adsorbent for adsorption using a TGA and a maximum of 781 mg CO_2/ g adsorbent for packed-bed column at 25 ℃, 1 bar and inlet gas flowrate of 25 ml/min. After chitosan impregnation, CO_2 adsorption capacity of SOD-ZMOF increased by 39 % and 16 % using the TGA and the packed-bed column respectively. For industrial purposes, the packed-bed column can be easily up-scaled as compared to the TGA. In addition, packed-bed column has better mass transfer between gas and adsorbent than the TGA.

6.5. Recommendations

As far as could be ascertained, this is the first study on the scale-up study of the synthesis and evaluation of chitosan impregnated SOD-ZMOF for post-combustion CO_2 capture. It is recommended that future work should consider improving the synthesis procedure of the SOD-ZMOF-chitosan in order to minimize or avoid interpenetration of the solvent. The information provided in this study could pave the way for future investigation on up-scaling of the synthesis method of SOD-ZMOF for mass production of the material for CO_2 capture.

Synthesis of SOD-ZMOF-chitosan should be optimized by varying the concentration of chitosan to be impregnated on SOD-ZMOF. Traditional method was used to investigate the effect of operating variables such as adsorption temperature and influent flowrate. It is recommended that future work makes use of a statistical approach to investigate the effect of operating conditions on the CO_2 adsorption capacity of SOD-ZMOF-chitosan because the traditional approach always overlooks the interaction effects of these variables.

It is recommended that studies on desorption of SOD-ZMOF-chitosan are carried out. Desorption is an important process that recovers CO_2 from the adsorbent. Moisture is a challenge when it comes to post-combustion capture; therefore it is recommended that the effect of the presence of moisture in flue gas is investigated. Performance of the adsorbent for CO_2 capture should also be investigated using real flue from power plants.

Future work should look into optimization of the adsorption process using SOD-ZMOF-chitosan as adsorbents. It is important to identify conditions at which SOD-ZMOF-chitosan is more effective in order to optimize its CO_2 adsorption capacity.

Lastly, it was discovered in this study that the custom-built packed-bed adsorption column used for the evaluation of the performance of the up-scaled adsorbent might have over-estimated the adsorption capacity due to systematic error from the set-up. In addition, analysis of the N_2 gas effluent from the adsorption column was not possible with the gas analyser attached to the set-up. It is hereby recommended that the trouble-shooting of the set-up should be carried out to identify the problem leading to the systematic error. In addition, the set-up should be provided with a gas analyser that could measure N_2 as well.

APPENDICES

Appendix A

For analysis XRD characterization was done using a cobalt XRD radiation with a wavelength of 1.78897 angstroms. Results obtained from this characterization had to be compared with that from literature. In literature, XRD characterization was done using copper radiation with a wavelength of 1.542 angstroms. For the sake of comparison, a ratio was calculated in order to normalize the two different wavelengths. Calculations were done as follow:

Cobalt XRD ⟶ Copper XRD

Wavelength=1.78897 angstroms Wavelength=1.542 angstroms

Ratio of cobalt wavelength to copper wavelength

Ratio = $\frac{1.78897\ angstroms}{1.542\ angstroms}$ =1.162

This ratio was then used to normalize the wavelength of XRD cobalt data with copper wavelength by dividing cobalt raw XRD data by this ratio.

Appendix B: Adsorption runs and calculations results

B1. TGA

This shows the TGA adsorption data used to calculate the adsorption capacity

B.1.1. TGA Raw results

B.1.1.1 SOD-ZMOF and Chitosan

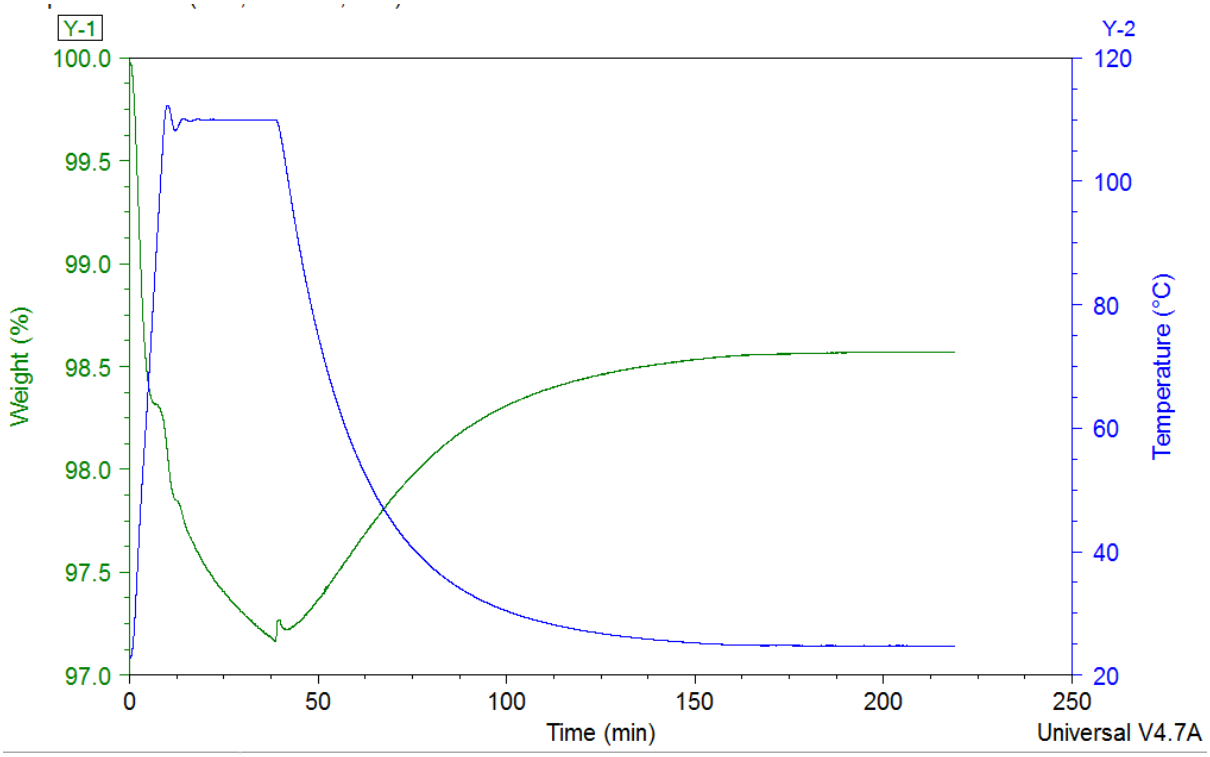

Figure B1: TGA for SOD-ZMOF at a flowrate of 30 ml/min, 1 bar and 25 ℃

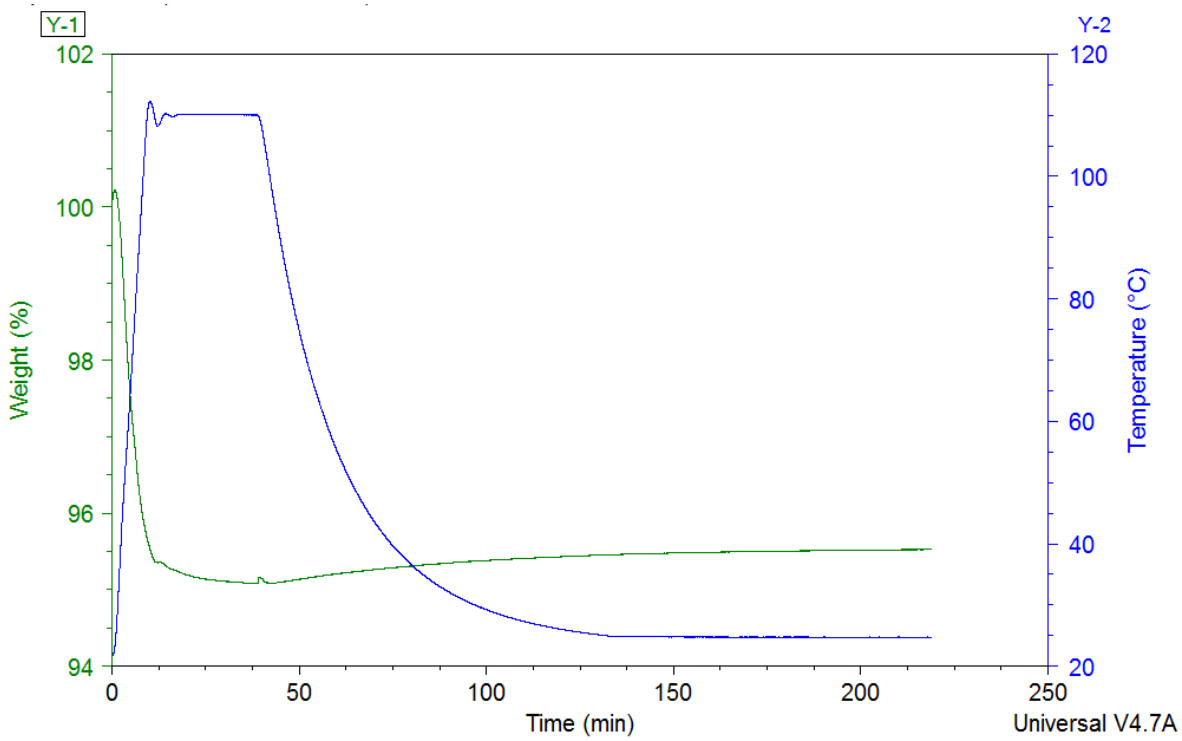

Figure B2: TGA for chitosan at a flowrate of 30 ml/min, 1 bar and 25 ℃

B.1.2. SOD-ZMOF-Chitosan

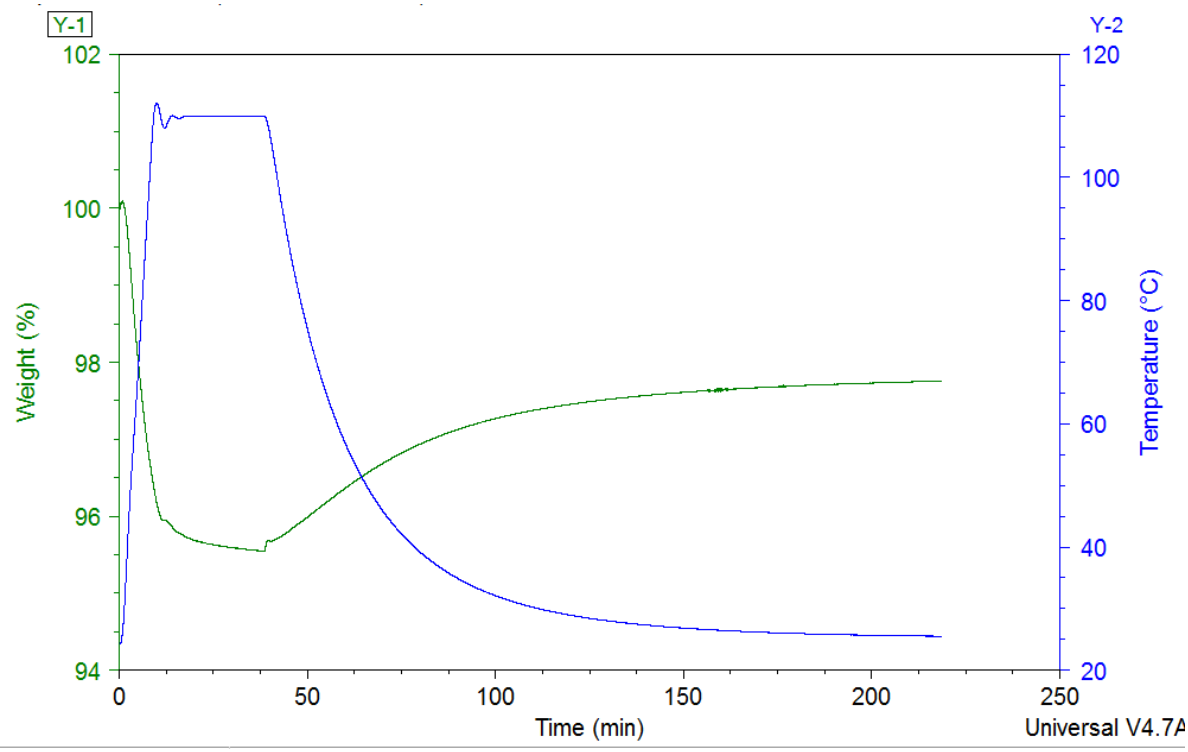

Figure B3: TGA for SOD-ZMOF-chitosan at a flowrate of 30 ml/min, 1 bar and 25 ℃

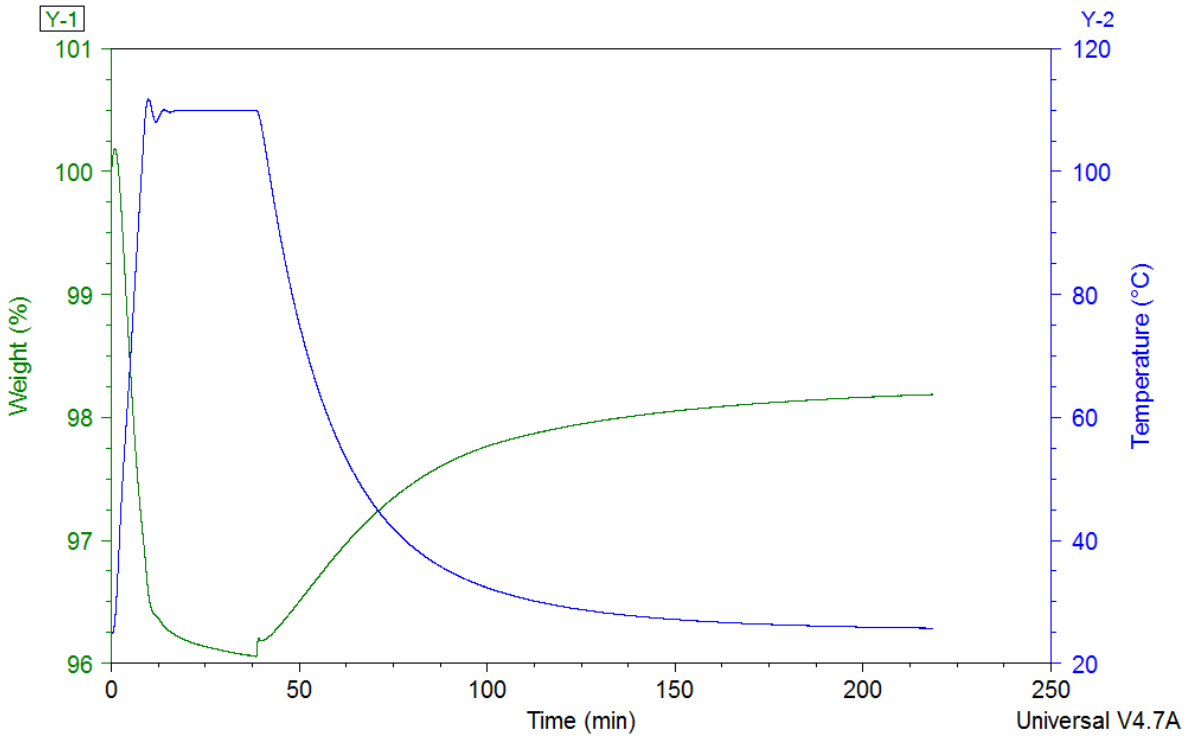

Figure B4: TGA for SOD-ZMOF-chitosan at a flowrate of 45 ml/min, 1 bar and 25℃

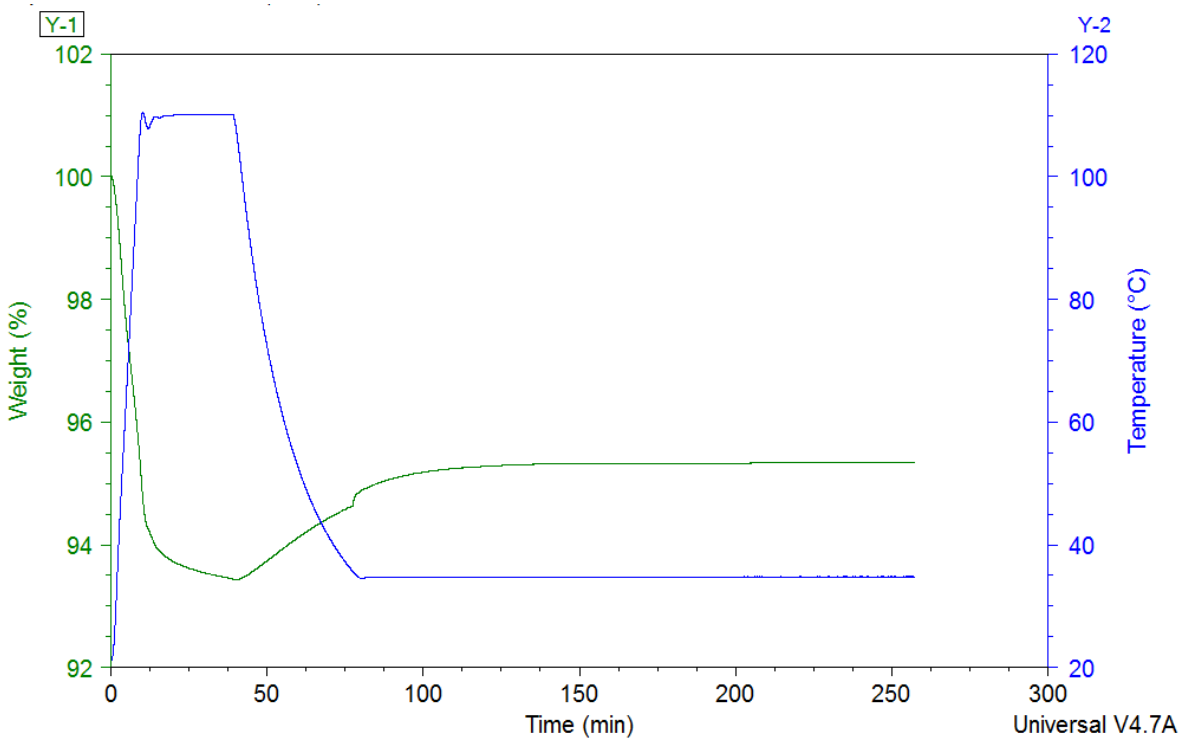

Figure B5: TGA for SOD-ZMOF-chitosan at a flowrate of 60 ml/min, 1 bar and 25 ℃

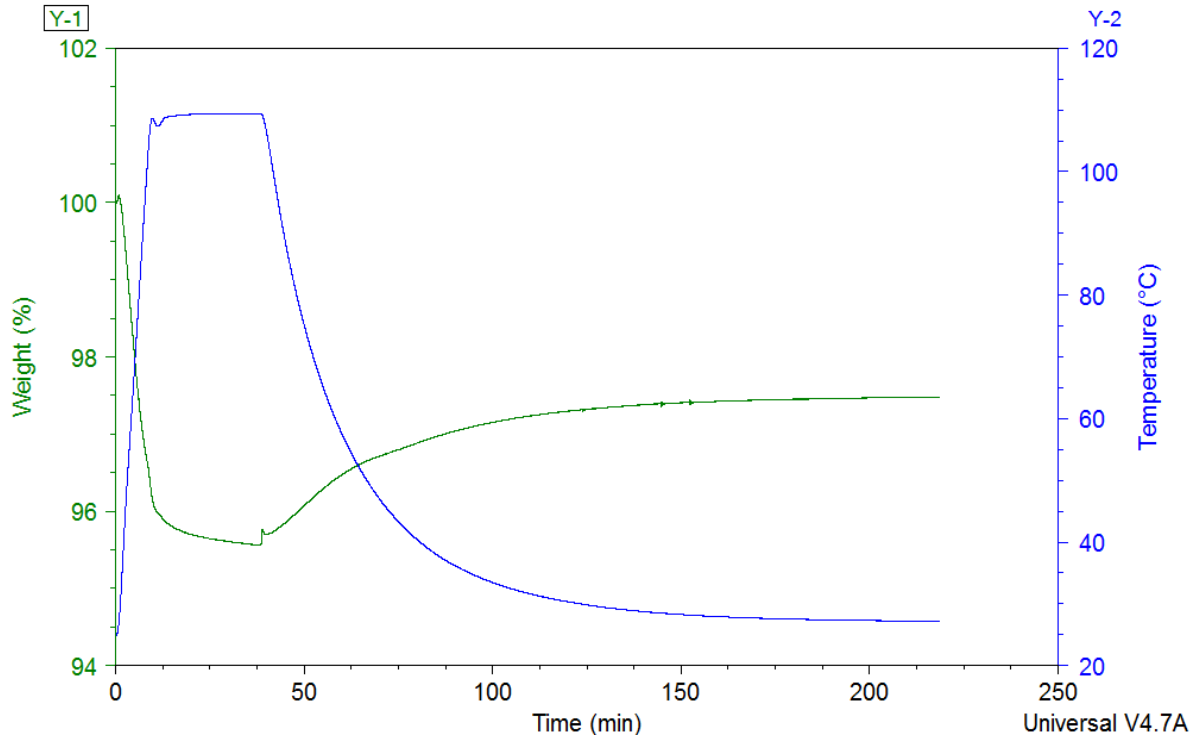

Figure B6: TGA for SOD-ZMOF-chitosan at a flowrate of 75 ml/min, 1 bar and 25 ℃

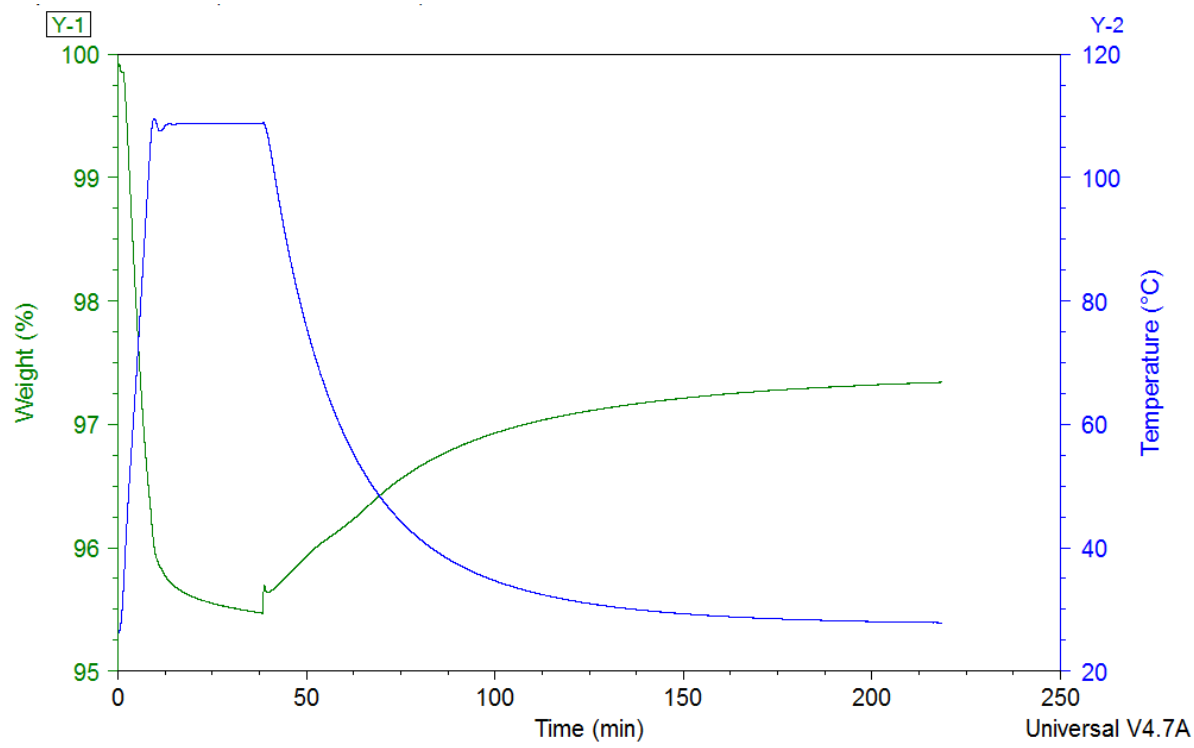

Figure B7: TGA for SOD-ZMOF-chitosan at a flowrate of 75 ml/min, 1 bar and 25 ℃

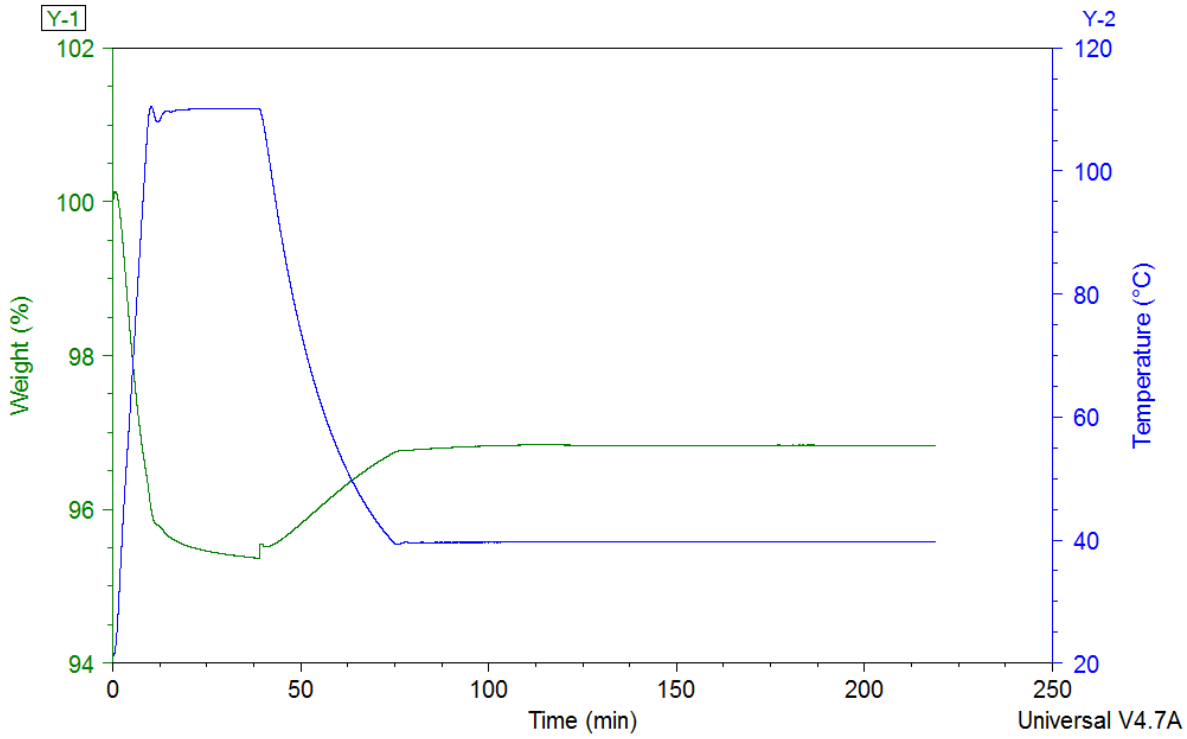

Figure B8: TGA for SOD-ZMOF-chitosan at a flowrate of 60 ml/min, 1 bar and 40 ℃

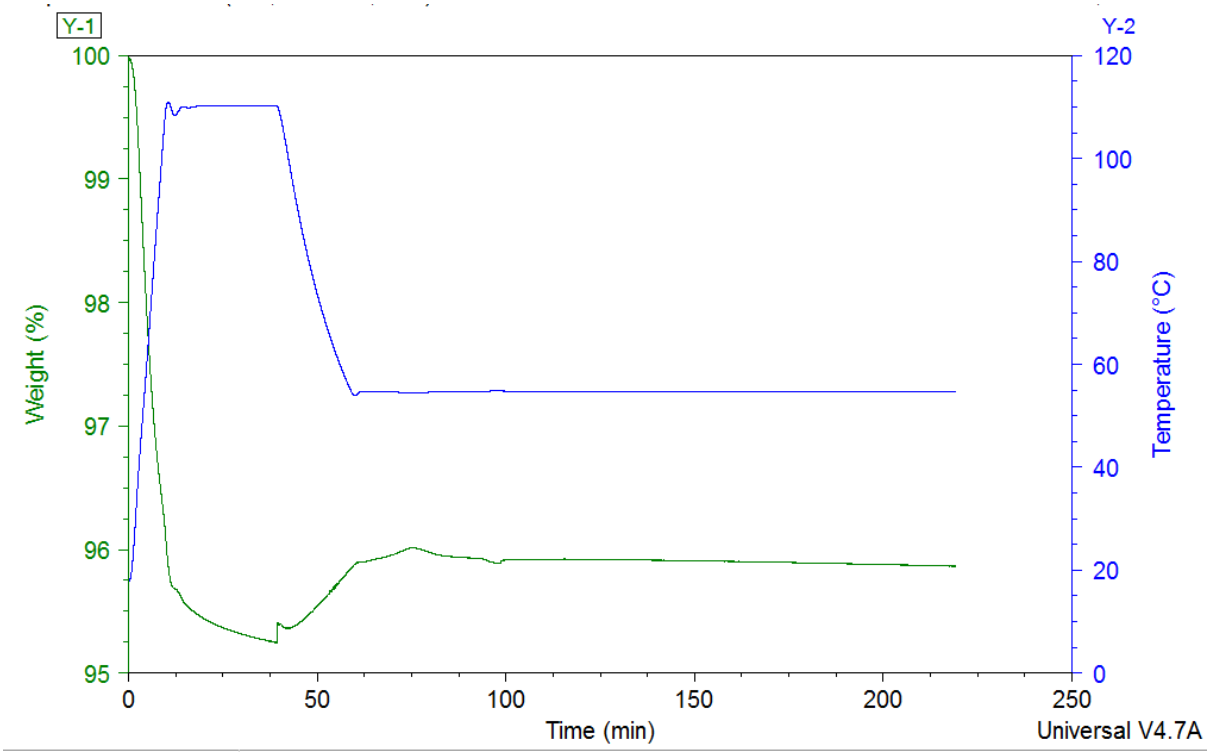

Figure B9: TGA for SOD-ZMOF-chitosan at a flowrate of 60 ml/min, 1 bar and 55 ℃

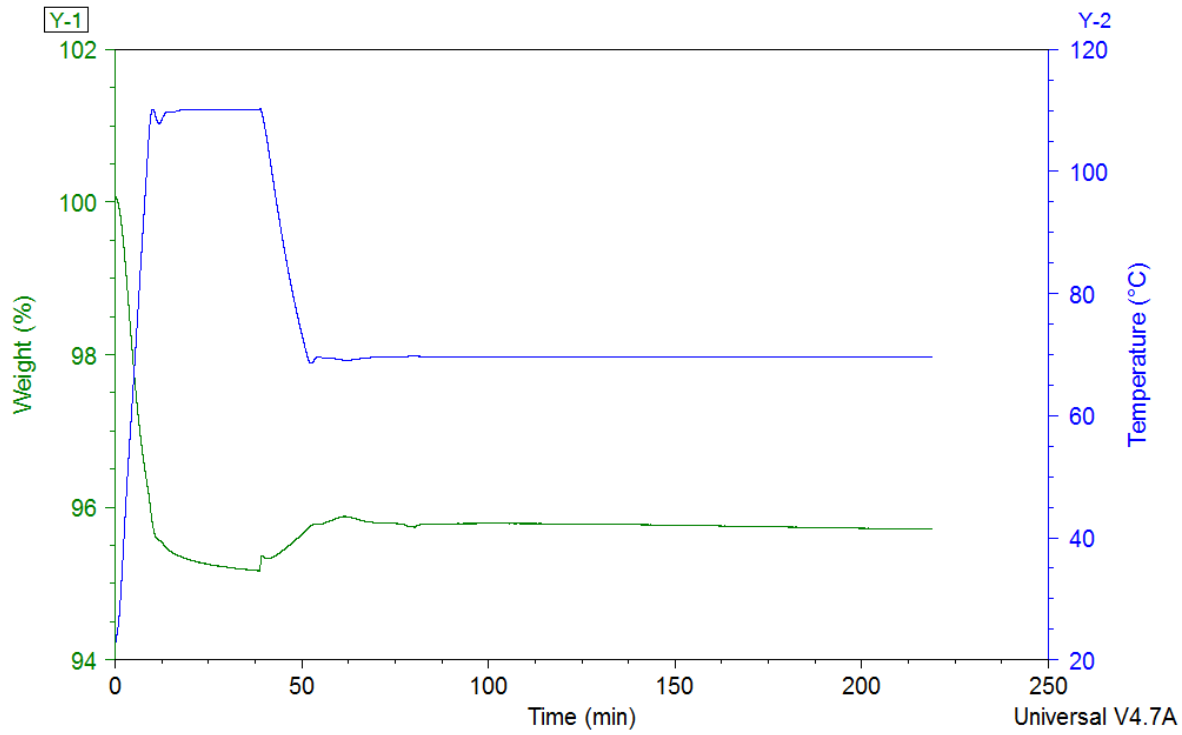

Figure B10: TGA for SOD-ZMOF-chitosan at a flowrate of 60 ml/min, 1 bar and 70 ℃

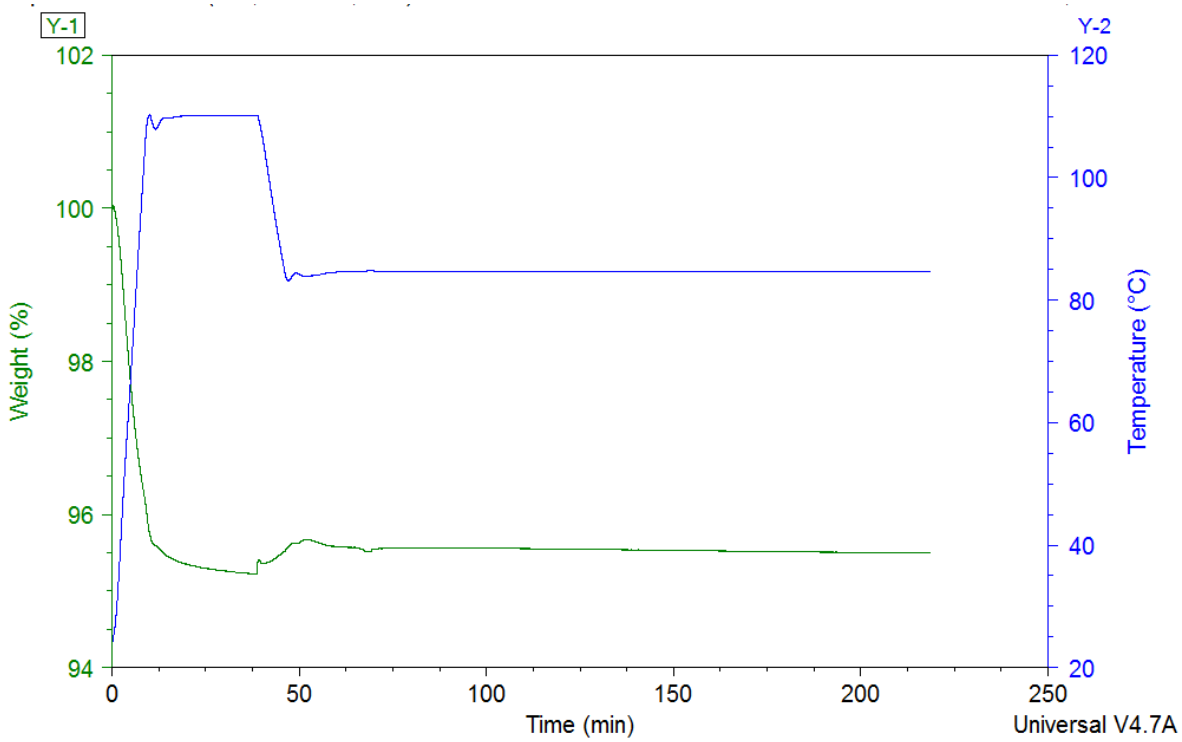

Figure B11: TGA for SOD-ZMOF-chitosan at a flowrate of 60 ml/min, 1 bar and 85 ℃

B1.2: Adsorption capacity as a function of time calculations

Table B1: TGA Adsorption capacity calculations for at 25℃, 1 bar and 30 ml/min

Experimental time (minutes)	Adsorption time (minutes)	Weight (%)	Adsorption Capacity (mg CO_2/ g adsorbent)
36	0	96	0
48	12	96	4
60	24	96	9
72	36	97	13
84	48	97	15
97	60	97	17
109	72	97	19
121	84	97	20
133	97	98	21
145	109	98	21
157	121	98	22
169	133	98	22
181	145	98	22
192	156	98	23
205	169	98	23
217	181	98	23

Table B2: TGA Adsorption capacity calculations for at 25℃, 1 bar and 45 ml/min

Experimental time (min)	Adsorption time (min)	Weight (%)	Adsorption capacity (mg CO_2/g adsorbent)
36	0	96	0
48	12	96	4
60	24	97	9
72	36	97	13
84	48	98	15
97	60	98	17
109	72	98	18
121	84	98	19
133	96	98	20
145	109	98	20
157	121	98	21
169	133	98	21
181	145	98	21
193	157	98	22
205	169	98	22
217	181	98	22

Table B3: TGA Adsorption capacity calculations for at 25℃, 1 bar and 60 ml/min

Experimental time (min)	Adsorption time (min)	Weight (%)	Adsorption capacity (mg CO_2/ g adsorbent)
36	0	95	0
48	12	96	4
60	24	96	9
72	36	97	14
85	48	97	16
97	60	97	17
109	72	97	18
125	89	97	19
137	101	97	20
145	109	97	20
157	121	97	21
169	133	97	21
181	145	97	21
193	157	97	21
205	169	98	21
217	181	98	21

Table B4: TGA Adsorption capacity calculations for at 25℃, 1 bar and 75 ml/min

Experimental time (min)	Adsorption time (min)	Weight (%)	Adsorption capacity (mg CO_2/ g adsorbent)
36	0	96	0
48	12	96	4
60	24	96	10
72	36	97	12
84	48	97	15
96	60	97	16
109	72	97	17
121	84	97	18
133	96	97	19
145	109	97	19
157	121	97	19
169	133	97	19
181	145	97	20
193	157	97	20
205	169	97	20
217	181	97	20

Table B5: TGA Adsorption capacity calculations for at 25℃, 1 bar and 90 ml/min

Experimental time (min)	Adsorption time (min)	Weight (%)	Adsorption capacity (mg CO_2/ g adsorbent)
36	0	95	0
48	12	96	4
60	24	96	7
72	36	97	11
85	49	97	13
96	60	97	15
108	72	97	16
121	84	97	17
133	96	97	17
145	108	97	18
157	120	97	18
169	133	97	19
181	145	97	19
193	157	97	19
205	169	97	19
217	181	97	19

Table B6: TGA Adsorption capacity calculations for at 25℃, 1 bar and 45 ml/min

Experimental time (min)	Adsorption time (min)	Weight (%)	Adsorption capacity (mg CO_2/ g adsorbent)
36	0	95	0
48	12	96	4
60	24	96	9
73	36	97	14
85	48	97	15
97	60	97	15
109	73	97	15
121	85	97	15
139	103	97	15
145	109	97	15
157	121	97	15
169	133	97	15
181	145	97	15
193	157	97	15
205	169	97	15
217	181	97	15

Table B7: TGA Adsorption capacity calculations for at 25℃, 1 bar and 60 ml/min

Experimental time (min)	Adsorption time (min)	Weight (%)	Adsorption capacity (mg CO_2/ g adsorbent)
36	0	95	0
48	12	95	2
61	24	96	7
73	36	96	8
88	52	96	7
97	61	96	7
109	73	96	7
121	85	96	7
133	97	96	7
145	109	96	7
157	121	96	7
169	133	96	7
182	145	96	7
194	157	96	7
206	170	96	6
218	182	96	6

Table B8: TGA Adsorption capacity calculations for at 25℃, 1 bar and 75 ml/min

Experimental time (min)	Adsorption time (min)	Weight (%)	Adsorption capacity (mg CO_2/g adsorbent)
36	0	95	0
48	12	96	4
60	24	98	28
72	36	96	6
85	48	96	6
97	60	96	6
109	73	96	6
121	85	96	6
133	97	96	6
145	109	96	6
157	121	96	6
169	133	96	6
181	145	96	6
193	157	96	6
205	169	96	6
217	181	96	6

Table B9: Packed-bed Adsorption capacity calculations for at 25℃, 1 bar and 25 ml/min

y_f	0.152
y	0.132
Q_f (ml/min)	22.90268
Time (min)	55.04
t_t (min)	7.242105
T_s (K)	273
P_s (bar)	1
E_t	0.15
V_b (ml)	0.150816
P_b (bar)	0.7
R (ml.bar/K.mol)	83.1451
T_b (K)	297.5
Mass of adsorbent (g)	0.05
Adsorption capacity (mol/mg)	0.022212
Adsorption capacity (mg/g)	977.3275

Table B10: Packed-bed Adsorption capacity calculations for at 40℃, 1 bar and 25 ml/min

y_f	0.151
y	0.12
Q_f (ml/min)	21.80511
Time	25.28
t_t (min)	5.189934
T_s (K)	273
P_s (bar)	1
E_t	0.15
V_b (ml)	0.150816
P_b (bar)	0.7
R (ml.bar/K.mol)	83.1451
T_b (K)	313
Mass of adsorbent (g)	0.05
Adsorption capacity (mol/mg)	0.015055
Adsorption capacity (mg/g)	662.4109

Table B11: Packed-bed Adsorption capacity calculations for at 55℃, 1 bar and 25 ml/min

y_f	0.151
y	0.123
Q_f (ml/min)	22.90268
Time	21.63
t_t (min)	4.010861
T_s (K)	273
P_s (bar)	1
E_t	0.15
V_b (ml)	0.150816
P_b (bar)	0.7
R (ml.bar/K.mol)	83.1451
T_b (K)	328
Mass of adsorbent (g)	0.05
Adsorption capacity (mol/mg)	0.01222
Adsorption capacity (mg/g)	537.6777

Table B12: Packed-bed Adsorption capacity calculations for at 25℃, 1 bar and 70 ml/min

y_f	0.151
y	0.13
Q_f (ml/min)	45.80537
Time	11.73
t_t (min)	1.631325
T_s (K)	273
P_s (bar)	1
E_t	0.15
V_b (ml)	0.150816
P_b (bar)	0.7
R (ml.bar/K.mol)	83.1451
T_b (K)	298
Mass of adsorbent (g)	0.05
Adsorption capacity (mol/mg)	0.00994
Adsorption capacity (mg/g)	437.3536

Appendix C: Adsorption Equipment

C1. Packed-bed column

Figure D1 depicts the actual adsorption set-up of the packed-bed column used for CO2 adsorption evaluation in this work. The set- up is connected to nitrogen and 15% (balance being nitrogen) gas cylinders. The set-up is also connected to a CO_2 gas analyser which detects the CO2 concentration before, during and after adsorption. It also consists of a flowmeter that reads the inlet CO_2 flowrate in ml/min as it enters the system, a temperature and pressure control system used to set either temperature or pressure to desired values. An overview of this equipment is in figure 3.2

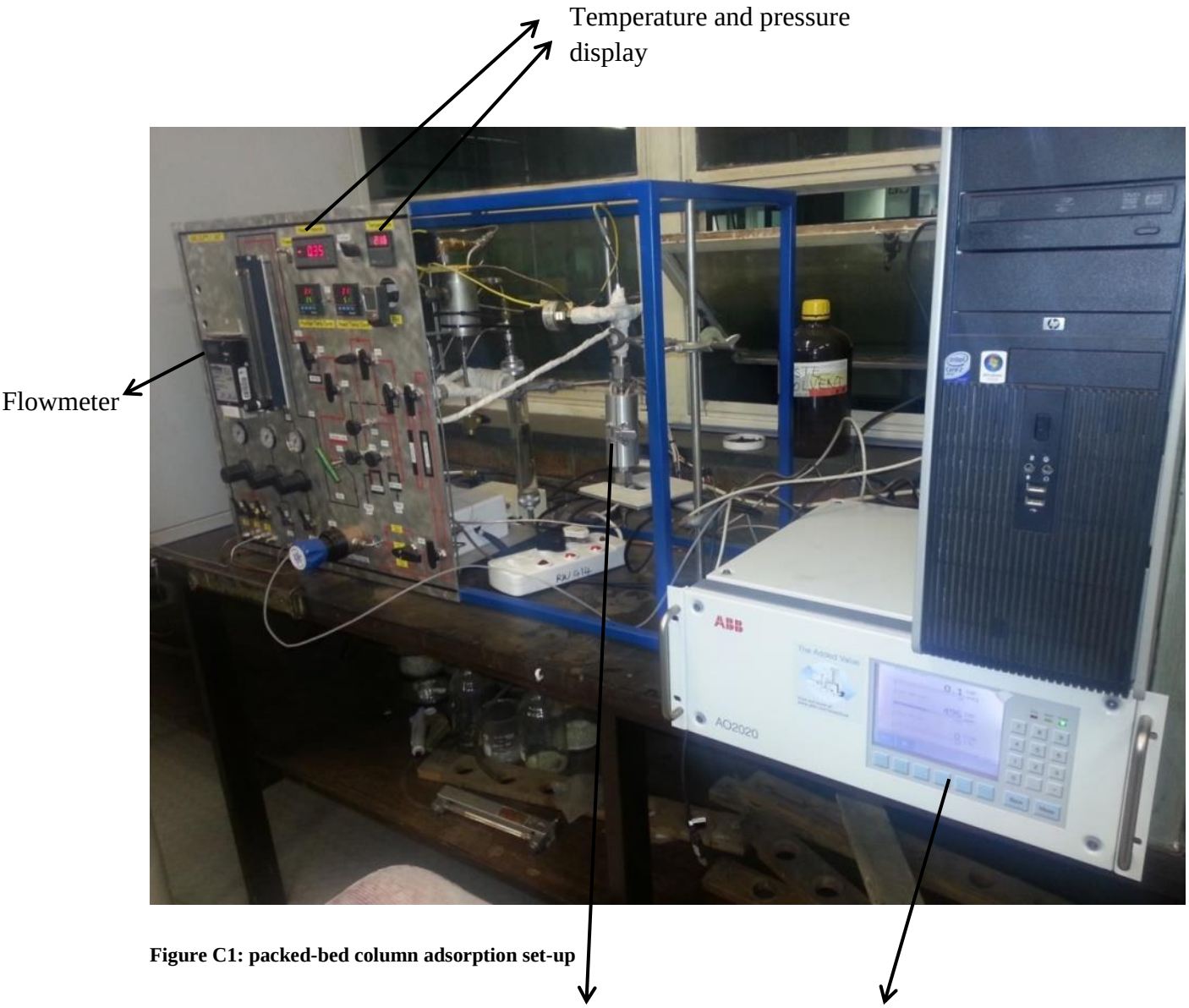

Figure C1: packed-bed column adsorption set-up

Appendix D: Published papers

Available online at www.sciencedirect.com

ScienceDirect

Energy Procedia 114 (2017) 2429 – 2440

Energy Procedia

13th International Conference on Greenhouse Gas Control Technologies, GHGT-13, 14-18 November 2016, Lausanne, Switzerland

Chitosan-impregnated sod-Metal Organic Frameworks (sod-ZMOF) for CO_2 capture: Synthesis and performance evaluation

Muofhe. C .Singo[a], Xitivhane. C. Molepo[a], Olugbenga O. Oluwasina[b], Michael.O.Daramola[a]*

[a]*School of Chemical and Metallurgical Engineering, Faculty of Engineering and the Built Environment, University of the Witwatersrand, Private Bag X3, Wits 2050, Johannesburg, South Africa*

[b]*Department of Chemistry, Federal University of Technology, Akure, Ondo State, Nigeria*

Abstract

A sodalite zeolite-like metal organic framework (sod-ZMOF) was impregnated with chitosan and evaluated for carbon dioxide (CO_2) capture. Sod-ZMOF before and after impregnation was characterized by x-ray diffraction (XRD), Fourier transform infrared spectroscopy (FTIR) and N_2 physisorption. Chitosan impregnated sod-ZMOF (sod-ZMOF-chitosan) was then evaluated for CO_2 adsorption using a packed bed column using a gas mixture containing 15% CO_2 and 85% N_2. Sod-ZMOF-chitosan was evaluated at different temperatures and flow rates to understand the effect of these variables on the adsorption performance of the material. Sod-ZMOF-chitosan reached its best adsorption capacity of 978 mg CO_2/g adsorbent at a temperature of 25℃, flow rate of 25 ml/min and a pressure of 1 bar.

Peer-review under responsibility of the organizing committee of GHGT-13.

Keywords: Adsorption; Chitosan; CO_2 capture; MOFs; Packed-bed column

* Corresponding author. Tel.: +27117177536.
E-mail address: michael.daramola@wits.ac.za

Peer-review under responsibility of the organizing committee of GHGT-13.
doi:10.1016/j.egypro.2017.03.1390

1. Introduction

Climate change is among one of the major challenges that the world is facing today. This is due to increase in greenhouse gases concentration, especially CO_2 in the atmosphere. Increase in atmospheric concentration of CO_2 has created an interest to reduce due to its effect on the environment. About 85% of the worlds energy needs is produced from fossil fuel [1] Fossil fuels will continue to be the primary source of energy for the world [2]. Fossil fuels are combusted to produce energy and CO_2 is an inevitable by-product. Removal of CO_2 from post combustion outlet streams is achieved through CO_2 capture. This is the first stage in a process called carbon capture and storage (CCS). CCS reduces the amount of CO_2 released into the atmosphere by capturing it from fossil fuel powered plants and storing it in a way that will not affect the atmosphere. However, the capture stage is challenging due to the high temperature and low partial pressure of CO_2 in the flue gas from the combustion outlet stream [3]. It is therefore essential to investigate capture technologies for CO_2 reduction. Various technologies including absorption, membrane separation and adsorption have been developed and are being actively investigated.

Absorption using synthetic liquid amines is the most mature and commercialized CO_2 capture technology. However, this technology possesses several drawbacks such as the large amount of energy required to regenerate the solvent and corrosive nature of the solvent [1, 4]. This calls for an efficient alternative for CO_2 capture. Adsorption using solid adsorbents exhibits many advantages in dealing with CO_2 post combustion capture [3]. Adsorption is the attachment of gas or solid molecules on a solid surface [5]. The aforementioned technology is less energy intensive as it can operate at moderate temperature and pressure [6]. Several kinds of solid materials such as carbon based materials, Silica based materials, zeolites and metal organic frameworks (MOFs) have been developed and investigated for CO_2 adsorption [1, 4].

MOFs are highly crystalline materials that have metal ions as centres and organic materials as linkers [7]. MOFs have been synthesized and investigated for CO_2 capture due to their high surface area, high porosity, open metal sites and desirable chemical properties [7]. There are different types of MOFs depending on choice of building blocks (metal ion, organic linker and structure directing agent). Zeolite-like metal organic frameworks (ZMOFs) are a member of the MOF family with topologies similar to that of zeolites [8]. ZMOFs with sodalite (sod) and *rho* topologies have been investigated for CO_2 capture by Chen et al [8]. Chen et al. [8] reported adsorption capacity of 53 and 51 mg CO_2/ g adsorbent for sod-ZMOF and rho-ZMOF respectively [8]. These ZMOFs showed relatively high CO_2 adsorption capacity and selectivity at ambient temperature and pressure as compared to other types of MOFs.
Additionally, the properties of MOFs can be enhanced by incorporating appropriate functional groups to the MOF structure through grafting, impregnation and ion exchange to improve its CO_2 adsorption capacity [9]. The Amine functional group is of particular interest for incorporating in solid adsorbents. This is because the interaction between basic modified amine active sites and acidic CO_2 enables adsorption by covalent bonding [4]. A major advantage of amine based adsorbents is that they require low heat of regeneration as compared to aqueous amines [4]. Chen *et al* [10], grafted ethylenediamine (EDA) on sod-ZMOF to enhance its adsorption capacity and EDA grafted sod-ZMOF gave a 30% increase in adsorption capacity as compared to the ordinary sod-ZMOF [10].

In spite of the aforementioned advantages, amine-based adsorbents have drawbacks such as high cost and the environmental impact associated with synthetic amines; making it challenging for this adsorbents to be commercialized [4]. This calls for an alternative material that has strong affinity for CO_2 but which is also less expensive and has less impact on the environment. This work proposes chitosan as an alternative source of amine functional group to be impregnated on sod-ZMOF. Chitosan is a biocompatible, biodegradable and non-toxic polymer derived from chitin [11]. Chitin is a natural resource produced from crabs, insects and shrimps [11, 12]. Chitosan is a green material and is the second largest most abundant polymer on earth [11]. Properties of chitosan include high viscosity, high solubility in various media, ability to form films and capability to bind with various metal ions [11]. Due to its unique properties, chitosan has been applied in industries such as wastewater treatment, food industry, cosmetics, and agriculture and biomedical [11]. The presence of functionalities such as amine ($-NH_2$) and hydroxyl (-OH) in the chitosan molecules provides basis for interaction with other materials [13]. Therefore, of recent chitosan has been receiving great attention to be used as novel functional composite material [11]. Chitosan, being a biodegradable organic material with several anime groups depending on its degree of deacetylation, can be a

green material that could be used to substitute synthetic liquid amine chemical. Also, the final product; sod-ZMOF-chitosan would have very little environmental effect.

Against this background, the current work investigated the synthesis of sod-ZMOF-chitosan adsorbent through impregnation of chitosan onto sod-ZMOF as well as the evaluation of the adsorbent. Furthermore, the influence of temperature and gas flow rate on chitosan-impregnated sod-ZMOF CO_2 adsorption capacity was investigated. Chitosan was impregnated into sod-ZMOF in order to improve the chemical surface of sod-ZMOF so as to enhance the adsorption capacity of sod-ZMOF.

2. Experimental

2.1. Materials

The chemicals used in the study: 4,5-Imidazoledicarboxylic acid, imidazole, indium (III) nitrate hydrate, hydrochloric acid, sodium hydroxide and solvents; N,N-dimethylformamide (DMF), nitric acid, acetonitrile and acetic acid were all purchased from Sigma Aldrich South Africa. The chitin was obtained from the shell of crabs (usually a waste material from restaurants). The gas mixture, 15%-85% CO_2-N_2, and nitrogen baseline were obtained from Afrox, South Africa.

2.2. Synthesis of sod-ZMOF and sod-ZMOF-chitosan

2.2.1. Synthesis of Sod-ZMOF

The method used to synthesize sod-ZMOF in this study was adapted from the work reported by Chen *et al* [8]. About 2.1 g of 4.5-imidazoledicarboxylic acid, 1.5 g of indium (III) nitrate hydrate ($In(NO_3)_3.2H_2O$), 150 mL N,N-dimethylformamide (DMF), 50 mL acetonitrile (CH_3CN), 2.0 g imidazole in 20 mL DMF and 4.4 mL nitric acid (HNO_3) in 30 mL DMF were added into a 1000 mL flask. The solution was mixed thoroughly until a clear solution was obtained. The solution was heated up to 85℃ under reflux for 12 h. After 12 h, the temperature was increased to 105℃ and heating continued for 23 hours. Polyhedral crystals formed were collected by filtration; washed with methanol to remove any DMF from the pores and surface and then dried in an oven at 100 ℃ for 2 h. The dried white poly crystals obtained were sod-ZMOF.

2.2.2. Preparation of chitosan

The crab flesh was removed, and the exoskeletons were thoroughly washed and sun dried. The dried exoskeletons were then chopped into smaller sizes, pulverized to a particle size of < 74 nm. For preparation of chitosan, chitin was sieved and subjected to demineralization, deproteinization and decolonization. Chitin was added to 10 % (v/v) hydrochloric acid (HCl) with a solvent to solid ratio of 1:10. The reaction was carried out at 65 ℃ for 2 h with continuous stirring, after which the obtained material was filtered and washed with distilled water until filtrate pH was neutral. The resulting sample was dried in an oven at 50 ℃ for 24 h. The demineralized chitin was added to 4 % (w/v) sodium hydroxide (NaOH) with a solvent to solid ratio of 1:10 and heated at 65 ℃ for two h with continuous stirring. The resulting product was then filtered and washed with distilled water to a neutral pH. The sample was dried in an oven at 50 ℃ for 24 h. Thereafter, about 50 g of the deproteinized chitin was added to 50% (w/v) of sodium hydroxide (NaOH) at 90 ℃ for 5 h with continuous stirring. The resultant product was filtered, washed with distilled water to a neutral pH and dried in an oven at 50 ℃ for 24 h.

2.2.3. Impregnation of chitosan in sod-ZMOF

The procedure used for the impregnation of chitosan onto sod-ZMOF was adapted from the work reported by Sun *et al*. [14]. Chitosan was dissolved in 2 wt. % acetic acid solution and stirred at 80 ℃ for 1 h to obtain 2 wt. % chitosan

solution. 1 g of sod-ZMOF was added into the solution under stirring for 1 h. The suspension mixture was filtered and the obtained product dried in an oven at 50 ℃ for about 2 h.

2.3. Characterization

X-ray diffraction (XRD) analysis was carried out on the sample in order to check the purity and crystallinity of synthesized adsorbent. The XRD patterns in this study were obtained using a CoKα radiation with a wavelength (λ) of 1.79$\dot{A}$. Fourier transform infrared spectroscopy (FTIR) analysis was carried out for surface chemistry of the synthesized adsorbent. N_2 physisorption at 77 K was carried out to determine the BET surface area, pore volume and the pore size of the synthesized adsorbent.

2.4. Performance evaluation of the adsorbent for post-combustion CO_2 capture

Adsorption set-up depleted in Figure 1 was used to evaluate the CO_2 adsorption performance of the synthesized sod-ZMOF-chitosan. The set-up consisted of a packed-bed column connected to a CO_2 detector in order to read the CO_2 concentration before, during and after adsorption. About 0.05 g of the adsorbent was packed in the column. The sample in the column was then heated from room temperature to 110℃ under continuous flow of nitrogen through the sample and held for another 30 minutes at 110^{o}C to remove impurities such as moisture from the adsorbent. Then the temperature was reduced to 25 ^{o}C. A gas mixture, containing 15% CO_2 and 85% N_2, was passed through the sample at a flow rate of 50 ml/min and a pressure of 1 bar for 1 h. The initial CO_2 concentration in the feed stream was determined using a gas analyser by by-passing the adsorption column. Amount of CO_2 adsorbed during the experiment was obtained according to Becnel et al. [15] using Equation (1):

$$q = \frac{\frac{y_f Q_f t_t P_s}{RT_s} - \frac{y_f \varepsilon_T V_b P_b}{RT_b}}{m_{adsorbent}} \quad (1)$$

Where q is the amount of CO_2 adsorbed in mol/g adsorbent (to express the amount in mg CO_2/ g adsorbent, q was multiplied by the molar mass of CO_2), y_f is the mole fraction of CO_2 in the feed, Q_f is the volumetric flow rate of the feed stream. P_s and T_s are the standard pressure and temperature, respectively. R is the universal gas constant; ε_T is the total porosity of the bed; $m_{adsorbent}$ is the mass of the adsorbent and t_t, is the adsorption time. The aforementioned procedure was repeated at 40 ^{o}C, and 70 ^{o}C with constant feed flow rate and then repeated for varying feed flow rate keeping temperature and pressure constant at 25 ^{o}C and at 1 bar, respectively. The gas mixture employed in the study was used to mimic the composition of flue gas expected from a typical coal-fired power plant.

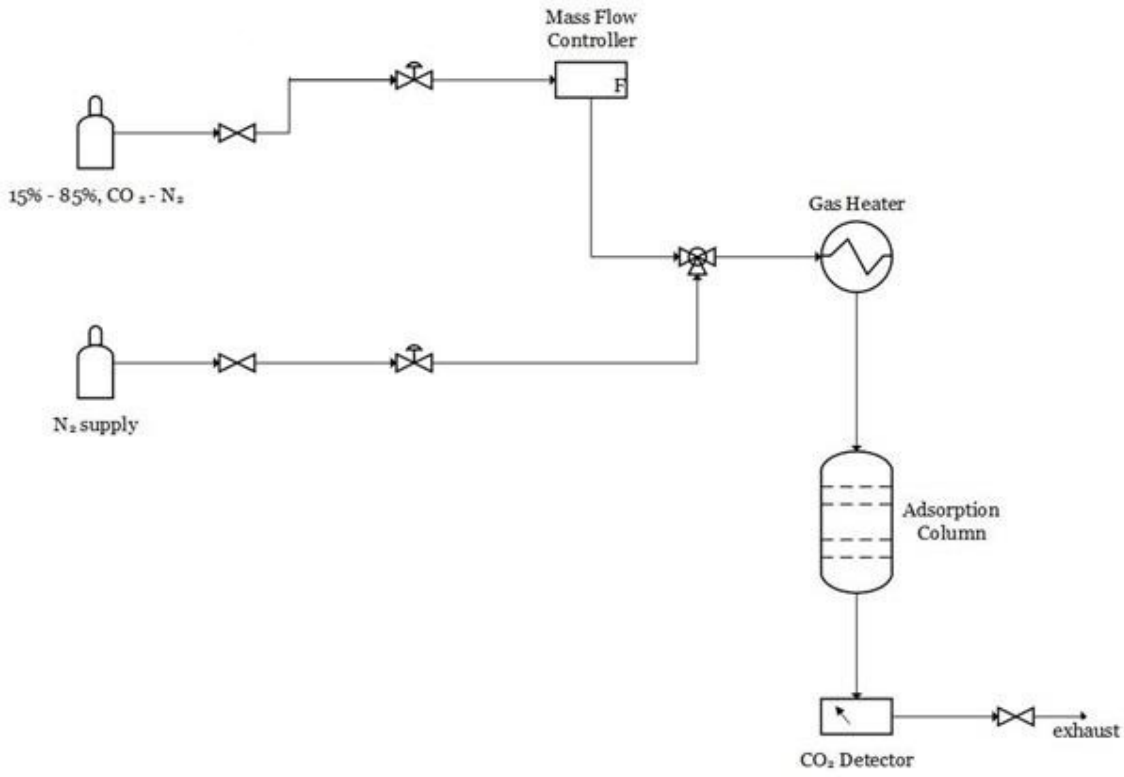

Figure 1: Adsorption set-up for CO_2 adsorption

3. Results and Discussion

3.1. Physicochemical characterization

Figure 3 depicts the XRD patterns of sod-ZMOF before and after chitosan impregnation. XRD pattern of sod-ZMOF was compared with those from Calleja *et al* [16] which confirmed that the synthesized material is crystalline and similar to that reported in literature. XRD pattern were obtained for chitosan impregnated sod-ZMOF in order to determine if sod-ZMOF maintained its crystanallity after chitosan impregnation. The XRD pattern of chitosan impregnated sod-ZMOF shows a similar shape to that of sod-ZMOF. This indicates that the structure of sod-ZMOF was still conserved after chitosan impregnation.

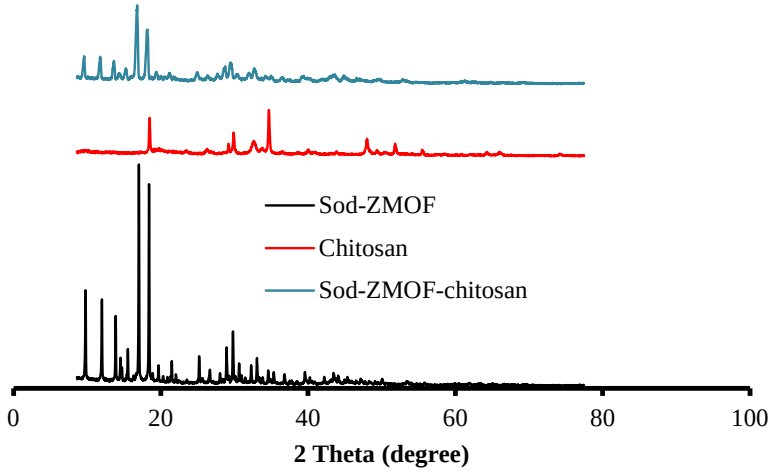

Figure 2: XRD pattern of sod-ZMOF before and after chitosan impregnation

The FTIR spectra of sod-ZMOF and sod-ZMOF-chitosan are depicted in figure 4. The organic linker in sod-ZMOF is 4.5-Imidazoledicarboxylic acid and as such it is expected that sod-ZMOF and this organic linker have similar functional groups. The functional groups present in 4.5-Imidazoledicarboxylic acid are amine (N-H), carboxylic acid (O-H), aromatics (C-C (in ring)), aromatic amine (CN) and (C=O). The FTIR analysis of sod-ZMOF in Figure 3 shows the presence of COOH at a wavelength of 3178 cm^{-1}, C-C (in ring) at a wavelength of 1476 cm^{-1}, C-N at a wavelength of 1105 cm^{-1}, N-H at a wavelength of 779 cm^{-1} and C=O at a wavelength of 1700 cm^{-1}, which therefore confirms the successful synthesis of sod-ZMOF. Refer to table 1 for interpretation. Figure 3 also shows FTIR spectrum for sod-ZMOF-chitosan. The FTIR spectrum of sod-ZMOF-chitosan showed functional groups similar to those found in sod-ZMOF. However, there is a drastic decrease in the intensity of the O-H (carboxylic acid) band in the spectrum for sod-ZMOF-chitosan as compared to the ordinary sod-ZMOF. When Chen *et al.* [10] grafted sod-ZMOF with ethylenediamine (EDA), the FTIR also showed a decrease in O-H band after grafting. Chen *et al.* [10] speculated that the decrease in O-H band could be as a result of carboxylic acids being transformed to amide groups. In this work, the decrease in the O-H band could also be due to the impregnation of chitosan which then confirms the presence of chitosan (amine group) in sod-ZMOF chitosan

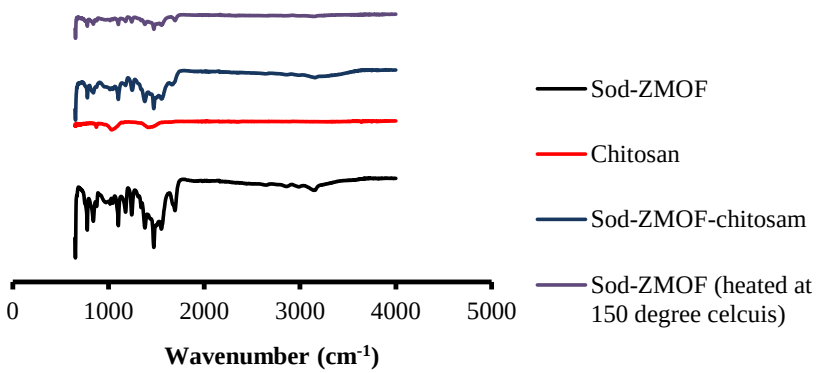

Figure 3: FTIR spectra of sod-ZMOF before and after chitosan impregnation

Table 1: Interpretation of characteristics of IR absorption

Wavelength	Functional group	Interpretation
3300–2500	COOH	Carboxylic group
1710–1665	C=O	Unsaturated aldehydes
1500–1400	C-C (in ring)	Aromatics
1250–1020	C-N	aromatic amines
910–665	N-H	1°, 2° amines

3.2. Surface area and pore volume

The Nitrogen physi-sorption at 77 K was conducted on sod-ZMOF before and after chitosan in order to determine the pore volume and BET surface area. Table 2 shows a summary of the results obtained in this study. From work done by Chen *et al.* [8], sod-ZMOF has a pore volume of 0.16 cm^3/g and a BET surface area of 375 cm^2/g. In this study, sod-ZMOF had a pore volume and BET surface which were much less than that from the work done by Chen *et al.* [8] The low pore volume and the BET surface area could be attributed to the presence of material such as Structure Direction Agent (SDA) occluded in the structure that was not completely removed. In order to remove the occluded material from the sod-ZMOF, drying temperature was increased from 100℃ to 150℃. However, this resulted in the structure of sod-ZMOF being affected as the FTIR spectra in Figure 4 illustrates the FTIR spectra of the sod-ZMOF where drying occurred at 100℃ and 150℃ are different. The carboxylic acid at a wavelength of about 3116 cm^{-1} completely disappeared for the sod-ZMOF that was dried at 150℃ as compared to the one dried at 100℃. This shows that the structure of sod-ZMOF was affected. This is expected as metal organic frameworks are unstable at high temperatures [17]. As this study is preliminary, effort will be made to remove the material from the structure in the subsequent optimization study of the material.

In addition, impregnation of chitosan on sod-ZMOF resulted in a decrease in surface area and pore volume. The decrease in surface area and pore volume is expected as chitosan impregnated occupies the surface area and pore volume in sod-ZMOF. The decrease in surface area is a significant indication of the successful impregnation of chitosan. Chen *et al.* [8] also observed a decrease in surface area and pore volume when they grafted amine onto

sod-ZMOF.

3.3. CO_2 adsorption performance

CO_2 adsorption performance of sod-ZMOF-chitosan was evaluated using the adsorption set-up depicted in Figure 1. The performance evaluation of sod-ZMOF-chitosan was determined using a gas mixture containing CO_2 (15%) and N_2 (85%). During the indication of the CO_2 by the gas analyser, the CO_2 reading starts to decrease with time indicating that some of the CO_2 was adsorbed onto the adsorbent from the inlet stream. After a certain time, the gas analyser displayed an increase in the CO_2 concentration until it reached the initial concentration in the feed stream, indicating the completeness of the adsorption process. Figure 2 depicts the CO_2 concentration profile of the adsorption process as obtained from the CO_2 gas analyser.

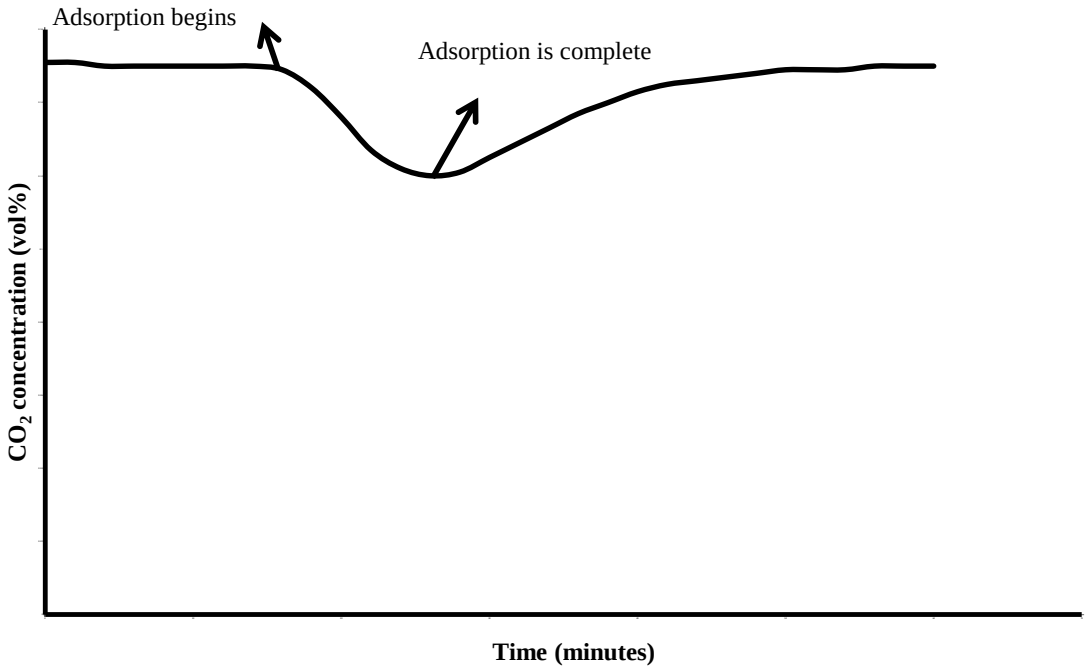

Figure 4: CO_2 concentration profile from the adsorption process

Figure 5 depicts the adsorption performance of sod-ZMOF-chitosan as a function of temperature. Adsorption capacity is increased with decreasing in temperature. At the lowest temperature of 25℃, adsorption capacity was 978 mg CO_2/ g adsorbent and reduced to 546 mg CO_2/ g adsorbent at 70℃. This is expected as adsorption is an exothermic process [15]. When gas molecules come into contact with the adsorbent, the gas molecules are taken by the adsorbent and heat is generated (that is heat of adsorption) [18]. Increasing temperature increases the kinetic energy of gas molecules so at high temperatures thus CO_2 molecules have high kinetic energy and as such they spend less time on the adsorbent surface which results in low adsorption capacity at high temperature.

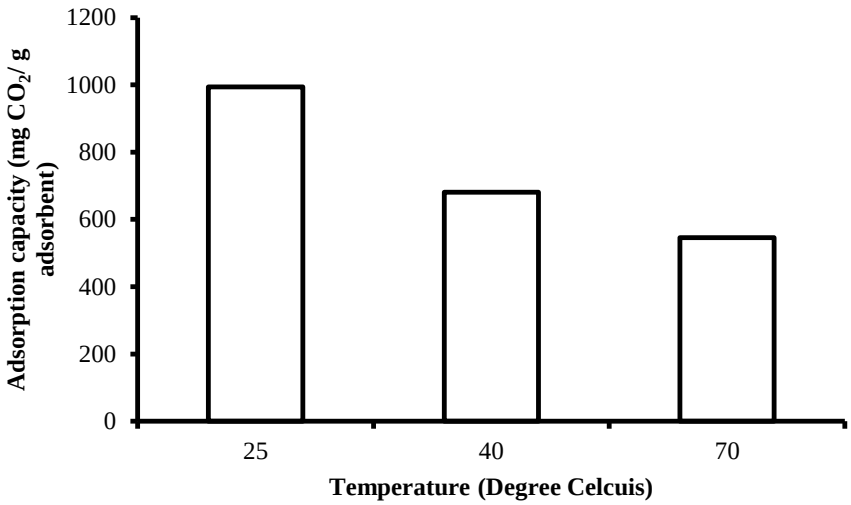

Figure 5: CO_2 adsorption performance of sod-ZMOF-chitosan as a function of temperature

Figure 6 depicts the results of the investigation of the CO_2 adsorption performance of the adsorbent at different feed flow rates. The CO_2 adsorption performance of sod-ZMOF-chitosan was evaluated at feed flow rates of 25, 50 and 70 ml/min keeping constant temperature and pressure at 25℃ and at 1 bar, respectively. Amount of CO_2 decreased with increase in the feed flow rate. At the lowest flow rate of 25 ml/min, the amount of CO_2 adsorbed by sod-ZMOF-chitosan was 978 mg CO_2/ g adsorbent, and at a high flow rate of 70 ml/ min, the mount of CO_2 adsorbed was 170 mg CO_2/ g adsorbent. This behaviour could be attributed to the reduction in the contact time between the adsorbate and the adsorbent at higher feed flowrates. More contact time means the gas spends more time at the surface of the adsorbent thus more gas molecules will be adsorbed.

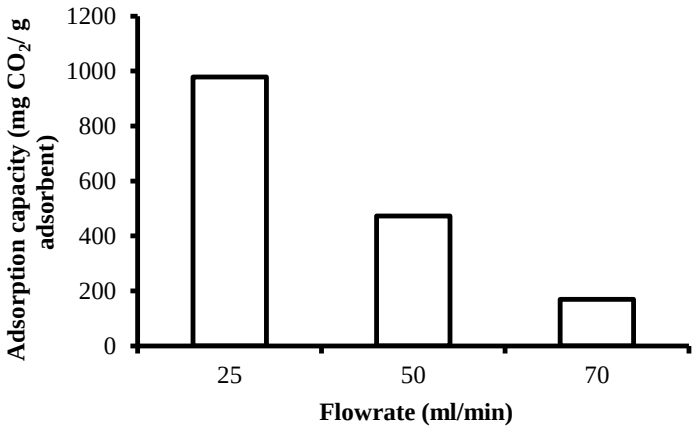

Figure 6: CO_2 adsorption performance of sod-ZMOF-chitosan as a function of feed flowrate

Since some researchers commonly use TGA to investigate CO_2 adsorption performance of their adsorbents during post-combustion CO_2 capture, performance evaluation of our adsorbent was carried out using TGA as well at

different temperatures and feed flowrates. The CO_2 adsorption performance of our adsorbent with the use of TGA was similar to that observed when the packed-bed adsorption column was used. Figure 7 and Figure 8 depict the CO_2 adsorption performance of our adsorbent using TGA. However, the amount of CO_2 adsorbed obtained when a TGA was used was much less than that obtained using the packed-bed adsorption column, even at 100% CO_2 which was used for the TGA. In a packed-bed adsorption column, mass transfer between the adsorbent and adsorbate (CO_2) in greatly enhanced. This is because with a packed-bed adsorption column, the gas flows through the packed adsorbent particles while with the TGA; the gas just flows over the sample pan that contains the adsorbent with little contact with the adsorbent particles.

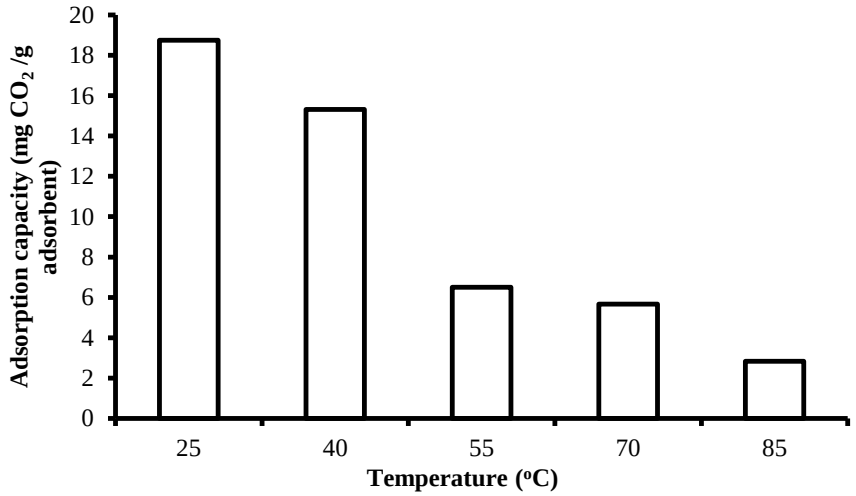

Figure 7: CO_2 adsorption performance of sod-ZMOF-chitosan as a function of temperature using TGA

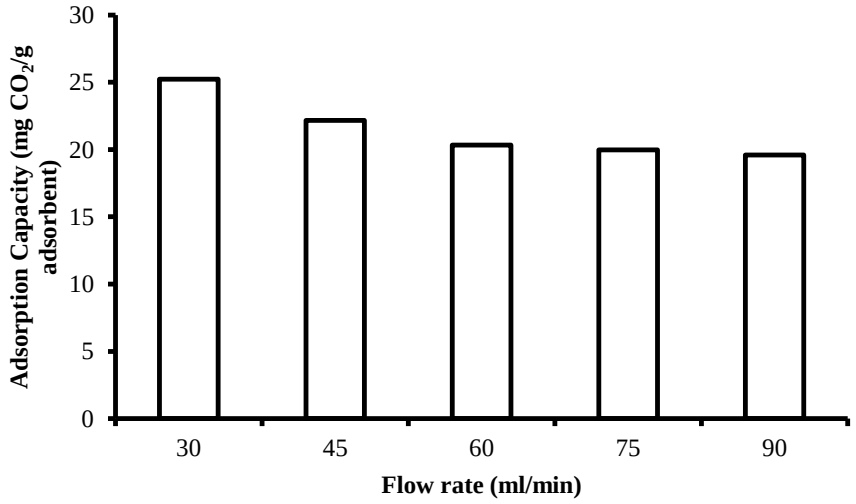

Figure 8: CO_2 adsorption performance of sod-ZMOF-chitosan s a function of feed flowrate using TGA.

4. Conclusion

In this work sod-ZMOF-chitosan was successfully synthesized and evaluated for CO_2 capture. XRD analysis showed that sod-ZMOF maintained its crystallinity after chitosan impregnation. FTIR and BET analysis showed successful impregnation of chitosan onto sod-ZMOF. The highest amount of CO_2 adsorbed was 2132 mg CO_2/ g adsorbent at 25℃, 50 ml/min and 1 bar. In addition, amount of CO2 adsorbed decreased as temperature and feed flowrates were increased.

5. Acknowledgements

The authors acknowledge the financial assistance from the National Research Foundation (NRF) of South Africa, the South African Centre for Carbon Capture and Storage (SACCCS) and the University of the Witwatersrand (WITS). In addition, the authors thank ABB for the provision of the gas detector utilized in this research.

References

1. Ngoy JM, Wagner N, Riboldi L, Bolland O. A CO_2 capture technology using multi-walled carbon nanotubes with polyaspartamide surfactant. Energy Procedia. 2014; 2230 : 2248
2. Geol C, Kaur H, Bhunia H, Bajpai PK. Carbon dioxide adsorption on nitrogen enriched carbon adsorbents: Experimental, kinetics, isothermal and thermodynamic studies. Journal of CO_2 Utilization. 2016; 50:63-16
3. Liu D, Xia Q , Li Z , Xi H. Experimental and molecular simulation studies of CO_2 adsorption on zeolitic imidazolate frameworks: ZIF-8 and amine-modified ZIF-8. Springer Science and Business Media. 2013; 19:25–37
4. Yu C, Huang C, Tan C. A Review of CO_2 Capture by Absorption and Adsorption. Taiwan Association for Aerosol Research. 2012; 745:769-12
5. Wang M, Lawal A, Stephenson P, Sidders J, Ramshaw C. Post-combustion CO_2 capture with chemical absorption: A state-of-the-art review. Chemical Engineering Research and Design. 2 0 1 1: 1609;1624
6. Chitsiga T, Daramola MO, Wagner N, Ngoy J. Effect of the presence of water-soluble amines on the carbon dioxide (CO_2) adsorption capacity of amine-grafted polysuccinimide (PSI) adsorbent during CO_2 capture. Energy Procedia. 2016; 90:105-86.
7. Rowsell J & Yaghi O. Metal-organic frameworks: a new class of porous materials. Microporous and Mesoporous Materials.2004; 3:14
8. Chen C, Kim J, Yang D, Ahn W. Carbon dioxide adsorption over zeolite-like metal organic frameworks (ZMOFs) having a sod topology: structure and ion exchange effect. Chemical Engineering Journal. 2011; 1134:1139-168
9. Imteaz A, Sung H. Composite of metal organic framework: Preparation and Application in adsorption. Materials today. 2014; 136:146.
10. Chen C, Kim J, Park D, Ahn, W. Ethylenediamine grafting on zeolite like metal organic frameworks (ZMOF) for CO_2 capture. Materials letters. 2013; 344:347.
11. Shukla S, Mishra A, Arotiba O, Mamba B. Chitosan-based nanomaterials: A state-of the-art review. International Journal of Biological Macromolecules. 2013; 46:58.
12. Ma J, Xin C, Tan C. Preparation, physicochemical and pharmaceutical characterization of chitosan from Catharsius molossus residue. International Journal of Biological Macromolecules. 2015; 547:556
13. Xie J, Li C, Chi L, Wu D. Chitosan modified zeolite as a versatile adsorbent for the removal of different Pollutants from water. Fuel. 2013; 480:485
14. Sun H, Lu L, Chen, X, Jiang Z. Surface modified zeolite-filled chitosan membranes for pervaporation dehydration of ethanol. Applied surface science. 2008;5367:5374.

15. Becnel JM, Holland CE, McIntyre J, Matthews MA, Ritter JA. Fundamentals of fixed bed adsorption processes: Analysis of Adsorption Breakthrough and Desorption Elution curves. Department of Chemical Engineering, University of Carolina.
16. Calleja G, Botas JA, Sa´nchez-Sa´nchez M, Orcajo MG. Hydrogen adsorption over Zeolite-like MOF materials modified by ion exchange. 2010; 9916:9923
17. Lee S, Park S. A review on solid adsorbents for carbon dioxide capture. Journal of Industrial and Engineering Chemistry. 2015; 1:11
18. Mori Y, Yamada A. Dynamic behaviour of an adsorption column heat exchanger. Proceedings of the tenth international heat transfer conference. Brighton, UK.1994; 161:166

Available online at www.sciencedirect.com

ScienceDirect

Energy Procedia 114 (2017) 1643 – 1664

Energy Procedia

13th International Conference on Greenhouse Gas Control Technologies, GHGT-13, 14-18 November 2016, Lausanne, Switzerland

Modelling and Experimental Study of the CO_2 Adsorption Behaviour of Polyaspartamide as an Adsorbent during Post-Combustion CO_2 Capture

Kelvin O. Yoro, Muofhe Singo, Jean L. Mulopo, Michael O. Daramola*

School of Chemical and Metallurgical Engineering, Faculty of Engineering and the Built Environment, University of the Witwatersrand, Private Bag X3, Wits 2050, Johannesburg, South Africa.

Abstract

Adsorption technology due to its potentially low energy consumption, simple operation and flexibility in design to meet different demands is fast becoming popular and is now widely considered in the area of CO_2 capture. Adsorbents play a vital role in any adsorption technology. Therefore, the behavior of adsorbents under different conditions during an adsorption process needs to be investigated. In this study, the behavior of polyaspartamide as an adsorbent during post-combustion CO_2 capture was investigated using kinetic and non-kinetic models. Bohart-Adams and Thomas models were the non-kinetic models explored to ascertain whether external mass transfer dominated the overall system kinetics during the CO_2 adsorption onto polyaspartamide. The kinetics of adsorption of polyaspartamide was studied using Lagergen's

* Corresponding author. Tel.: +27 11 717 7536.

E-mail address: michael.daramola@wits.ac.za

Peer-review under responsibility of the organizing committee of GHGT-13.
doi:10.1016/j.egypro.2017.03.1294

pseudo 1st order, Lagergen's pseudo 2nd order and the Avrami kinetic models in order to understand whether the adsorption process was a physical, chemical or physiochemical process. The experimental validation of the model prediction was carried out in a laboratory-sized packed bed adsorption column at an operating pressure of 2 bar; gas flow rate of 1.5-2.5 ml/s, and a temperature range of 303-333 K using 0.1 g of the adsorbent. The experimental breakthrough curve showed a superior fit with the Bohart-Adams model. For the kinetic study, Avrami kinetic model displayed a better fit with kinetic data at all temperatures studied. The non-kinetic model revealed that external mass transfer governed the adsorption of CO_2 onto polyaspartamide while the kinetic study revealed that the mechanism of adsorption of CO_2 onto polyaspartamide was more of physical than chemical (physiochemical).

Peer-review under responsibility of the organizing committee of GHGT-13.

Keywords: Adsorbents; Adsorption; Breakthrough curves; CO_2 capture; Polyaspartamide;

1. Introduction

The interest in CO_2 capture is rising continuously around the globe. Carbon capture and storage (CCS) is a promising technology for mitigating climate change and meeting CO_2 emission reduction targets [1]. Anthropogenic CO_2 emitted into the atmosphere must be reduced in order to mitigate the unfettered release of greenhouse gases into the atmosphere [2, 3]. The Capture of CO_2 from flue gas emitted from power plants via post combustion capture is very useful in addressing the problem of its emission into the atmosphere. Post-combustion CO_2 capture via the adsorption technology ensures that the adsorbent is in direct contact with the CO_2 gas in an adsorption column. Mathematical models describing the behavior of the adsorbent during the post-combustion CO_2 capture is very essential in designing, optimizing and scaling-up of the CO_2 capture process[3, 4]. Furthermore, thermodynamic and kinetic study play a role in understanding the performance of any adsorbent [4]. The solute uptake rate which determines the residence time required for completion of the adsorption process can also be established from the kinetic analysis. Several mathematical models have been developed to describe adsorption behavior of adsorbents during post-combustion CO_2 capture. Due to the complex nature of the mathematical model solutions, the use of accurate and simplified models have been explored to

reduce the computational time [5]. Mathematical modeling of adsorption processes have attracted a considerably high attention amongst researchers today because mathematical models are capable of estimating the breakthrough curve, adsorption kinetics and temperature profile for a certain adsorbent and adsorbate in all locations within the adsorption column [5-6]. The model, if experimentally verified can be used to study the effect of various process parameters such as pressure, temperature, flow rate and concentration on the adsorption behavior of an adsorbent. CO_2 capture using solid adsorbents involves a selective separation of CO_2 based on a gas–solid interaction [7]. The adsorbent in most adsorption processes is always in contact with the gas in a packed bed adsorption column [8]. An understanding of the behavior and performance of the adsorbent and also the dynamic behavior of the adsorption system is required for a rational process design, scale-up and optimization [9-11].

In recent times, several adsorbents have been synthesized and investigated for CO_2 capture using experimental and modeling approach [12-14]. Examples are synthetic zeolites, activated carbon, carbon molecular sieves, silica, metal oxides, chitosan, carbon nanotubes, Sodalite zeolite metal organic frameworks (Sod-ZMOFs) etc. Before designing an adsorption process, selecting an appropriate adsorbent with high working capacity as well as a strong desorption capability is key for post combustion CO_2 capture [9]. This simply means that adsorbents play a key role in any adsorption technology [15]. For instance, adsorbents determine the overall CO_2 capture performance in the vacuum swing adsorption (VSA) technology [16]. The key elements for a good adsorbent in CO_2 capture technology are; high selectivity of CO_2 , high adsorption capacity, rapid adsorption/desorption kinetics, stable adsorption capacity after repeated cycles and adequate mechanical strength of the particles [17]. Amine-modified polymer-based adsorbents have been developed recently [18]. Polyaspartamide has been studied as a potential adsorbent for post-combustion CO_2 capture [19]. Polyaspartamide (PAA) is an amine grafted polymer from polysuccinimide obtained when polysuccinimide reacts with Ethylene diamine (EDA). Polyaspartamide is considered as a potentially good adsorbent for post combustion CO_2 capture because of its large surface area, non-toxic nature, biodegradable nature and its good geometry [20]. The behavior and performance of polyaspartamide as an adsorbent is assessed in terms of various desired attributes, such as its equilibrium adsorption capacity, regeneration,

multi cycle durability, and adsorption/desorption kinetics. In this study, existing gas-solid kinetic and non-kinetic adsorption models will be used to assess the behavior of polyaspartamide during post combustion CO_2 capture using a balanced flue gas stream of 15% CO_2 and 85% N_2. This study focused on investigating the adsorption behavior of polyaspartamide as an adsorbent during post combustion CO_2 capture using mathematical modeling and experimental validation approach. Other properties to test for the performance of polyaspartamide during CO_2 capture such as adsorption kinetics was also studied using kinetic models.

Nomenclature

% E	Percentage Error
C	Final concentration of CO_2
CCS	carbon capture and storage
C_e	Concentration of CO_2 at equilibrium
C_o	Initial concentration of CO_2
EDA	Ethylene Diamine
K_A	Avrami constant (s^{-1})
K_f	Pseudo 1st order constant (S^{-1})
K_s	Pseudo 2nd order constant ($gmol^{-1}s^{-1}$)
N	Number of experimental runs
nA	Avrami exponent
PAA	Polyaspartamide
qe	Amount of CO_2 adsorbed at equilibrium ($mol\ g^{-1}$)
Q_{Exp}	Amount of CO_2 adsorbed from experiment ($mol\ g^{-1}$)
Q_{mod}	Amount of CO_2 adsorbged predicted by the model ($mol\ g^{-1}$)
q_t	Amount of CO_2 adsorbed at a particular time ($mol\ g^{-1}$)
t	Time (seconds)
VSA	Vacuum swing adsorption

2. Experimental Section

2.1 Materials

The adsorbent considered in this study is polyaspartamide. Detailed information about the synthesis and characterization of the adsorbent can be obtained elsewhere [10, 19]. As such, it will not be repeated in this study. The gas used was a balanced mixture of CO_2 and N_2 (15% CO_2, 85 % N_2) purchased from Afrox (pty) South Africa. The experiment was carried out in a laboratory-scale packed bed adsorption column. The experimental conditions for this study are summarized in Table 1.

Table 1. Experimental conditions for adsorption

Operating conditions	
Adsorption temperatures (K)	303 - 333
Adsorption total pressure (bar)	2
Inlet flow rates (ml/s)	1.5 – 2.0
Inlet gas concentration (vol. %)	15.0
Mass of adsorbent (g)	0.1

2.2 Method

0.1 g of polyaspartamide was fed into the packing in the adsorption column and degassed by passing in dry Nitrogen gas through the packed bed at an inlet flow rate of 1.5 ml/s and a temperature of 373 K for 1 hour to remove CO_2 that could be present within the adsorption column. Polyaspartamide was heated to 373 K within the adsorption column to remove moisture that could be present on the adsorbent and also improve its porosity. After the degassing and heating stage, the temperature of the adsorption bed was lowered to 303 K under N_2 flow. The flue gas mixture (15% CO_2, 85 % N_2) was fed to the packed bed adsorption column at a flow rate of 2.5 ml/s while by-passing the reactor in order to determine the inlet concentration of CO_2 from the gas analyzer (model: ABB-AO2020). The flue gas was then allowed to pass through the reactor containing the adsorbent. The gas flow rate was regulated using a mass flow controller while the CO_2 uptake onto the polyaspartamide material was monitored as a function of time from the CO_2 gas analyzer. The experiment was repeated at temperatures of 318 and 333 K and flow rates of 1.5 and 2.0 ml/s to determine the behavior of the adsorbent at higher temperatures and different flow rates. The experiment lasted for 1200 seconds until equilibrium was reached. A schematic process flow diagram for this experiment is depicted in Figure 1.

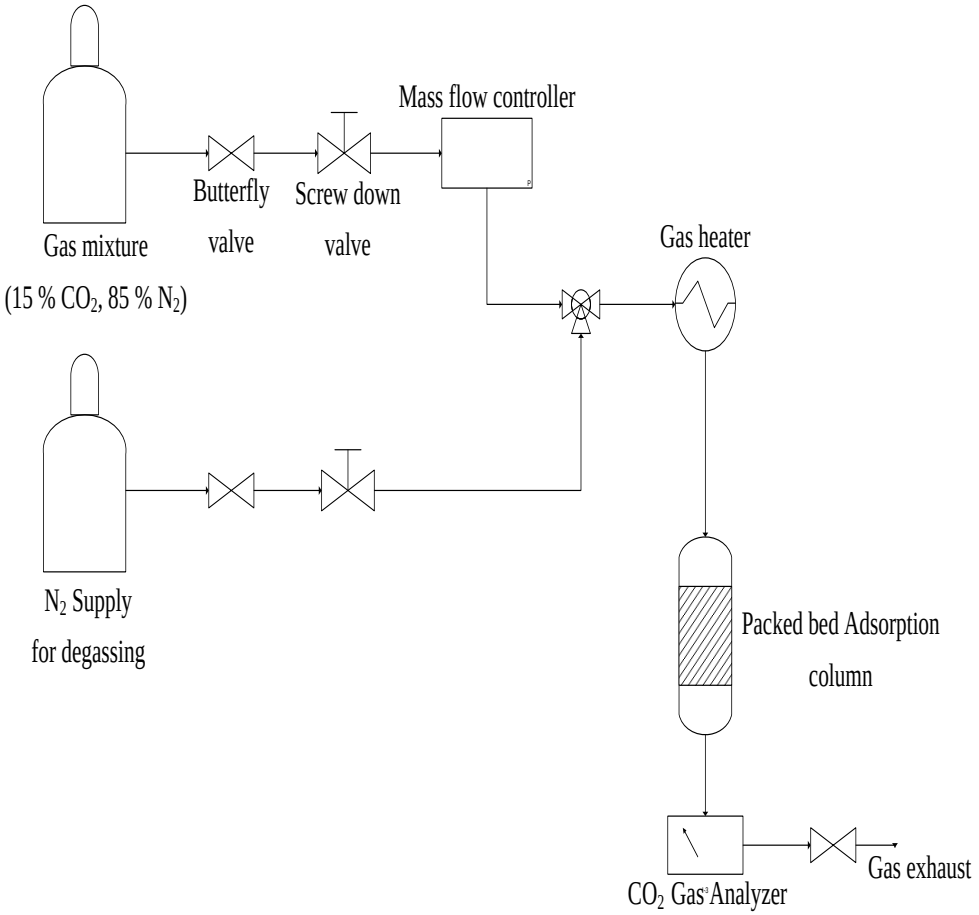

Figure 1. Experimental set up for CO_2 adsorption onto polyaspartamide material in a packed bed column.

3. Model description and Implementation

3.1 Model description

The models considered in this study were existing gas-solid adsorption models derived from the mass balance around an adsorption column. Assumptions for the models explored in this study are summarized in Table 2.

Table 2. Models explored and the basic assumptions made

Models Studied	Assumptions
Bohart-Adams model	1. Rectangle or step isotherm is assumed for the model and adsorption bed is homogenous 2. Gradients occur only in the axial direction and they are negligible 3. At time t = 0, the bed is free of adsorbate (CO_2) 4. The model assumes that equilibrium is not instantaneous 5. Irreversible adsorption isotherm
Thomas Model	1. The axial and radial dispersion in the column is negligible 2. Constant separation factor 3. Adsorption is described by a pseudo-second order reaction rate principle and reduces to a Langmuir isotherm at equilibrium. 4. The column void fraction is constant 5. Constant temperature and pressure process conditions 6. Negligible external resistance during mass transfer process.
Lagergen's pseudo 1st order model	1. The rate of adsorption increases as the number of vacant site on the adsorbent increases 2. Local equilibrium is achieved instantaneously and the primary resistance is mass transfer resistance.
Lagergen's pseudo 2nd order model	1. The rate of adsorption is proportional to the square of the number of vacant sites
Avrami kinetic model	1. There are random nucleation sites across the reaction surface

3.2 Model implementation

Experimental data were fit into the Bohart-Adams model, Thomas model, Lagergen Pseudo 1^{st} and 2^{nd} order models as well as the Avrami kinetic model, to describe the behavior of the adsorbent. Kinetic data significantly influence the residence time required for the completion of any adsorption process as well as the unit capital cost [21]. In this study, the kinetics of adsorption of polyaspartamide was investigated using the Lagergen's pseudo 1^{st} order, 2^{nd} order and Avrami kinetic models. The kinetic models used to describe the adsorption kinetics were validated using kinetic data obtained from the experiment conducted. Due to complexities associated with the description of model parameters, this study considered a common approach which involves fitting of the data obtained from experiments to a number of mathematical models. The model that fits best with the experimental data is always considered as the best model describing the behavior of the adsorbent [22]. Breakthrough curves in this study were obtained by plotting the normalized concentration of CO_2 (C/C_o) against time. The breakthrough curves were obtained at various temperatures and also different flow rates. The breakthrough curves in this study were described using the Bohart-Adams and the Thomas model [23, 24]. The model results were validated using the experimental data. Model parameters obtained from the solution in MATLAB R2014a are presented in Table 4.

4.0 Results and Discussion

4.1 Adsorption behavior

In order to understand the adsorption behavior of CO_2 onto polyaspartamide, the adsorbent was experimentally studied under different adsorption conditions such as temperature, pressure and flow rates. The experimental breakthrough curve obtained for the adsorbent is shown in Figure 2. The breakthrough curve in Figure 2 was obtained at various isothermal conditions (i.e. 303, 318 and 333 K). The curves exhibited a common behavior at different adsorption temperature, constant pressure and flowrates. The general shape of the breakthrough curves for the adsorption of CO_2 onto polyaspartamide was achieved as expected; it was similar to breakthrough curves obtained for other polymer-based adsorbents reported in literature [25, 26]. The breakthrough curve explains that the amount of CO_2 captured by the adsorption sites on polyaspartamide increases with a decrease in adsorption temperature and increased operating pressure. The breakthrough curves depicted in this study showed a plot of the ratio of the final concentration at the outlet C and the inlet concentration Co against the contact time within the packed bed at different operating pressures and temperatures. The experimental conditions considered in this study are summarized in Table 1. The CO_2 adsorption breakthrough time for polyaspartamide occurred at 700 seconds at a pressure of 200 KPa and temperature of 303 K . Longer breakthrough times were observed when the temperature was increased to 318 and 333 K. This shows that the pore diameter of polyaspartamide is sufficient for CO_2 to fill in depending on the operating temperature. The saturation time for adsorption of CO_2 on polyaspartamide was quite long as deduced from the experimental breakthrough curve in Figure 2. This could be attributed to the large pore volume of polyaspartamide. The effect of feed flow rate on the adsorption of CO_2 onto polyaspartamide was investigated by operating the adsorption process at different flow rates (1.5 and 2.0 ml/s) at a constant adsorption temperature of 303 K and pressure of 2 bars as shown in Figure 3. According to the breakthrough curve in Figure 3, at higher flowrates, the packed bed adsorption column was saturated early and lower flow rates resulted in a shallower adsorption zone and longer contact time between the CO_2 and the adsorbent in the packed bed. Early breakthrough time resulted in a less CO_2 uptake by polyaspartamide. The high CO_2 adsorption capacity displayed by polyaspartamide in this study is attributed to the large

surface area of the amine grafted polyaspartamide. The Bohart-Adams and Thomas non kinetic models were used to fit the experimental breakthrough curve at 303 K. It was observed that the Bohart-Adams model gave a better fitting with the experimental data as shown in Figure 4. This means that external mass transfer dominated the overall system kinetics during the CO_2 adsorption process in this study. In order to determine the accuracy of each model explored in this study, an error function based on the normalized standard deviation adapted from a related study [27] was applied as shown in equation (1) ;

$$\% \, E = \sqrt{\frac{\sum_{i=1}^{N=3}\left(\frac{Q_{exp} - Q_{mod}}{Q_{exp}}\right)^2}{N-1}} \times 100 \quad (1)$$

Where % E is the error function from the study in percentages, Q_{exp} is the average amount of CO_2 adsorbed experimentally at a given time, Q_{mod} is the amount of CO_2 adsorbed as predicted by the mathematical model and N is the total number of experimental runs.

The CO_2 capture efficiency of the adsorbent was calculated on percentage basis by dividing the equilibrium concentration of CO_2 by the initial CO_2 concentration according to Equation 2.

$$\% \quad CO_2 \text{ capture efficiency} = \frac{C_e}{C_o} \times 100 \quad (2)$$

Where C_e is the gas concentration at equilibrium and C_o is the initial concentration of the gas. The percentage CO_2 capture efficiency was obtained at all temperatures considered in this study using Equation 2 and presented in Table 3.

Table 3. CO_2 capture efficiency of polyaspartamide at different adsorption temperatures and constant pressure.

Temperature (K)	Pressure (bar)	CO_2 capture efficiency (%)
303	2	92.67
318	2	90.00
333	2	86.67

4.2 Kinetics of Adsorption

A good adsorbent is expected to have fast adsorption kinetics. More so, kinetic data of the adsorption process is another characteristic that is very important in the design of a CO_2 capture system. The Lagergen's pseudo 1st order, pseudo 2nd order and Avrami kinetic models were used to investigate the kinetics of adsorption CO_2 onto polyaspartamide as presented in Figure 5. The Lagergen's pseudo 1st and 2nd order kinetic models had some limitations with respect to the adsorption of CO_2 onto polyaspartamide. After few seconds, the Lagergen's pseudo 1st order model under-estimated the uptake of CO_2 till about 120 seconds and afterwards, CO_2 uptake was still under-estimated consistently until the adsorption process attained equilibrium. The pseudo second order model also did not perfectly fit into the experimental data. This therefore suggests that the Lagergen's pseudo 1st order model which described mainly the early stage of adsorption is applicable only under low surface coverage as previously reported in literature [28-33]. However, the best fit for the adsorption kinetics was consistently obtained at different temperatures with the Avrami kinetic model because of the model's ability to account for CO_2 adsorption by both physical and chemical adsorption as shown in Figure 6. Going by the results of the Avrami kinetic model in this study, the adsorption of CO_2 onto polyaspartamide could be described as a physiochemical process. The kinetic constant of the Avrami model is independent

of the initial concentration of CO_2. The kinetic models and their corresponding parameters are presented in Table 4. The Avrami kinetic model consistently displayed the least percentage error at all temperatures studied as seen in Table 4. Hence, it could be inferred that the kinetics of adsorption of CO_2 onto polyaspartamide was best described by the Avrami kinetic model.

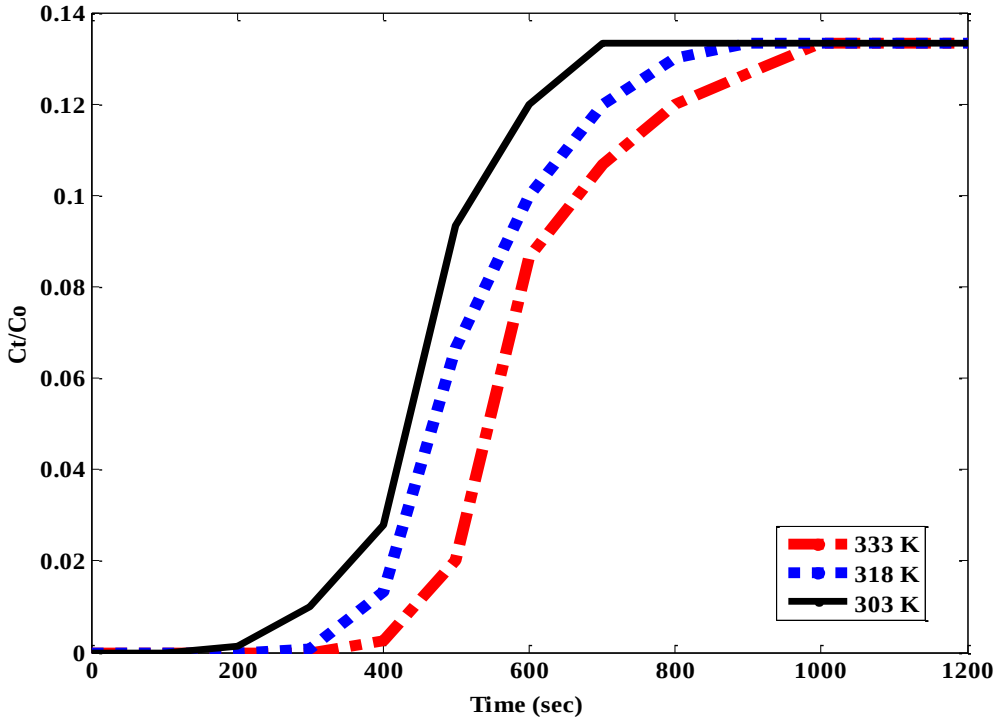

Figure 2. Experimental breakthrough curves at various adsorption temperatures, constant flow rate and constant pressure.

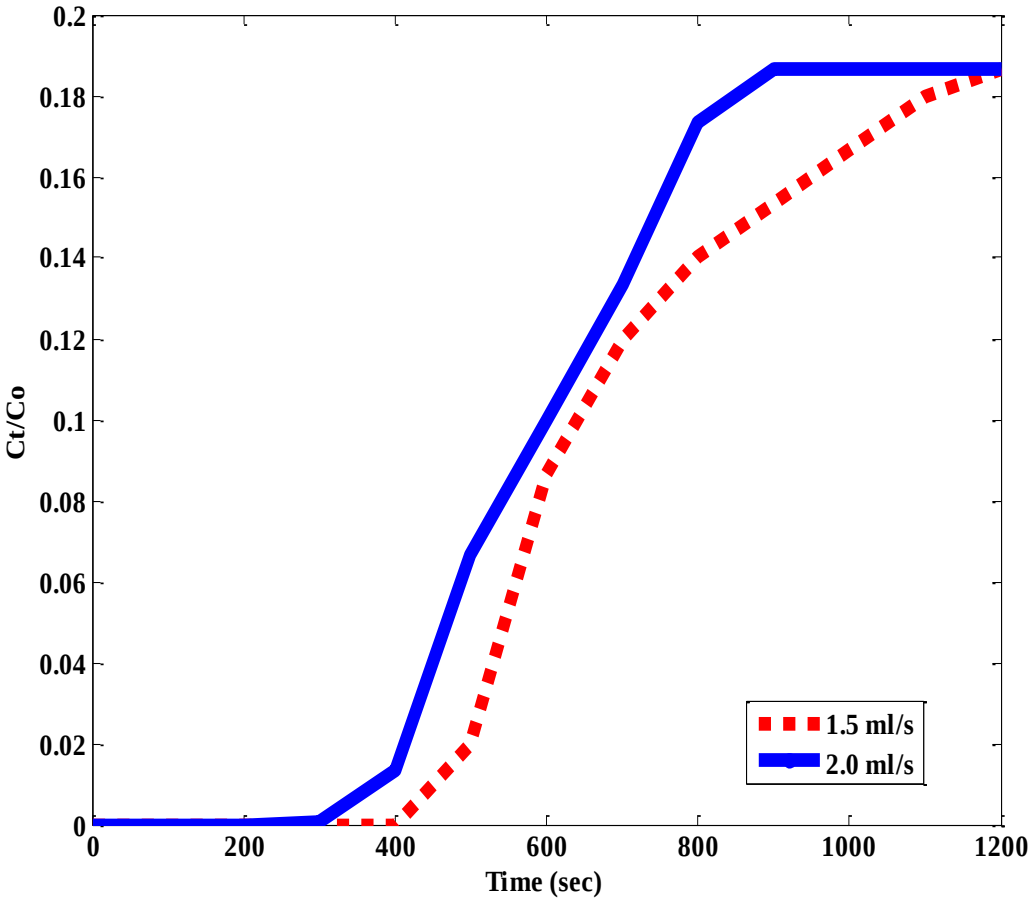

Figure 3. Effect of feed flow rate as a function of time. (Experimental conditions: feed pressure, 2 bar, and temperature 303 K).

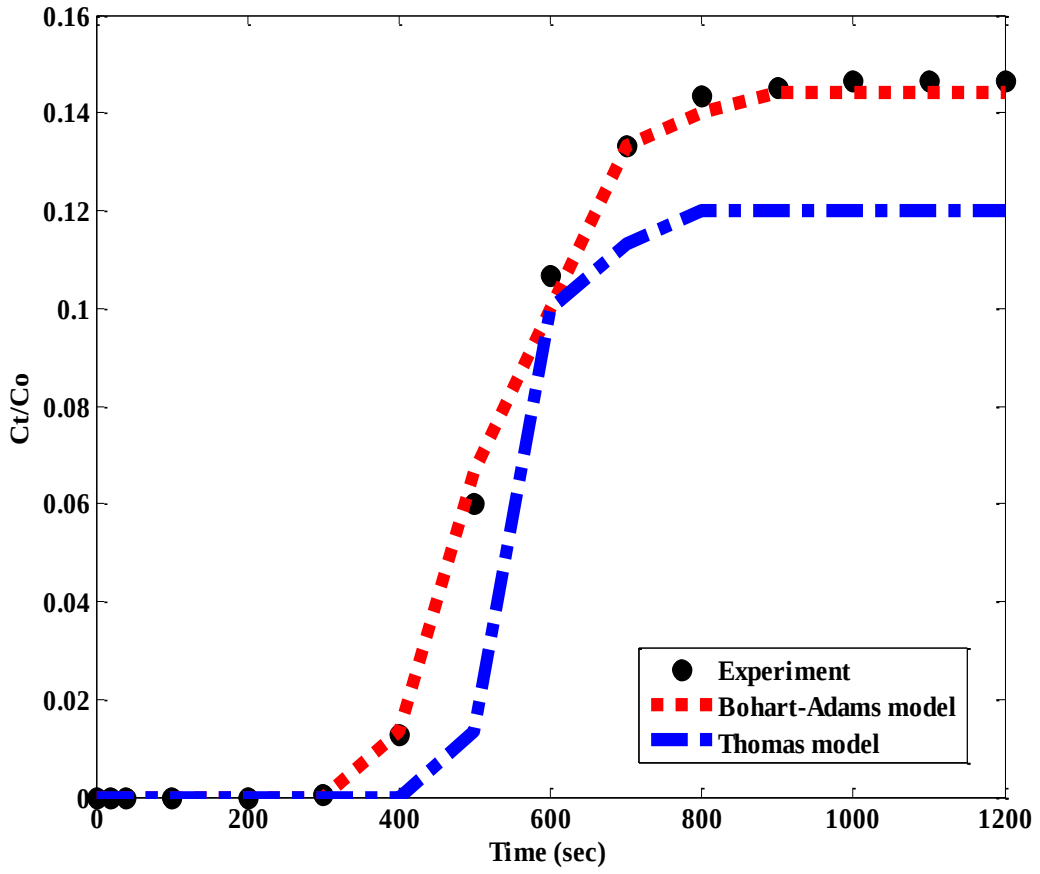

Figure 4. Experimental result versus model results. (Experimental conditions: 303 K, 2 bar)

Table 4. Kinetic model parameters for adsorption of CO_2 on polyaspartamide

Kinetic models	Parameters	303 K	318 K	333 K
Pseudo-first order model $q_t = q_e(1 - e^{-K_f t})$	Kf (s^{-1})	3.2 x 10^{-2}	3.53 x 10^{-2}	3.92 x10^{-2}
	Error (%)	1.33	5.27	2.8
	q_e (mol g^{-1})	4.97	4.72	4.37
Pseudo-second order model $q_t = \frac{q_e^2 + tK_S}{1 + q_e K_S t}$	Ks ($gmol^{-1}s^{-1}$)	2.24 x 10^{-2}	3.14 x 10^{-2}	4.42x10^{-2}
	Error (%)	8.81	3.88	2.33
	q_e (mol g^{-1})	5.2	4.82	4.4
Avrami model $q_t = q_e[1\text{-}\exp(-(K_A t^{nA})]$	K_A (s^{-1})	3.99 x 10^{-2}	4.17 x 10^{-2}	4.31x10^{-2}
	Error (%)	2.38	2.22	1.55
	q_e (mol g^{-1})	5.74	4.94	4.45
	nA	1.76	1.46	1.38

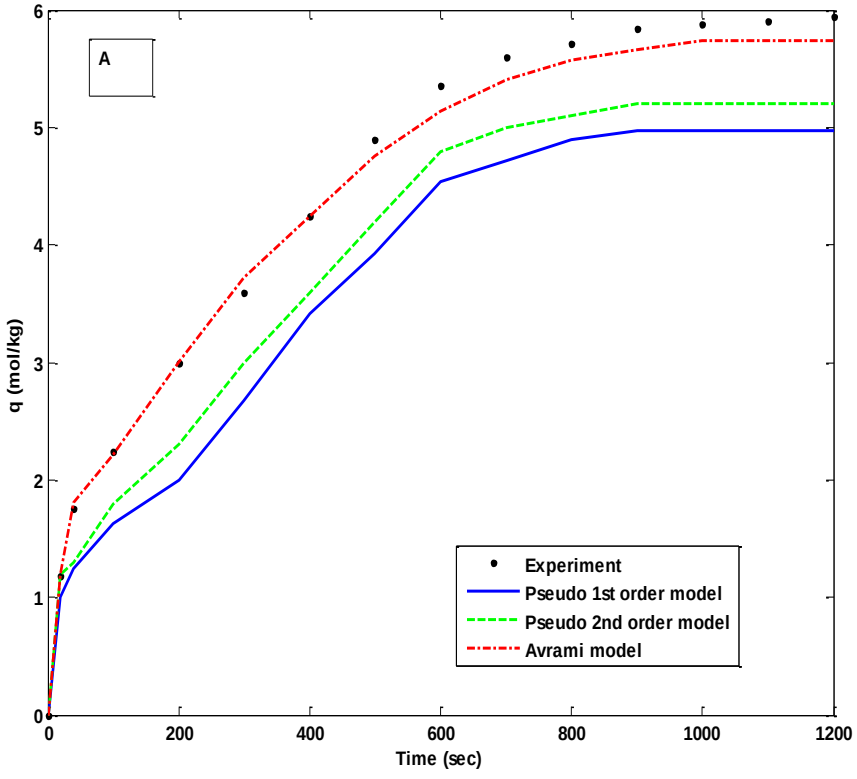

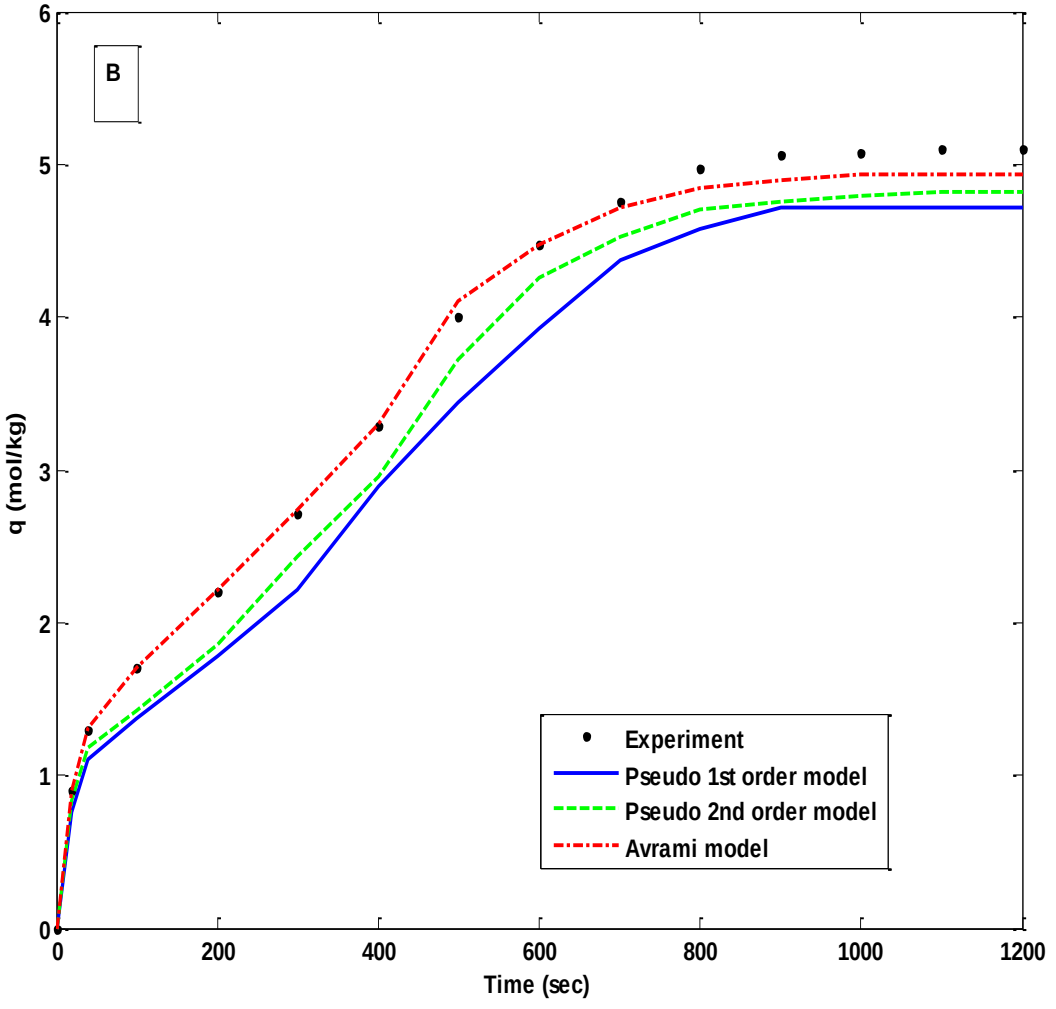
B
q (mol/kg)
Time (sec)
0
1
2
3
4
5
6
0
200
400
600
800
1000
1200
Experiment
Pseudo 1st order model
Pseudo 2nd order model
Avrami model

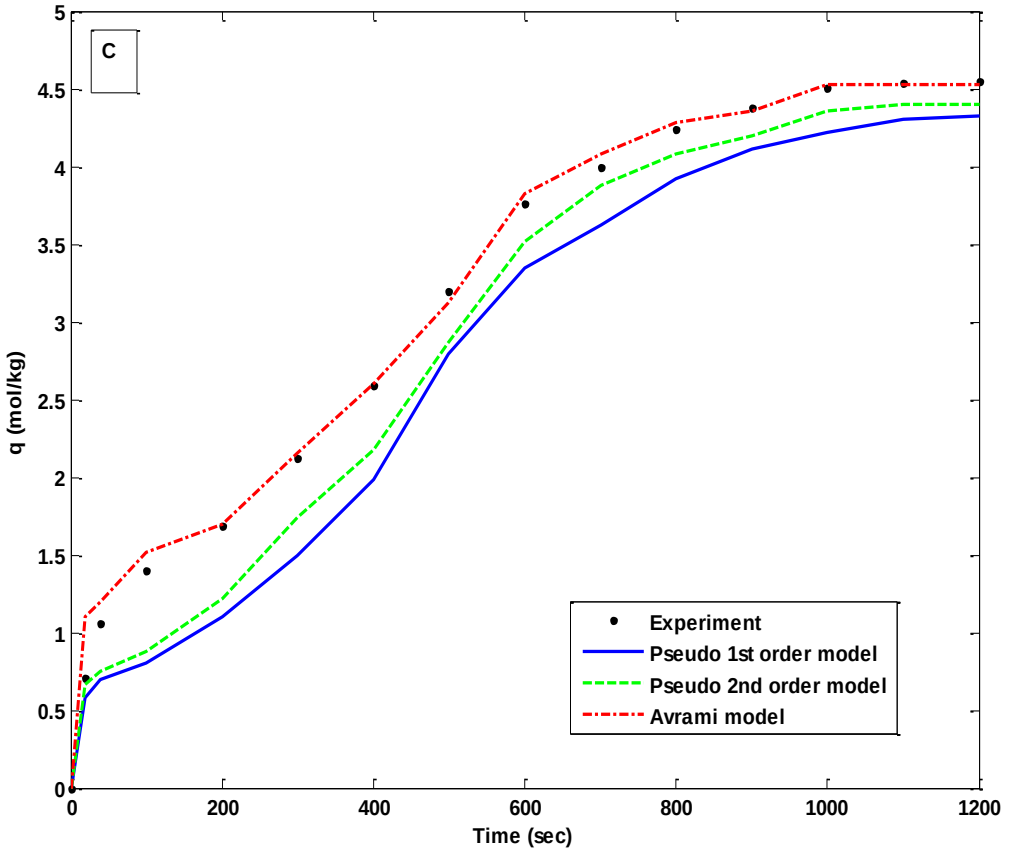

Figure 5: Experimental and predicted kinetics of adsorption of CO_2 onto polyaspartamide at (A) 303 K, 2 bar, (B) 318 K, 2 bar, (C) 333 K, 2 bar.

5. Conclusions

This study successfully investigated the adsorption behavior of polyaspartamide as an adsorbent during post-combustion CO_2 capture using kinetics and breakthrough curves under different adsorption conditions and also attempted modeling these behaviors. Based on the outcome of this study, it can be concluded that polyaspartamide is a promising adsorbent for post-combustion CO_2 capture. The breakthrough curve was successfully described using the Bohart-Adams model which could be attributed to the flexible assumptions of the Bohart-Adams

model considered in this study. From the results of the Bohart-Adams model (non-kinetic model), it can be logically concluded that mass transfer dominated the adsorption of CO_2 onto polyaspartamide. The shape of the breakthrough curve as predicted by the model was in close agreement with experimental data and equilibrium was attained at various temperatures studied after 1000 seconds as depicted in Figure 2. The Avrami kinetic model consistently and successfully described the kinetics of adsorption of CO_2 onto polyaspartamide at all temperatures studied as shown in Figure 5. This simply implies that the adsorption of CO_2 onto polyaspartamide is more of a physical than chemical adsorption process (Physiochemical). Increasing the feed (i.e. CO_2) flow rate decreased the breakthrough time because faster flow rate decreases the retention time of the gas molecules on the adsorbent within the packed bed resulting in a decreased amount of CO_2 adsorbed by polyaspartamide. This simply means that, longer breakthrough times are required for a higher amount of CO_2 to be adsorbed by polyaspartamide which subsequently results to a higher adsorption capacity.

Acknowledgements

The authors are grateful to the National Research Foundation (NRF) of South Africa - grant number **94874** and the University of the Witwatersrand, Johannesburg for their financial support.

REFERENCES

[1] Xu, Z., Chai, J., Pan, B., Mathematically modeling fixed-bed adsorption in aqueous systems, *J. Zhejiang Univ. Sci.*, 2013, **14**(3), pp.155–176.

[2] Shafeeyan, M. S., Daud, W. M. A., Shamiri, A., A review of mathematical modeling of fixed-bed columns for carbon dioxide adsorption, *Chem. Eng. Res. Des.*, 2014, **92**(5), pp.961–988.

[3] Sekoai P.T., Yoro, K.O., Biofuel Development Initiatives in Sub-Saharan Africa: Opportunities and Challenges, *Climate*, 2016, **4**(2), pp. 33.

[4] Qiu, H., Lv, L., Pan, B., Zhang, Q., Zhang, W., Zhang, Q., Critical review in adsorption kinetic models, *J. Zhejiang Univ. Sci. A*, 2009, **10** (5), pp.716–724.

[5] Sun, W., Shen, Y., Zhang, D., Yang, H., Ma, H., A Systematic Simulation and Proposed Optimization of the Pressure Swing Adsorption Process for N2/CH4 Separation under External Disturbances, *Ind. Eng. Chem. Res.*, 2015,**54**(30), pp.7489–7501.

[6] Plaza, M.G., Duran, I., Querejeta, N., Rubiera, F., Pevida C., Experimental and Simulation Study of Adsorption in Post combustion Conditions Using a Microporous Biochar. 1. CO_2 and N_2 Adsorption, *Ind. Eng. Chem. Res.*, 2016, **55**, pp.3097−3112.

[7] Dantas, T. L. P., Luna, F. M. T., S., Torres, A. E. B., Azevedo, D., Rodrigues, A. E., Moreira, R. F. P. M., Modeling of the fixed - bed adsorption of carbon dioxide and a carbon dioxide - nitrogen mixture on zeolite 13X, *Braz. J. Chem. Eng.*, 2011,**28** (3), pp.533–544.

[8] Yoo, C., Lee, L., Jones, C.W., Probing Intramolecular versus Intermolecular CO_2 Adsorption on Amine-Grafted SBA-15, Langmuir. 2015, **31**, pp.13350 − 13360.

[9] Xu, C., Hedin N., Microporous adsorbents for CO_2 capture – a case for microporous polymers?, *Materials Today*., 2014, **17** (8), pp.397–403

[10] Chitsiga, T., Daramola, M.O., Wagner, N., Ngoy, J., Effect of the Presence of Water-soluble Amines on the Carbon Dioxide (CO_2) Adsorption Capacity of Amine-grafted Poly-succinimide (PSI) Adsorbent During CO_2 Capture, *Energy Procedia*, 2016, **86**, pp.90–105.

[11] Chowdhury, Z. Z., Zain, S. M., Rashid, A. K., Rafique, R. F., Khalid, K., Breakthrough Curve Analysis for Column Dynamics Sorption of Mn(II) Ions from Wastewater by Using Mangostana garcinia Peel-Based Granular-Activated Carbon, *J. Chem.*, 2012, **2013**,pp. 959761.

[12] Aziz, A., S. A., Manaf, L. A., Man, H. C., Kumar, N. S., Column dynamic studies and breakthrough curve analysis for Cd(II) and Cu(II) ions adsorption onto palm oil boiler mill fly ash (POFA), *Environ. Sci. Pollut. Res. Int.*, 2014, **21**(13), pp.7996–8005.

[13] Ruthven, D.M., Principles of Adsorption and Adsorption Processes, *John Wiley & Sons*, 1984, pp.29-62.

[14] Dantas, T. L. P., Luna, F. M. T., Silva Jr, I. J., De Azevedo, D. C. S., Grande, C. A., Rodrigues, A. E., Moreira, R. F. P. M., Carbon dioxide–nitrogen separation through adsorption on activated carbon in a fixed bed, *Chem. Eng. J.*, 2011,**169**,(1–3), pp.11–19.

[15] Gibson, J. A. A., Mangano, E., Shiko, E., Greenaway, A. G., Gromov, A. V., Lozinska, M. M., Friedrich, D., Campbell, E. E. B., Wright, P. A., Brandani, S., Adsorption Materials and Processes for Carbon Capture from Gas-Fired Power Plants: AMP Gas, *Ind. Eng. Chem. Res.*, 2016, **55**(13), pp.3840–3851.

[16] Chaffee, A. L., Knowles, G. P., Liang, Z., Zhang, J., Xiao, P., Webley, P. A., CO_2 capture by adsorption: Materials and process development," *Int. J. Greenh. Gas Control*, 2007, **1**(1), pp.11–18.

[17] Gale, J., Herzog, H., Braitsch, J., Plaza, J.M., Wagener, D.V., Rochelle, G. T., Modeling CO_2 capture with aqueous monoethanolamine, *Energy Procedia*, 2009,**1**(1), pp.1171–1178.

[18] Creamer, A. E., Gao, B., Carbon-Based Adsorbents for Post combustion CO_2 Capture: A Critical Review, *Environ. Sci. Technol.*, 2016, **50**(14), pp. 7276–7289.

[19] Ngoy, J. M., Wagner, N., Riboldi, L., Bolland, O., A CO_2 Capture Technology Using Multi-walled Carbon Nanotubes with Polyaspartamide Surfactant, *Energy Procedia*, 2014, **63**, pp.2230–2248.

[20] Yoro, K.O., Sekoai, P.T., The Potential of CO_2 Capture and Storage Technology in South Africa's Coal-Fired Thermal Power Plants, *Environments,* 2016, **3**, pp.24.

[21] Belmabkhout Y., Sayari, A., Effect of pore expansion and amine functionalization of mesoporous silica on CO_2 adsorption over a wide range of conditions, Adsorption, 2009, **15** (3), pp.318–328.

[22] Serna-Guerrero R., Sayari, A., Modeling adsorption of CO_2 on amine-functionalized mesoporous silica. 2: Kinetics and breakthrough curves, *Chem. Eng. J.*, 2010, **161**(1–2), pp.182–190.

[23] Bohart G. S., Adams, E. Q., Some aspects of the behaviour of charcoal with respect to chlorine, J. *Frankl. Inst.*, 1920, **189**(5), pp.669.

[24] Thomas, H. C., Heterogeneous Ion Exchange in a Flowing System, *J. Am. Chem. Soc.*, 1944, **66**(10), pp.1664–1666.

[25] Rezaei, F., Subramanian, S., Kalyanaraman, J., Lively, R. P., Kawajiri, Y., Realff, M. J., Modeling of rapid temperature swing adsorption using hollow fiber sorbents, *Chemical Engineering Science.*, 2014, **113**, (3), pp.62–76

[26] Fan, Y., Lively, R.P., Labrechea, Y., Rezaeia, F., Korosa, W. J., Jonesa, C. W., Evaluation of CO_2 adsorption dynamics of polymer/silica supported poly(ethylenimine) hollow fiber sorbents in rapid temperature swing adsorption, *International Journal of Greenhouse Gas Control*, 2014, **21**, February, pp.61–71

[27] Borah, J. M., Sarma, J., Mahiuddin, S., Adsorption comparison at the α-alumina/water interface: 3, 4-Dihydroxybenzoic acid vs. catechol, *Colloids Surf. Physicochemical. Eng. Asp.* 2011, **387**(1–3), pp.50–56.

[28] Gupta, S. S., Bhattacharyya, K.G., Kinetics of adsorption of metal ions on inorganic materials: A review, *Adv. Colloid Interface Sci.*, 2011, **162**, (1–2), pp.39–58.

[29] Cheung, C. W., Porter, J. F., Mckay, G., Sorption kinetic analysis for the removal of cadmium ions from effluents using bone char, *Water Res.*, 2001, **35**(3), pp.605–612.

[30] Ho, Y.S., Review of second-order models for adsorption systems, *J. Hazard. Mater.*, 2006, **136**(3), pp.681–689.

[31] Ho Y. S., Mckay, G., The kinetics of sorption of basic dyes from aqueous solution by sphagnum moss peat., *Can. J. Chem. Eng.*, 1998, **76**(4), pp.822–827.

[32] Guo, B., Chang, L., Xie, K., Adsorption of Carbon Dioxide on Activated Carbon, *J. Nat. Gas Chem.*, 2006, **15** (3) ,pp.223–229.

[33] Song, G., Zhu, X., Chen, R., Liao, Q., Ding, Y., Chen, L., An investigation of CO_2 adsorption kinetics on porous magnesium oxide, *Chemical Engineering Journal*., 2016, **283**, pp. 175-183.